HOT CRACKING SUSCEPTIBILITY OF TWIN ROLL CAST Al – Mg ALLOYS

A THESIS SUBMITTED TO
THE GRADUATE SCHOOL OF NATURAL AND APPLIED SCIENCES
OF
MIDDLE EAST TECHNICAL UNIVERSITY

BY

SÜHA TİRKEŞ

IN PARTIAL FULFILLMENT OF THE REQUIREMENTS
FOR
THE DEGREE OF DOCTOR OF PHILOSOPHY
IN
METALLURGICAL AND MATERIALS ENGINEERING

OCTOBER 2009

Approval of the thesis:

HOT CRACKING SUSCEPTIBILITY OF TWIN ROLL CAST Al – Mg ALLOYS

submitted by **SÜHA TİRKEŞ** in partial fulfillment of the requirements for the degree of **Doctor of Philosophy in Metallurgical and Materials Engineering, Middle East Technical University** by

Prof.Dr. Canan Özgen
Dean, Graduate School of **Natural and Applied Sciences** _____

Prof.Dr. Tayfur Öztürk
Head of Department, **Metallurgical and Materials Engineering** _____

Prof.Dr. Alpay Ankara
Supervisor, **Metallurgical and Materials Engineering Dept., METU** _____

Examining Committee Members:

Prof. Dr. Rıza Gürbüz
Metallurgical and Materials Engineering Dept., METU _____

Prof. Dr. Alpay Ankara
Metallurgical and Materials Engineering Dept., METU _____

Prof. Dr. Bilgehan Ögel
Metallurgical and Materials Engineering Dept., METU _____

Prof. Dr. Ali Kalkanlı
Metallurgical and Materials Engineering Dept., METU _____

Assist. Prof. Dr. Kazım Tur
Materials Engineering Dept., Atılım University _____

I hereby declare that all information in this document has been obtained and presented in accordance with academic rules and ethical conduct. I also declare that, as required by these rules and conduct, I have fully cited and referenced all material and results that are not original to this work.

Name, Last name: Süha TİRKEŞ

Signature :

ABSTRACT

HOT CRACKING SUSCEPTIBILITY OF TWIN ROLL CAST Al-Mg ALLOYS

Tirkeş, Süha
Ph.D., Department of Metallurgical and Materials Engineering
Supervisor: Prof. Dr. Alpay Ankara

October 2009, 108 pages

Increasing use of aluminum alloys in the automotive industry increases the importance of the production of sheet aluminum. To provide cost effective sheet aluminum to the industry, twin-roll casting (TRC) is becoming more important compared to DC casting. Demand for usage of different aluminum alloys in sheet form introduces some difficulties that should be considered during their applications. The main problem encountered during the welding of aluminum alloys is hot cracking. The aim of this study is to understand the difference in hot cracking susceptibility of two twin roll cast (TRC) aluminum-magnesium alloys (5754 and 5049 alloys) during welding. Varestraint test method was used to evaluate the effect of welding parameters, strain levels, filler alloys and mid-plane segregation on hot cracking susceptibilities.

Hot cracking susceptibility of both 5049(Al-2wt%Mg) and 5754(Al-3wt%Mg) alloys increased with increasing strain level. Also, it was observed that hot cracking susceptibility was higher for the alloy having higher magnesium content. Thermal analysis results verified that hot cracking susceptibility indeed can be related to the

solidification range. As is suggested in the solidification range approach, the results of the present study confirm that the extent of solidification and liquation cracking depend on the magnitude of solidification range and the strain imposed during welding. Hot cracking susceptibility of 5754(Al-3wt%Mg) alloy has shown slightly decreasing behavior with addition of 5356 filler alloy. On the other hand, addition of 5183 filler alloy has increased solidification cracking susceptibility of two base alloys. The fracture surfaces of liquation and solidification cracks were investigated by scanning electron microscope with EDS. Liquation crack surfaces of the 5754(Al-3wt%Mg) alloy were found to have high Mg and Si content. For the 5754(Al-3wt%Mg) alloy, a quench test was designed to observe the effect of mid-plane segregation zone. It was observed that there was a eutectic reaction resulting in formation of liquid phase below solidus temperature of 5754(Al-3wt%Mg) alloy. Moreover, internal cracks have formed at the mid-plane segregation zone after Varestraint test. Results show that 5049(Al-2wt%Mg) alloy should be chosen compared to 5754(Al-3wt%Mg) alloy for welding. Moreover, low line energy should be applied and filler alloys with high magnesium content should be used during welding to decrease hot cracking tendency of welds.

Keywords: Varestraint Test, Hot Cracking, Aluminum-Magnesium Alloy, mid-plane segregation.

ÖZ

İKİZ MERDANE DÖKÜM TEKNOLOJİSİ İLE ÜRETİLMİŞ Al-Mg ALAŞIMLARININ SICAK ÇATLAK EĞİLİMİ

Tirkeş, Süha
Doktora, Metalurji ve Malzeme Mühendisliği Bölümü
Tez Yöneticisi : Prof. Dr. Alpay Ankara

Ekim 2009, 108 sayfa

Alüminyum alaşımlarının otomotiv endüstrisinde kullanımının artması alüminyum levha üretiminin önemini arttırmıştır. Kütük döküme kıyasla endüstriye düşük maliyetli levha sağlamak amacıyla ikiz merdane döküm teknolojisi önem kazanmaktadır. Çeşitli alüminyum levhalara olan taleble birlikte bunların kullanımı sırasında çıkabilecek sorunların çözümünü de zorunlu olmaktadır. Alüminyum alaşımlarının kaynağında başlıca sorun sıcak çatlaktır. Bu çalışmada amaçlanan ikiz merdane döküm teknolojisi ile üretilmiş aluminyum-magnesyum alaşımlarının (5754 ve 5049) sıcak çatlak eğilimlerindeki farklılığın nedenlerini anlamaktır. Kaynak değişkenlerinin, uygulanan gerinimlerin, farklı dolgu tellerinin ve orta segregasyonun sıcak çatlak eğilimine etkileri "Varesraint Test" yönemi ile değerlendirilmiştir.

Sıcak çatlak eğilimi her iki alaşımda da (5754 ve 5049) artan gerinim ile artış göstermiştir. Magnezyum oranı yüksek olan alaşımda çatlak eğiliminin daha yüksek olduğu görülmüştür. Termal analiz sonuçları da çatlak eğilimi ile katılaşma aralığının ilişkili olabileceğini göstermiştir. Çalışmanın sonuçları katılaşma aralığının ve

uygulanan gerinimin katılaşma ve erime çatlaklarının büyüklüğünü etkilediğini doğrulamıştır. 5754(Al-3wt%Mg) alaşımında 5356 dolgu telinin ilavesi ile katılaşma çatlağı miktarında azalma görülmüştür. 5183 dolgu telinde ise katılaşma çatlağı eğilimi artmıştır. Katılaşma ve erime çatlaklarına ait kırılma yüzeyleri taramalı elektron mikroskobu ve beraberinde EDS analizi kullanılarak inceleniştir. 5754(Al-3wt%Mg) alaşımına ait erime çatlağına ait yüzeyde yüksek miktarda magnezyum ve silisyum olduğu görülmüştür. Orta segregasyonun etkisini görmek amacıyla 5754(Al-3wt%Mg) alaşımı için su verme testi tasarlanmıştır. 5754(Al-3wt%Mg) alaşımının erime sıcaklığının altında sıvı faz oluşmasına sebep olan ötektik reaksiyon olduğu görülmüştür. Varestraint Test'i sonrasında orta segregasyon bölgesinde içten çatlamalar olduğu görülmüştür. Elde edilen sonuçlara göre kaynaklı kullanım için 5754(Al-3wt%Mg) alaşımı ile kıyaslandığında 5049(Al-2wt%Mg) alaşımının seçilmesinin daha uygun olduğu görülmüştür. Düşük hat enerjisi ve yüksek magnezyum içeren dolgu tellerinin kullanılması da çatlak eğilimini azaltacaktır.

Anahtar Kelimeler: Varestraint Test, Sıcak çatlak, Alüminyum-Magnezyum alaşımı, orta segregasyon.

ACKNOWLEDGMENTS

I would like to express his deepest gratitude to his supervisor, Prof. Dr. Alpay Ankara for his guidance, advice, and supports in the completion of this study.

I would like to thank Prof. Dr. Bilgehan Ögel, Prof. Dr. Ali Kalkanlı, Assistant Prof. Dr. Kazım Tur and Dr. Caner Batıgün for their suggestions and comments.

I am also grateful to the members of the METU Welding Technology and Nondestructive Testing Center for their technical assistance.

Finally, I would like to thank my family, Güliz and Baran Tirkeş for their patience and support.

TABLE OF CONTENTS

CHAPTER 1

INTRODUCTION

Aluminum and its alloys are widely used in defense, aerospace, automotive and marine industries. Low density, high corrosion resistance and good electrical and thermal conductivity increase the usage of aluminum alloys. Since the improvement of convenience, performance and safety increase vehicle weight in transportation, weight reduction becomes more important. Therefore, some of the steel parts have been replaced by cast and wrought aluminum alloys in automotive industry.

The production of sheet aluminum becomes more important with increasing demand. In the production of sheet aluminum, direct chill casting of slab and subsequent heating and rolling processes are more expensive compared to twin roll casting (TRC) process. In twin roll cast (TRC) process, sheet metal is directly produced from molten metal without additional heating and rolling steps, resulting in energy saving and lower production cost. However, only the alloys with narrow solidification range can be produced by this method. Moreover, there are some other problems like sticking, buckling and segregation encountered in twin roll cast (TRC) process which have to be overcome.

There are some problems that should be considered during the application of different aluminum alloys in cast and wrought form. The main problem encountered during casting and welding of aluminum alloys is hot cracking susceptibility. In welding, hot cracking can be seen as solidification cracking in the weld metal and liquation cracking in the heat affect zone (HAZ). Improvement of resistance to hot cracking can be possible by controlling the weld microstructure, chemical composition, welding

parameters and welding conditions for some alloys and they are explained in detail in the following sections.

For the evaluation of the susceptibility for hot cracking, *self-restrained test methods* and *externally loaded test methods* were developed. In self-restrained test methods whether the restrained weldment will crack due to the strains resulting from thermal contraction and weld metal solidification is examined. T-fillet, Houldcroft, lap fillet, ring cast, circular patch tests are examples of self-restrained test methods. Externally loaded test methods provide information about the relation between crack formation and welding and mechanical parameters. Evaluation of the hot cracking susceptibility can be made with respect to cracks formed in the solidifying weld metal and in the partially melted zone (PMZ). Number of cracks, total crack length and maximum crack length are the outputs of the externally loaded test methods that can easily be related to welding parameters and the strain applied during welding.

There are various studies on the hot cracking susceptibility of certain aluminum alloys conducted by self-restrained and externally augmented strain type test methods. However, the study of hot cracking susceptibility of twin roll cast (TRC) aluminum-magnesium alloys is lacking in the literature. Due to the increasing demand for twin roll cast (TRC) produced aluminum-magnesium alloys, the weldability of these alloys has become more important. The evaluation of hot cracking susceptibility is inevitable for examining the weldability of these alloys.

In the present study hot cracking susceptibility of two twin roll cast Al-Mg alloys with different magnesium contents, which are 5049(Al-2wt%Mg) and 5754(Al-3wt%Mg) is investigated. In the first part, hot crack formation on the two 5049(Al-2wt%Mg) and 5754(Al-3wt%Mg) Al-Mg alloys is examined. Varestraint test method with Gas Tungsten Arc Welding (GTAW) process was used for the evaluation of hot cracking susceptibility. Effect of chemical composition of the alloys, strain applied and line energy on hot cracking susceptibility were determined. Second part consists of obtaining bead-on-plate welds with different filler addition by Gas Tungsten Arc Welding (GTAW) process and evaluation of cracking susceptibility depending on filler alloys. The final stage includes characterization of mid-plane segregation and its effect on hot cracking susceptibility of two twin roll cast (TRC) aluminum-magnesium alloys.

CHAPTER 2

THEORY

2.1. Twin roll casting

Twin roll casting (TRC) is an alternative to conventional direct chill casting for the production of sheet and strip products. TRC has some advantages compared to direct chill casting like low energy consumption, low equipment and operating costs [2]. Molten metal is fed onto water cooled rolls, where it solidifies as a strip at high cooling rate compared to direct chill casting[3] (Figure 2.1). Then, strip is rolled into desired thickness.

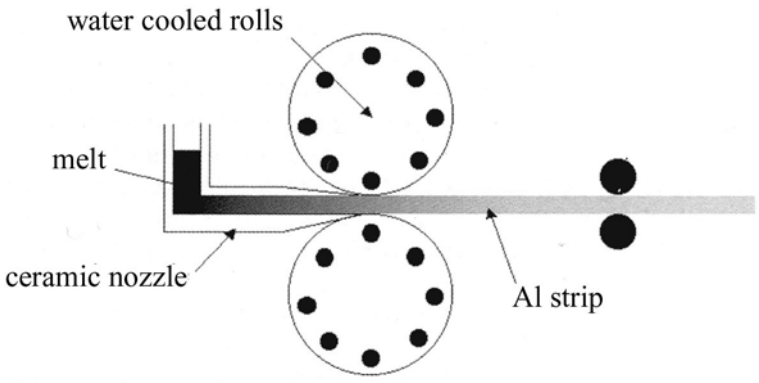

Figure 2.1 Schematic view of twin roll casting process[3].

In twin roll casting aluminum alloys with narrow freezing range are cast. The technique is not suitable for alloys with wide freezing range since strip cannot be cooled

sufficiently. Productivity of TRC process is low due to low casting speed of roll caster. There are some studies for improvement of productivity in TRC [2-5]. Moreover, buckling, sticking and segregation defects encountered in twin roll casting have been investigated. And wide range of alloys have been cast and studied with respect to convenience for TRC and defect formation [6, 7].

2.2. Weld regions

There are three main regions in the weldment. Weld metal (WM) is the completely melted and solidified region. Weld metal consists of base metal and filler material. As the weld pass increases chemical composition of the weld metal reaches to chemical composition of the filler metal. Weld metal is separated by fusion line from the base metal where temperature is liquidus temperature. There is a region which is affected from the heat input during welding between weld metal and base metal and it is named as heat affected zone (HAZ). In the heat affected zone, the region which starts from the fusion line and ends at the point where temperature is solidus temperature is named as partially melted zone (PMZ). The size of partially melted zone depends on solidification range of the base metal.

2.2.1. Weld metal

In fusion welding process heat for melting is provided by an arc burning between welding torch and base material. Dilution of weld metal, heat distribution, composition, pool shape and weld metal microstructure are related with welding parameters, like welding current, welding speed etc.

Base metal grains around the weld pool act as nucleation sites during solidification of weld metal. Solidification mode and microstructure of the weld metal depends on cooling rate, chemical composition, solute redistribution and growth rate. Effect of temperature gradient and growth rate on solidification mode is given in Figure 2.2[10]. Growth rate (R) and temperature gradient (G) determine solidification mode and size of microstructure as seen in Figure 2.2. G/R determines solidification mode and the GxR gives the size of solidification microstructure.

G/R ratio is affected by welding parameters like heat input and welding speed. Increasing line energy with constant welding speed, i.e. increasing heat input only results in decreasing temperature gradient. Then, G/R ratio decreases. Decreasing G/R can change the solidification mode from cellular to dendritic [10]. Moreover, heat input and welding speed also affect the size of microstructure. Size of microstructure, i.e. dendrite arm spacing, decreases with increasing cooling rate. And, cooling rate can be altered by lowering line energy (Q/V) where Q is heat input and V is welding speed. As the line energy decreases finer microstructure can be obtained.

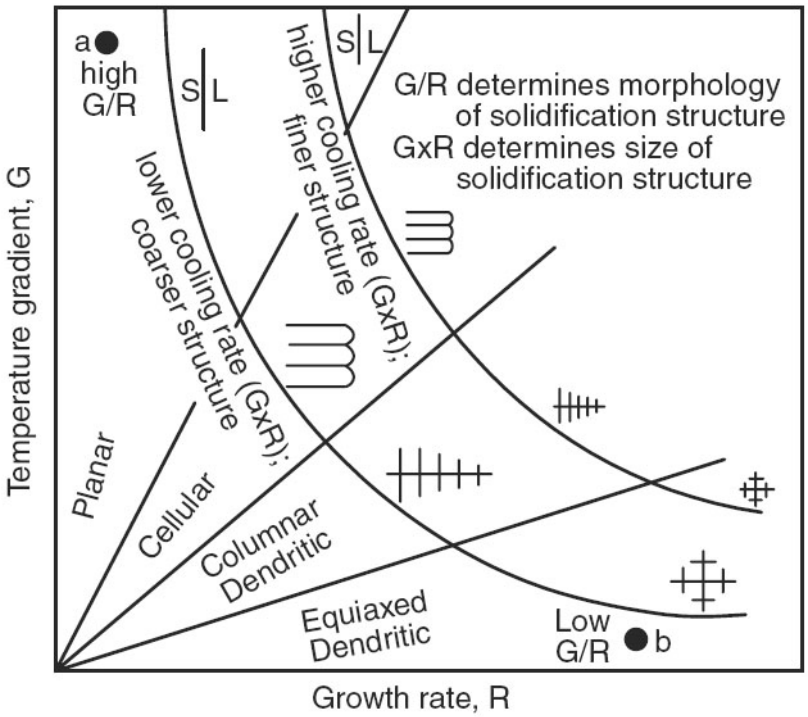

Figure 2.2 Effect of cooling rate and growth rate on weld metal solidification[10].

Growth rate and temperature gradient change along the weld pool boundary from center line to fusion line[10]. Therefore, solidification mode can change with respect to weld pool boundary. Growth rate (R) which depends on welding speed (V) changes from V to zero from centerline to fusion line as seen in Figure 2.3a. Moreover, temperature gradient is higher at the fusion line and decreases from fusion line to centerline of the

weld pool (Figure 2.3b). Thus, G/R ratio is much higher at the fusion line and this may result in presence of different solidification modes in a single weld metal (Figure 2.3c).

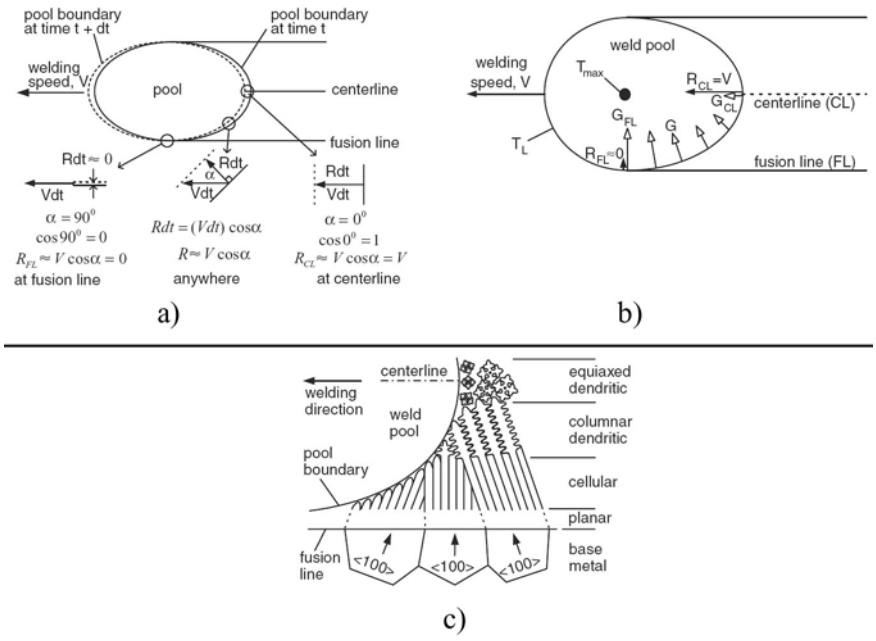

Figure 2.3 a) Growth rate (R), b) Temperature gradient (G) and c) Solidification mode along the weld pool [10].

2.2.2. Partially melted zone (PMZ)

Partially melted zone is a region in heat affected zone (HAZ) and more detectable in aluminum alloys due to wide solidification range. Partially melted zone starts from the fusion line of weld pool which is at liquidus temperature (T_L) and expands to the base material side and ends at the point where temperature is solidus temperature (T_S). However, heating and cooling occur very fast during welding and therefore liquation mechanisms can differ depending on composition of alloy[10]. These are defined in this section.

Welding affects the properties of the aluminum alloys depending on its type. Strength lost can be encountered after welding of aluminum alloys. Aluminum alloys gain

strength by work hardening, solution hardening and age hardening. However, heat generated from the welding process influence adversely mechanical properties of aluminum alloys. Heat treatable aluminum alloys can lose their strength but post weld heat treatment process can be applied for recovery of mechanical properties. Solution hardened alloys are not affected from welding. In work hardened alloys, on the other hand, strength decreases due to melting in weld region and recrystallization and grain growth in heat affected zone. And it is difficult to compensate strength loss.

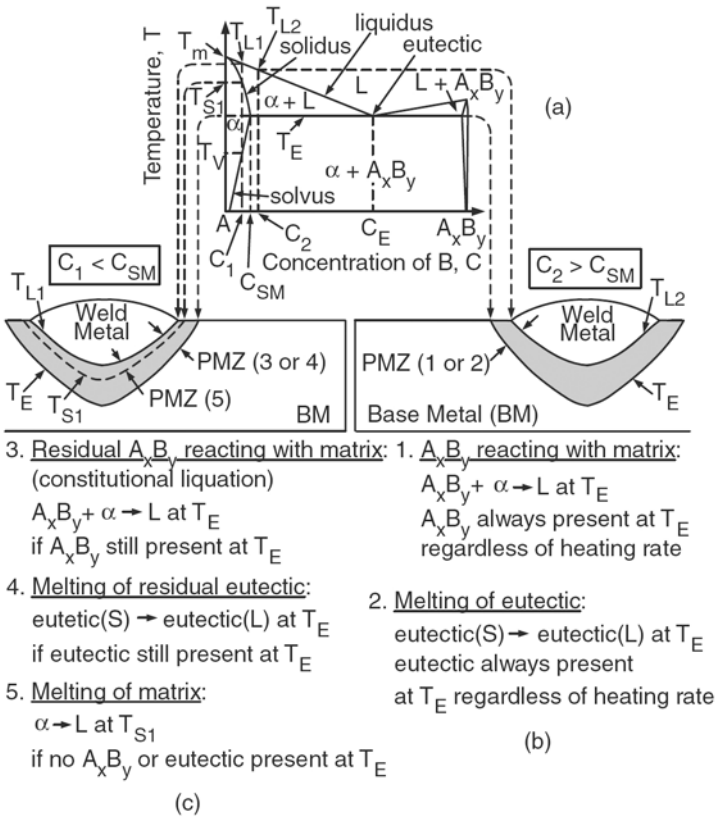

Figure 2.4 Liquation mechanisms for both solid solubility limit and above the solid solubility limit [10].

As mentioned above, heating is very fast during welding and this differs liquation mechanism of an alloy from equilibrium condition. Huang et al. [18,19, 21] states five different liquation mechanisms depending on alloy composition. First one is for an alloy having composition of C_2 as given in Figure 2.4a. At room temperature A_xB_y and α

phases present and during welding at temperature T_E eutectic reaction occurs between A_xB_y particles and α phase as shown in Figure 2.4b. Alloy C_2 also contains $\alpha + A_xB_y$ eutectics. When temperature reaches to T_E during melting eutectics melt and this is named as second mechanism (Figure 2.4b).

Third mechanism is called as constitutional liquation [56, 57]. Alloy C_1 contains A_xB_y particles and in equilibrium conditions when temperature reaches solvus temperature A_xB_y dissolves in α phase and there will be no liquation up to solidus line. However, A_xB_y particles can remain without dissolution in α phase during welding due to high heating rate. And at T_E temperature liquation occurs due to eutectic reaction between A_xB_y particles and α phase and this is defined as third mechanism (Figure 2.4c) in welding.

Solute segregation at grain boundaries may lead to formation of eutectics in C_1 alloy. During welding, because of high heating rate they do not dissolve and remain up to T_E temperature. At T_E temperature, residual eutectics melt at the grain boundaries. This is named as fourth mechanism and given in Figure 2.4c. Final liquation mechanism is melting of C_1 alloy consisting of only α phase. Since there is no A_xB_y particles and $\alpha+A_xB_y$ eutectics, melting does not occur before reaching solidus temperature (Figure 2.4c).

During welding of aluminum alloys solidification cracking in weld metal and liquation cracking in partially melted zone can be encountered. Wide solidification range, high thermal conductivity and solidification shrinkage are some reasons for high cracking susceptibility of aluminum alloys. Hot cracking theories and hot cracking in welds are the following sections containing details about hot cracking.

2.3. Hot cracking

Alloys solidify from liquid to solid over a temperature range. Solidifying metal contains both solid and liquid phases. At the beginning of the solidification, liquid metal with suspended solid particles is named as slurry. As the solid content increases solid particle interaction starts and this state is called mushy zone. During solidification, hot cracking

is the main problem encountered in the casting process at the mushy zone. Thermal gradients, solidification shrinkage and thermal contractions cause stress and strain evolution on the solidifying metal resulting in cracking between the dendrites. There are many theories explaining the hot cracking in the literature and collection of these mechanisms has been done by Eskin et. al.[32] and some of them are described in the following section.

According to permeability of the mushy zone solidification process is divided into four stages [31]. *Mass feeding* is the first stage at which liquid and solid phases are move freely. In second stage dendritic network is formed but interdendritic liquid still can flow and prevent pore or crack formation which is named as *interdendritic feeding*. *Interdendritic separation* is the third stage. Pores or cracks formed at this stage can not be healed since the interdendritic liquid can not flow due to very low permeability of the solid network. Solid phase develops considerable strength and resists any contraction at the *interdendritic bridging* state which is the final stage of the solidification. Hot cracking theories are related with third stage of the solidification which is susceptible for solidification cracking.

Ductility of the semi-solid body determines the hot crack formation [33, 34]. According to this theory, grain boundary sliding surrounded by liquid film is the mechanism to resist the strain on the semi-solid body. If strain evolved on the mushy zone greater than the ductility of the body than cracking occurs. And susceptibility to cracking is affected by grain size and its distribution and surrounding liquid film thickness. While decreasing grain size and increasing film thickness increases the fracture strain, inhomogeneous grain size reduces the fracture strain of the semi-solid body [34]. Moreover, it was proposed that [58] strain on the interdendritic liquid film causes the solidification cracking. Liquid film stage is most susceptible to cracking due to localized strain on the liquid film (Figure 2.5). As the presence time of the liquid film increases, strain on the film increases resulting in higher susceptibility to cracking (Figure 2.6). Liquid film stage is just before the complete solidification and duration of liquid film depends on alloy composition and cooling rate of the solidification.

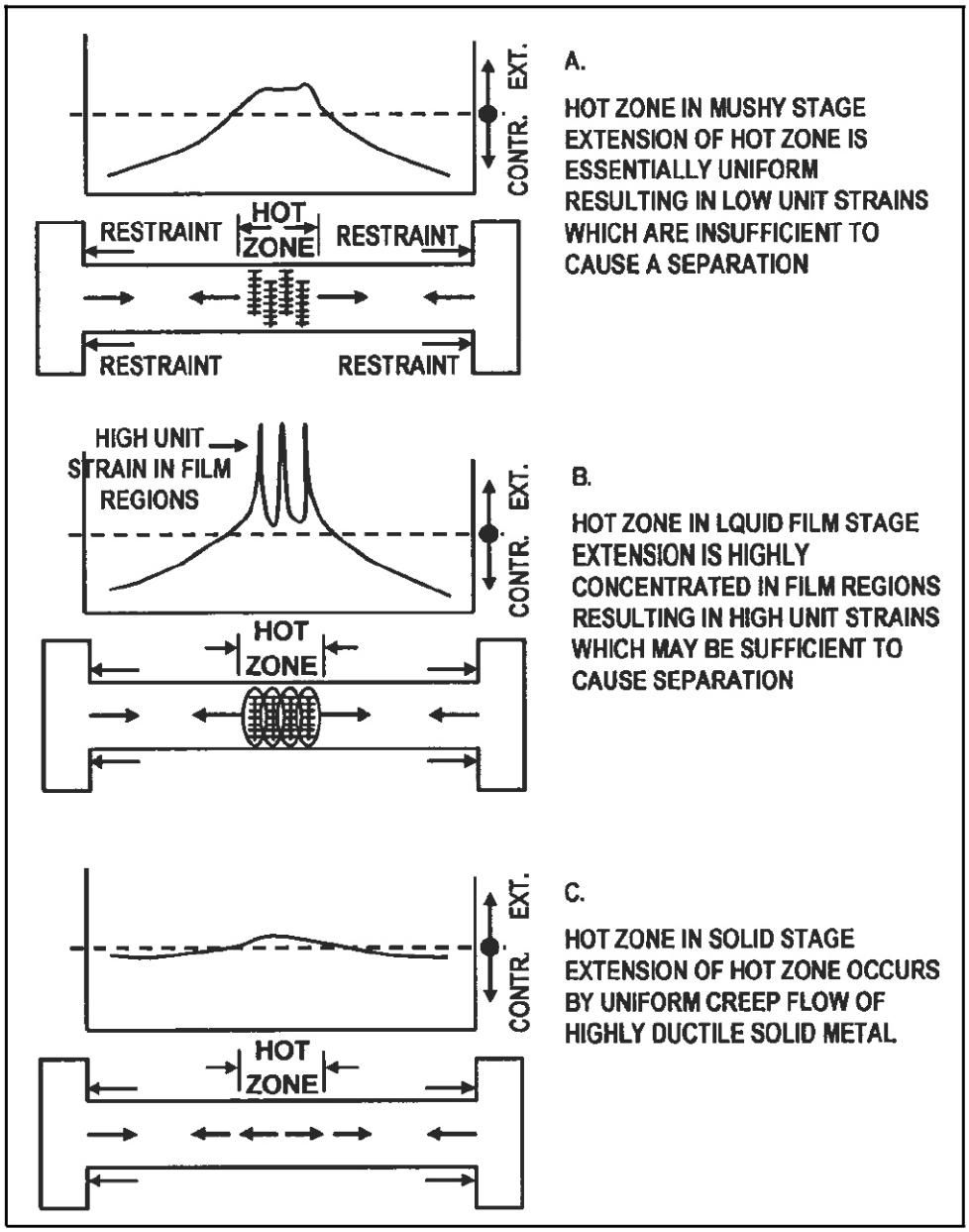

Figure 2.5 Strain distribution at three different stages [58]

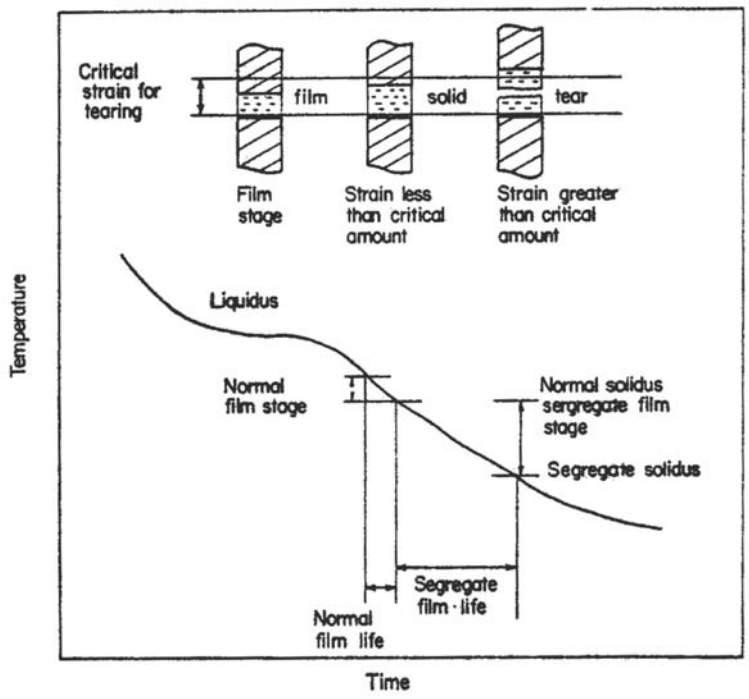

Figure 2.6 Effect of film life on strain accumulation causing crack formation [58]

As the permeability of the dendritic structure decreases flow of liquid is prevented. According to Pumphery and Jennings' theory named as shrinkage-brittleness theory [59], if strain accumulated is greater than the mushy zone can resist cracking occurs during solidification. Moreover, healing of any cracks or pores resulting from thermal contraction and solidification shrinkage can not be healed due to hindered feeding of the liquid.

Studies based on ductility of semi-solid structure showed that there is a region in which ductility is very low in a temperature range above the solidus. This temperature range is named as Brittle Temperature Range (BTR) and it has upper and lower limits as seen in Figure 2.7 [31]. If accumulated strain during solidification exceeds the strain at which semi-solid structure fractures then cracking occurs. The lower temperature is the solidus temperature below this limit ductility increases and the upper limit is the coherency temperature at which there is a dendrite coherency. Above this temperature liquid metal with low solid fraction, i.e there is not connection between solid particles gives no

response to strain. As the solidification range increases, brittle temperature range (BTR) increases and solidifying metal is more vulnerable to cracking.

In addition to critical strain needed for hot cracking, strain rate is also an important parameter for hot crack formation. As seen in Figure 2.7, there is a critical strain rate and if the rate of strain accumulation during solidification passes over this limit cracking occurs [61, 62].

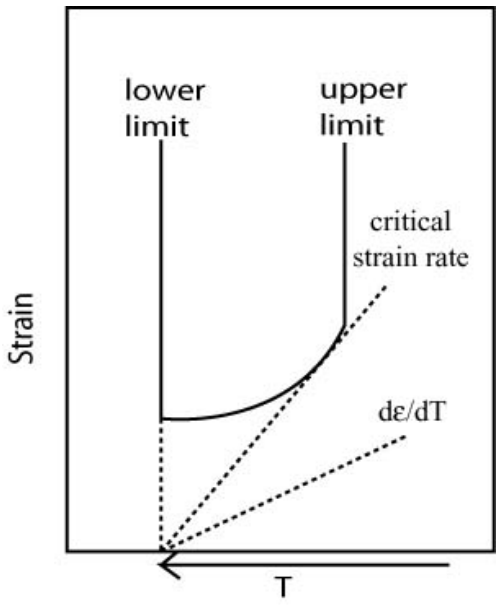

Figure 2.7 Schematic representation of Brittle Temperature Range (BTR) and strain rate.

The difference between average integrated strain for fracture (ε_p) and linear shrinkage/contraction (ε_{sh}) in the BTR defines the hot cracking susceptibility of the solidifying metal and this is named as "reserve of placticity" (p_r)(Figure 2.8).[63]

$$p_r = \frac{1}{\Delta T_{br}} \int (\varepsilon_p - \varepsilon_{sh}) dT \quad (1)$$

$$\varepsilon_{sh} = \alpha \Delta T_{br} \quad (2)$$

where ΔT_{br} is brittle temperature range (BTR) and α is thermal contraction coefficient. As the p_r increases hot cracking susceptibility decreases.

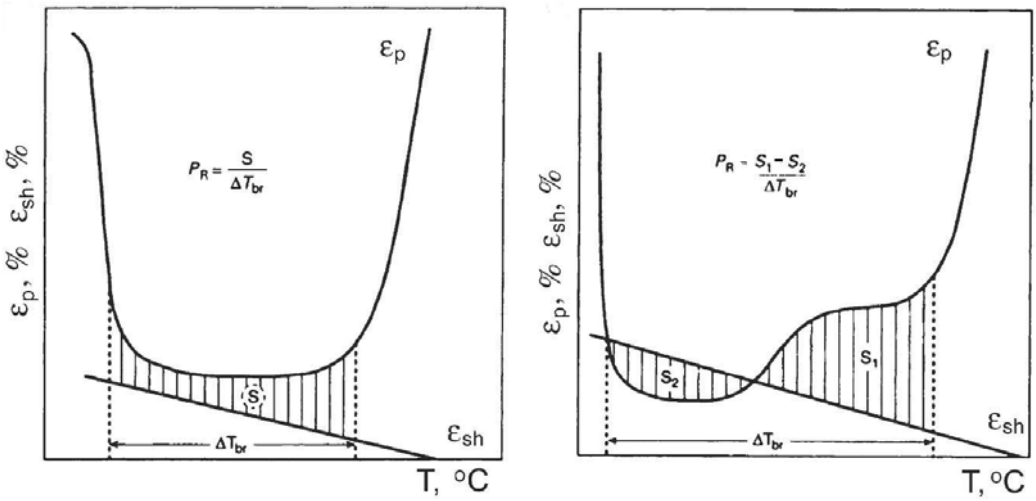

a) b)

Figure 2.8 Calculation of reserve of plasticity, p_r, a) $S/\Delta T_{br}$ and b) $(S_1\text{-}S_2)/\Delta T_{br}$ [63]

According to Borland's "generalized theory" [64] solidification process is divided into three stages as given in Figure 2.9. At first stage solids and liquid move freely and there is no strain accumulation. The second stage involves formation of dendritic network but still liquid flow is possible. Thus, healing of pores or cracks formed due to solidification shrinkage and thermal contraction is possible. In third stage, liquid flow is prevented due to low permeability of the dendritic network. In other words, if the strain accumulated is greater than the strain that semi-solid can resist crack forms and due to hindered feeding healing of cracks does not occur in this stage (Figure 2.9). As the solidification progresses strength of the interdendritic network increases and cracking

susceptibility decreases. As seen in Figure 2.9 hot cracking susceptibility of an alloy depends on it composition.

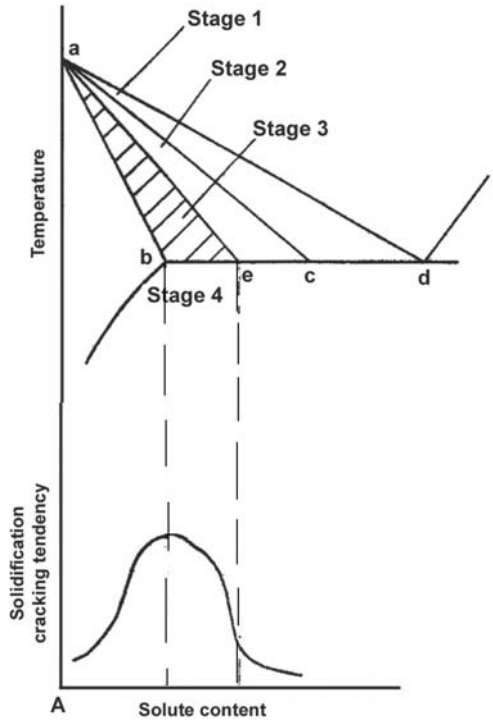

Figure 2.9 Relation between the solidification stages and cracking susceptibility[64].

Moreover, distribution of interdendritic liquid is also important [32]. Distribution of liquid depends on its wetting angle, ϕ, and it is a function of solid/solid and solid/liquid surface energies. At low dihedral angle liquid wets much grain boundary surface and increases the susceptibility (Figure 2.10). Cracking susceptibility decreases as the wetting angle increases. Wettability is given as;

$$\tau = \frac{\gamma_{SL}}{\gamma_{SS}} = \frac{1}{2\cos(\phi/2)} \qquad (3)$$

where γ_{SL} solid/liquid surface energy, γ_{SS} is solid/solid surface energy and ϕ is dihedral angle. As dihedral angle decreases wettability increases. For high wetting angle, e.g

120^{O} as given in Figure 2.10, wetting is low, so that there is more bridging between the grains resulting high resistance to cracking.

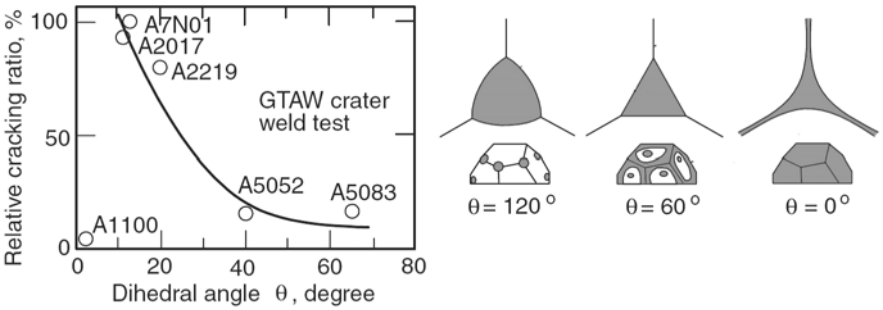

Figure 2.10 Relation between grain boundary liquid distribution and wetting angle on the hot cracking susceptibility [39].

Hot tearing criteria can be reviewed in two groups non-mechanical and mechanical. Process parameters, solidification range and phase diagram are involved in non-mechanical criteria. And mechanical criteria involve critical stress, strain and strain rate [65].

One of the non-mechanical criteria is proposed by Clyne and Davies [66]. Strain evolved during last stage of solidification can not be accommodated by mass and liquid feeding. As the solid fraction increases and interdendritic bridging is built, hot cracking is prevented. Following formula was proposed for hot cracking susceptibility [66].

$$HCS = \frac{t_V}{t_R} = \frac{t_{99} - t_{90}}{t_{90} - t_{40}} \tag{4}$$

where t_v is the susceptible time for hot cracking, t_R is the time available for stress-relief, time at the solid fraction is 99% is defined as t_{99} and t_{40} is the time at the fraction of solid is 40%.

The effect of solidification conditions and alloy composition on hot cracking properties of aluminum alloys was investigated by Feurer [67]. Composition of the alloy, shrinkage, solidification conditions and feeding were involved in this approach. This model based on that permeability of the dendritic network decreases during solidification and liquid metal feeding becomes difficult so that with addition of solidification shrinkage hot cracking occurs as given in Figure 2.11 [68]. According to Feurer model, if rate of feeding (ROF) is less than rate of shrinkage (ROS) hot cracking is possible.

$$ROF = \frac{f_L^2 \lambda_2^2 P_S}{24\pi c^3 \mu L^2} \tag{5}$$

$$ROS = \frac{\left(\rho_O - \rho_S + akC_L\right)\dot{T} f_L^{(2-k)}}{\rho(1-k)m_L C_O} \tag{6}$$

where f_L is liquid fraction, λ_2 is secondary dendrite arm spacing, P_S is effective feeding pressure, c is dendrite network tortuosity, μ is liquid viscosity, L is length of porous network, ρ_L and ρ_S are the densities at the liquidus and solidus temperatures, ρ is average density, ρ_O is liquid density at the melting point, a is composition coefficient of the liquid density, C_L is composition of the liquid at the solid-liquid interface, C_O is alloy composition, T is average cooling rate during solidification, k is equilibrium partitioning coefficient, m_L is slope of the liquidus line.

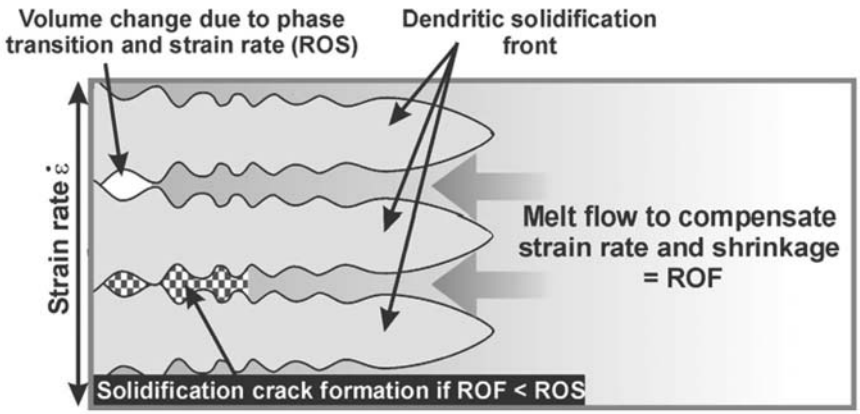

Figure 2.11 Relation between feeding, shrinkage and solidification cracking [68].

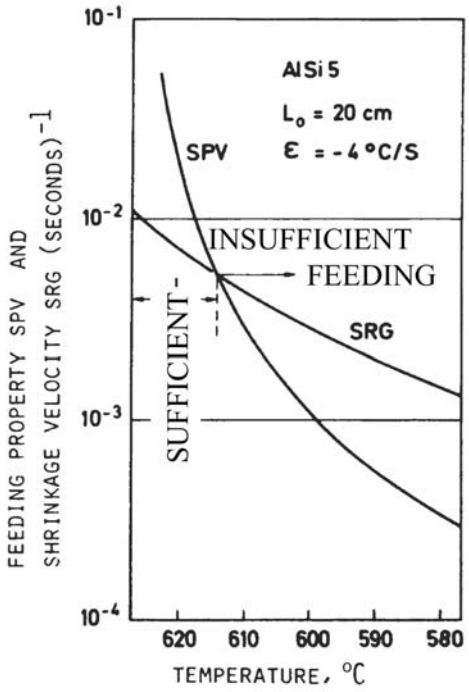

Figure 2.12 Maximum volumetric flow rate and volumetric solidification shrinkage values[67].

The third non-mechanical model is proposed by Katgerman [69] and it is derived from combination of two models mentioned above. Casting speed, ingot diameter and alloy

compositions are involved in this model. Hot cracking susceptibility index is given below.

$$HCS = \frac{t_{99} - t_{cr}}{t_{cr} - t_{40}} \quad (7)$$

where t_{99} is the time at solid fraction is 99%, t_{40} is the time at sold fraction is 40% and t_{cr} is the time feeding is insufficient.

2.3.1. Hot cracking in welding

Hot cracks in welding are divided into two groups as solidification cracks and liquation cracks. Solidification cracks in welding are almost same with the cracks formed during casting process mentioned in previous section. Similar to casting process, solidification cracks form when the mushy zone can not resist to the solidification shrinkage and thermal contraction.

High solute content at the intergranular region drops its melting temperature below the solidus of the base alloy. This results in higher liquation during welding at the grain boundaries. Liquation starts from the fusion line and expands through the base metal within the heat affected zone (HAZ) and it is named as partially melted zone (PMZ). Stresses due to solidification shrinkage and thermal contraction may form intergranular separation from the liquid film at grain boundaries called as liquation crack in the partially melted zone (PMZ).

2.3.1.1. Solidification cracking

At the final stage of the solidifying weld metal, shrinkage and thermal strains may result in cracking. During the solidification shrinkage and thermal contraction causes the solidifying weld metal to contract. And tensile strains form on the weld metal. If the mushy zone can not accommodate the strain evolved cracking occurs.

Solidification range consists of four stages (Figure 2.13). These stages are determined according to solid and liquid phase distribution. Continuous liquid phase containing

dispersed solid phase is the first stage. At this stage two phases can move freely. However, at the second stage since the solid dendrites are interlocked solid phase can not move. Only the continuous liquid phase can flow. This provides healing of the cracks. In third stage, increased solid fraction prevents the movement of the liquid. If the strains formed due to shrinkage or thermal contractions exceeds the ductility limit of the solidifying metal cracking occurs. In this stage cracks can not be healed since the amount of the liquid is very small and also its flow is prevented by solid phase. The last stage is the complete solidified metal and shrinkage and thermal strains can not cause cracking. [38].

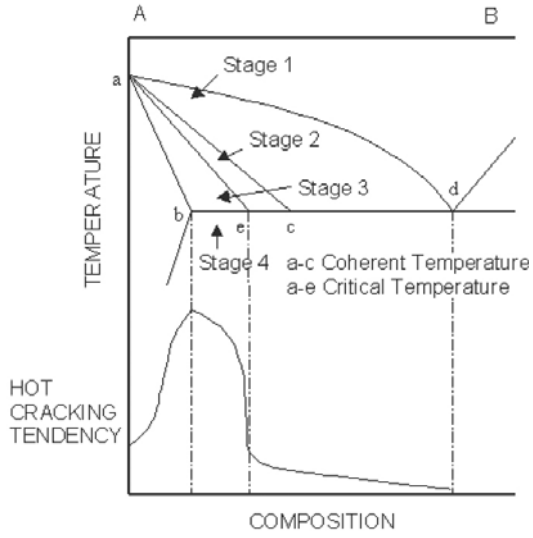

Figure 2.13 Hot cracking susceptibility change with composition and solidification stages according to the Borland's generalized theory [38].

Effect of brittle temperature range (BTR) on solidification cracking susceptibility is valid for weld solidification cracking. If brittle temperature range (BTR) expands, susceptibility to cracking increases. BTR range depends on solidification range. Increasing solidification range results in wider BTR. Solidification cracking susceptibility depending on composition of alloys which was mentioned above is also valid for solidifying weld metal. Moreover, Dupont et. al. [70] have shown that eutectic reactions expanding solidification ranges increases the solidification cracking susceptibility. Amount of liquid is also important during solidification of weld metal. If there is high amount of liquid at the final stage of the solidification, feeding of pores or

cracks is possible (Figure 2.14). Therefore increasing fraction of liquid at the last stage of solidification decreases cracking susceptibility. As seen from the Figure 2.14, little amount of solute (II) forms small amount of liquid between the grains resulting in higher susceptibility to solidification cracking. As the solute content increases healing of the cracks formed becomes easier during solidification [8].

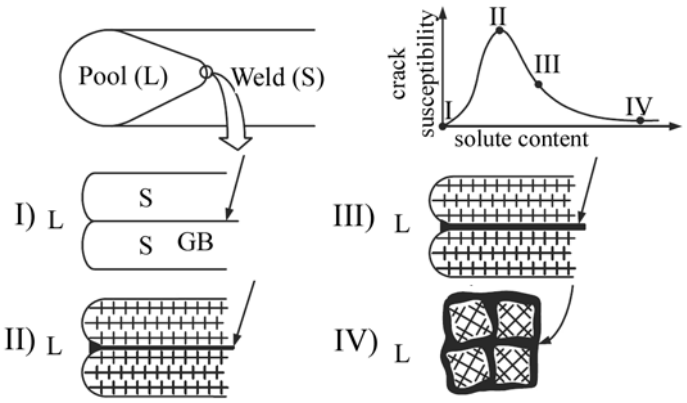

Figure 2.14 I. pure metal. II. some solute resulting in grain boundary film. III. more solute providing more grain boundary liquid for healing of the cracks IV. Higher amount of liquid least susceptible to cracking [10].

As mentioned previous section, ductility of solidifying metal and strain rate affect the hot cracking susceptibility. Brittle temperature ranges of different aluminum alloys and effect of strain rate on solidification cracking susceptibilities were investigated by Matsuda et.al. [39]. As seen in Figure 2.15a different aluminum alloys have different brittle temperature ranges. And, brittle temperature range (BTR) of an alloy increases with solidification range (Figure 2.15b). Also, results have showed that increasing strain rate decreases the critical strain for solidification cracking as seen in Figure 2.16. In other words, cracking susceptibility increases with increasing strain rate .

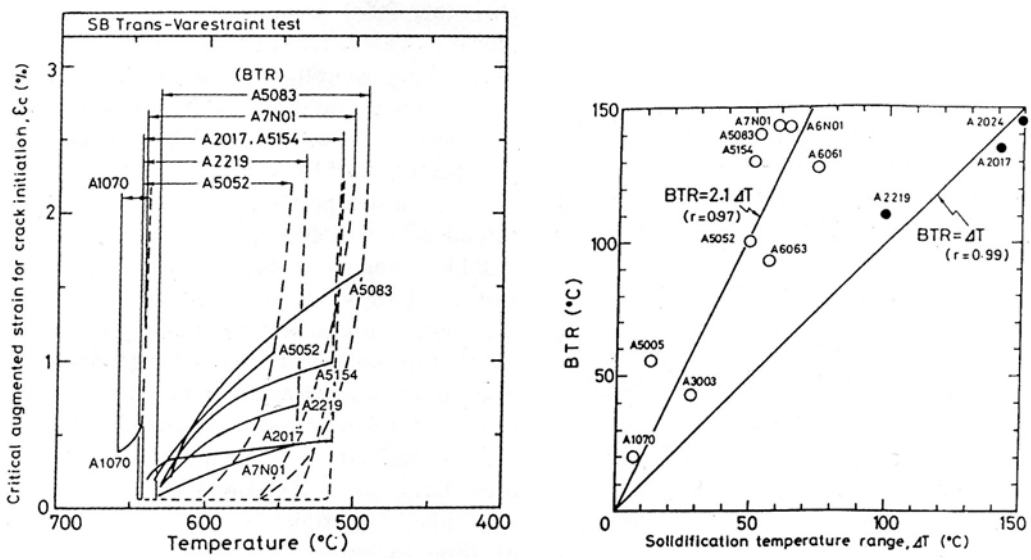

a) b)

Figure 2.15 a) Brittle temperature range (BTR) of aluminum alloys and b) relation between BTR and solidification range [39].

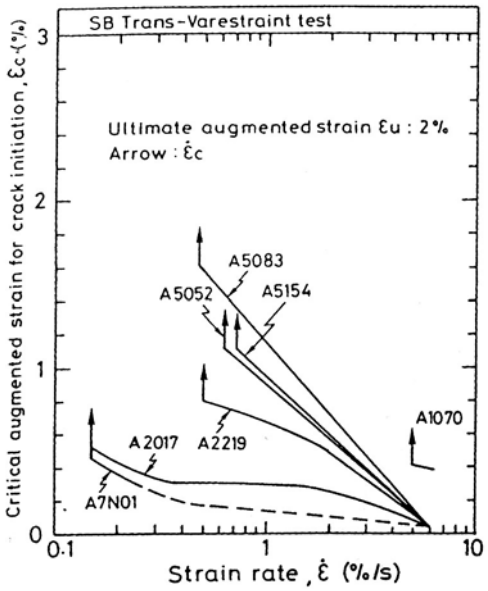

Figure 2.16 Effect of strain rate on critical strain for crack initiation [39].

Solute rich intergranular liquid increases the susceptibility of the solidifying weld metal. In addition to that, distribution of liquid is also important. Wetting of the remaining

liquid between the grains affects the cracking susceptibility. Form of the grain boundary liquid is important for the solidification cracking susceptibility. Depending on surface tension grain boundary liquid is globular or it forms a film between the grains. Lower surface tension between the grains and liquid, there will be a liquid film between the grains which results in higher solidification cracking susceptibility. If the surface tension is high then liquid is globular (Figure 2.17). This means there will be no wetting of the grains resulting in larger contact areas between the grains and they can resist the strain. Liquid film between grains instead of globular morphology increases the solidification cracking susceptibility.

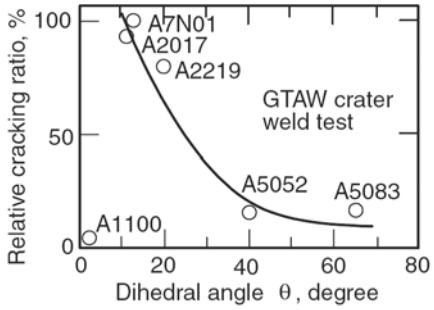

Figure 2.17 The effect of grain boundary liquid on the hot cracking susceptibility [39].

If the stress exceeds the strength of the solidifying metal then cracking occurs. According to Chihoski [71, 72] there are compression and tensile regions around the moving weld pool. These zones are given in Figure 2.18. Preheating of the welding torch results in thermal expansion in front of it so that there is a compression zone labeled as C_1. Tensile stresses develop on the solidifying weld pool (T_m) due to solidification shrinkage. Following region is under compression stresses, C_2, resulting from the thermal contraction. T_1 and T_2 are the tensile zones formed as a reaction to the compressive zones. Moreover, Chihoski states that, welding conditions affects these zones. Compressive region behind the weld pool, C_2, disappear with decreasing welding speed and this results in developing tensile stresses on the mushy zone. In other words, decreasing line energy increases the cracking susceptibility of the weld metal.

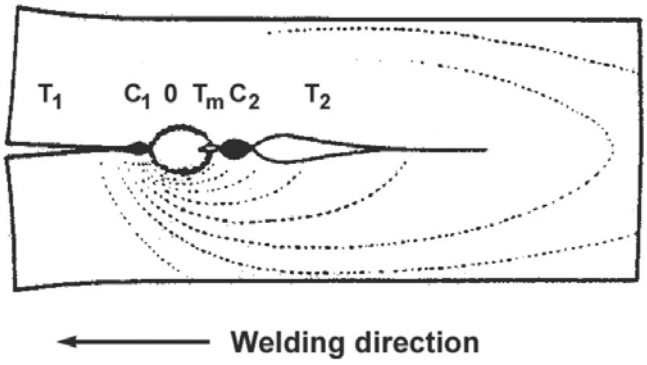

Figure 2.18 Tensile and compressive regions formed during welding

Fine grained materials show high resistance to solidification cracking. Moreover, decreasing grain size results in increasing grain boundary area. So that, amount of solute contents causing low melting point liquid per unit area decreases and cracking susceptibility decreases. Grain refining by the addition of refining agents[40] and magnetic arc oscillation[41] are the ways of increasing resistance to solidification cracking. Matsuda et al.[40] has studied to decrease the solidification cracking susceptibility of the Al-Zn-Mg alloy. With addition of some elements to the weld metal grain refining has obtained and solidification cracking susceptibility has decreased. The relation between the grain size and crack length is given in Figure 2.19. Reddy et al. [24] have also improved resistance to cracking susceptibility by small addition of Sc to both base and filler alloys. Besides grain refinement, formation of continuous grain boundary products is prevented with Sc.

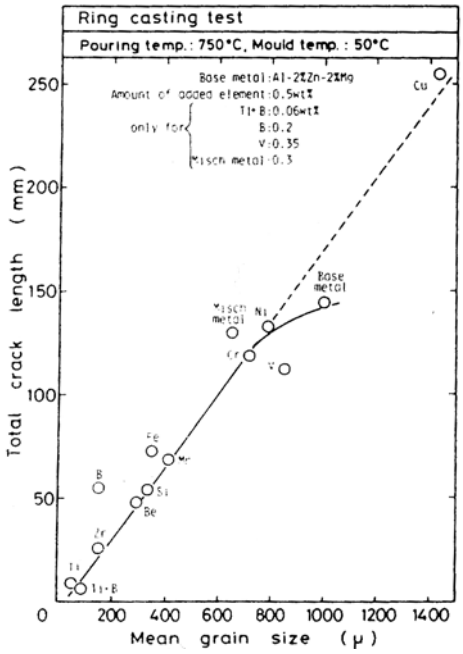

Figure 2.19 Relation between mean grain size and crack length of Al-2%Zn-2%Mg [40].

2.3.1.2. Liquation cracking

In the heat affected zone (HAZ) there is a region near the fusion line of which temperature is between liquidus (fusion line) and solidus called partially melted zone (PMZ). In PMZ melting starts at the grain boundaries first. Due to segregation of the solutes at the grain boundaries melting points are lower at these regions. As the solidification range of the base metal increases PMZ in the heat affected zone becomes wider. Also increasing line energy (heat input, kJ/cm) increases the size of the partially melted region. As mentioned in previous section during welding shrinkage and thermal strains on the weld zone may cause cracking during solidification (Figure 2.20). Same effect can be seen in the PMZ. When the partially melted zone cannot accommodate these strains cracking occurs called liquation cracking. Therefore, as the size of the partially meted zone (PMZ) increases it results in higher liquation cracking susceptibility. As the amount of liquation increases due to segregation of high amount of solute content cracking susceptibility increases in the partially melted zone. Besides segregation at the grain boundaries, base metal grain structure also important. As the

grain size decreases grain boundary area increases resulting in less solute segregation per unit area. As a result finer grain size increases the resistance to liquation cracking.

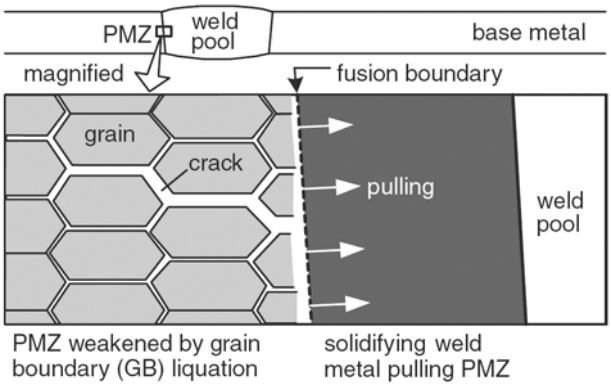

Figure 2.20 Schematic view of the partially melted zone (PMZ) and formation of liquation crack [10].

Liquation cracking can be reduced by lowering degree of restraint. Moreover, size of partially melted zone (PMZ) can be decreased with lowering line energy during welding, so that, liquation cracking susceptibility can be decreased by decreasing liquation.

Also liquation cracking susceptibility depends on the solid fraction (fs) of the weld metal during partially melted zone (PMZ) solidification [10, 21, 42, 43, 44]. If the tensile strains coming from the solidifying weld metal is greater than the strength of the solidifying PMZ then liquation cracking occurs. In case of solid fraction of the weld metal is greater than the fs of solidifying PMZ than the liquation cracking susceptibility is high. Susceptibility of the partially melted zone depends on type of alloy, segregation, welding parameters like welding speeds and heat input, thickness of the plate and also design and application of the weldment.

2.4. Test methods for hot cracking susceptibility

There are numerous tests for the evaluation of the hot cracking susceptibility. These tests are divided into two groups. One is the self restraint test and the other is external

augmented straint test methods. Houldcroft test, circular patch test, ring cast cracking test, T-fillet test, weld crater cracking test and lap fillet test are self restraint type of tests. These types of tests do not provide an opportunity to see the effect of different strain and strain rate on hot cracking susceptibility of the alloy. While some of these test has low reproducibility, some of them are very practical with regard to specimen preparation and test equipment. According to Matsuda et. al.[45] lap-fillet test (Figure 2.21a) is not very suitable due to scattering in the results obtained in gas shielded metal arc welding. Simplicity of T-fillet test (Figure 2.21b) makes it favorable for cracking test. However, this test method is not suitable to evaluate the effect of composition changes on cracking susceptibility since it is not so sensitive. Matsuda states that Houldcroft test (Figure 2.21c) method is more favorable test method to see the effect of different filler alloys and base materials. In addition to that, it is very sensitive to the effect of chemical changes in the filler alloy. Circular patch test [10] is also useful self-restraint test method to evaluate solidification and liquation cracking susceptibility.

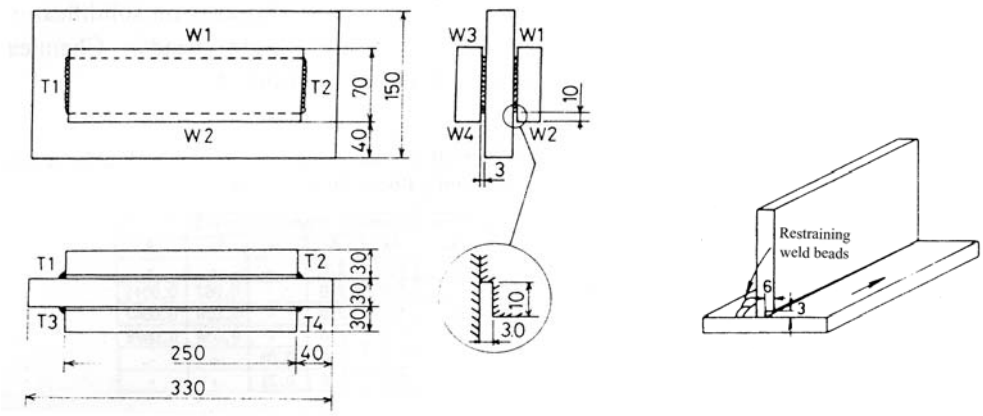

a) b)

Figure 2.21 Self-restraint test methods a) lap-fillet, b) T-fillet, c) Houldcroft [45] and d) circular patch test [10].

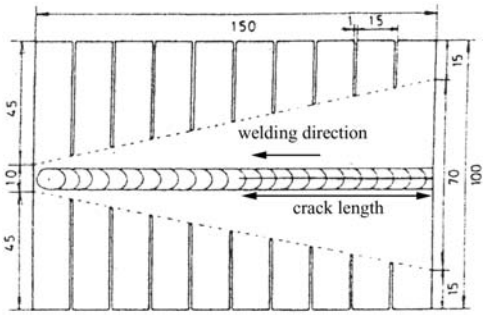

c)

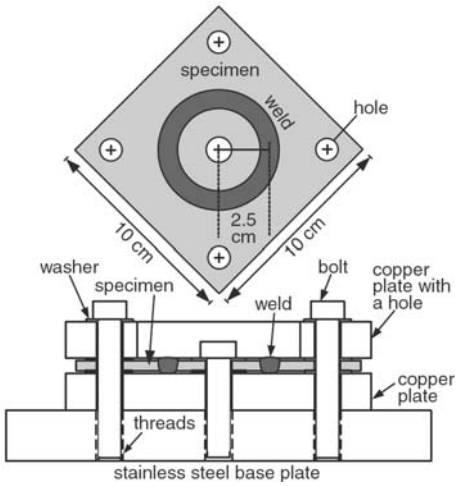

d)

Figure 2.21 Self-restraint test methods a) lap-fillet, b) T-fillet c) Houldcroft [45] and d) circular patch test [10] *(continued)*.

With external augmented straint test methods in addition to welding parameters mechanical parameters can be changed. Moreover, it provides quantitative results like total crack length, number of cracks, maximum crack distance etc. with respect to base material, welding parameters, applied strain and strain rate. Varestraint, trans-varestraint and spot varestraint test are externally loaded test methods for hot cracking suscepitiblity.

In Varestraint Test method, test specimen undergoes autogeneous welding, i.e without filler addition, and during welding bending is applied on a die having certain radius.

(Figure 2.22). In this study Modified Varestraint Test method (MVT) was applied. It provides semi-automatic testing resulting in higher reproducibility[73]. At the beginning of MVT, welding current, welding speed, shielding gas flow rate, strain rate, weld start and end position can be adjusted. Bending position is the point at which specimen contacts with die. Different strains can be applied to the specimen by changing the die radius. Solidification cracks in weld metal and liquation cracks in partially melted zone are observed at the end of the test. These cracks can be evaluated as total crack length (TCL), total number of cracks (T#C) and maximum crack length (MCL). Different base materials, filler alloys, welding conditions and strain and strain rates can be evaluated to see the effects on hot cracking susceptibility.

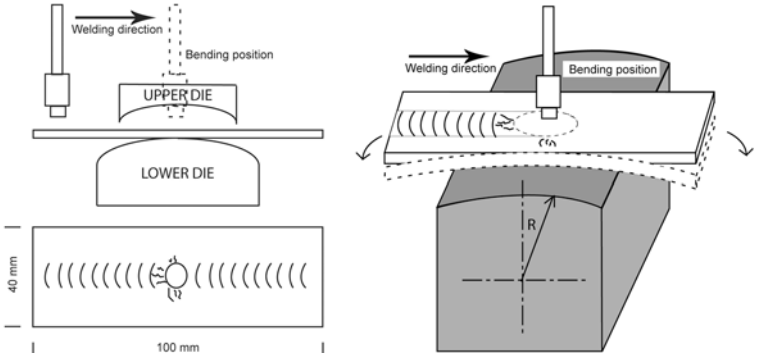

Figure 2.22 Schematic illustration of Varestraint test setup.

For each strain level applied crack length measurement is done under stereo microscope. To evaluate the cracks easily specimen surface is etched and measurement is done under high magnification. And results, that can be TCL, T#C or MCL, are represented with respect to applied strain as given in Figure 2.23.

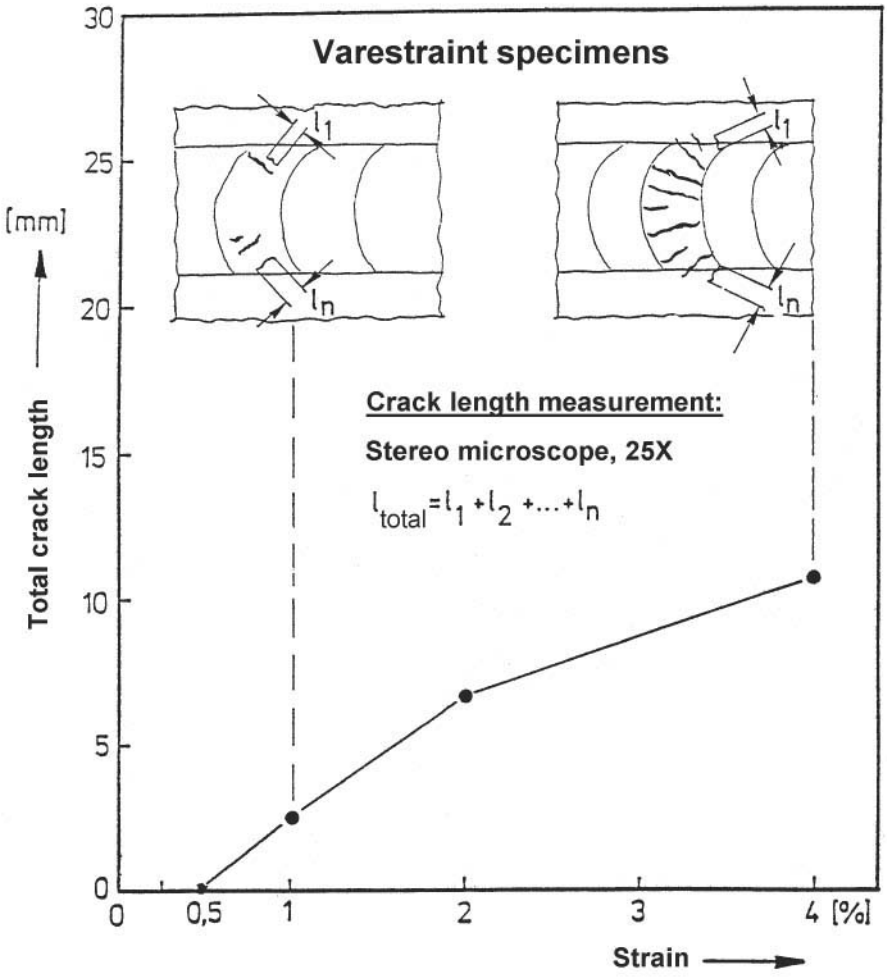

Figure 2.23 Representation of varestraint test results [73].

2.5. Gas Tungsten Arc Welding (GTAW)

There are two welding processes used for welding of aluminum alloys. Gas Shielded Metal Arc Welding (GMAW) and Gas Tungsten Arc Welding (GTAW) are the preferred fusion welding methods with argon shielding. In this study, GTAW method was used for Varestraint tests and production of the weldment.

Welding torch, shielding gas, filler wire and a power source are the parts of GTAW. Schematic representation of welding process is given in Figure 2.24. There is an arc between the tungsten electrode and workpiece as a heat source for melting. Direct current and alternating current can be used with this method. Negative polarity is used

for tungsten electrode during welding. However, for aluminum welding, since the oxide layer (Al_2O_3) on the workpiece has very high melting point compared to aluminum alloy, it must be removed during welding. Otherwise, workpieces melt down without joining since the weld pool is not reachable due to oxide layer. When the electrode is positive, ions moves from the electrode to the workpiece and breaks the oxide layer. Thus, electrode connected to the positive pole is preferred during welding of aluminum alloys. However, positive polarity of the electrode (DCEP) results in melting of the electrode due to overheating. Hence, alternating current is used instead of direct current so that electrode cools when it is negative pole. Also polarity of the electrode affects the penetration during welding. When electrode is negative under direct current (DCEN) high penetration is obtained but oxide surface can not be removed. When DCEP is used oxide removing is possible but penetration is very low and heat on the electrode increases. Thus, alternating current is preferred during welding of aluminum since provides oxide cleaning and intermediate penetration (Figure 2.25).

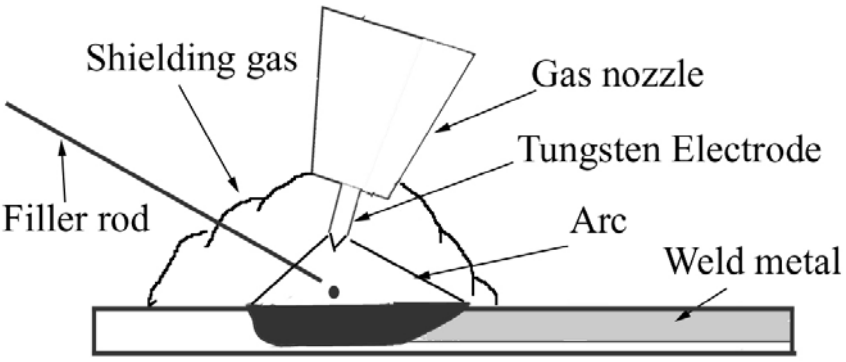

Figure 2.24 Welding area of the GTAW method

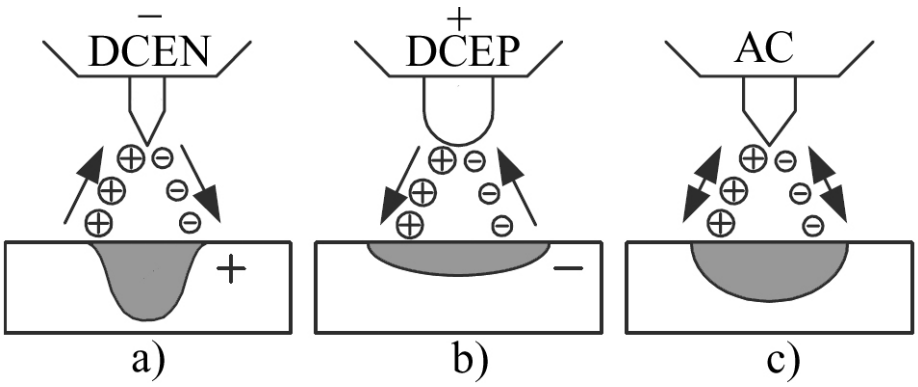

Figure 2.25 Effect of polarity on weld penetration a) good penetration without oxide removing, b) low penetration with oxide removing and c) intermediate penetration with oxide removing

In GTAW method inert gas is preferred for shielding of the weld pool, filler rod and tungsten electrode from atmosphere. Argon is the widely used shielding gas in GTAW process. Also, helium or mixture of argon-helium can be used with GTAW method. Since the ionization energy of argon gas is lower than the helium, initiation of the arc during welding is easier. Besides low cost, more effective shielding can be obtained with argon due to higher density Thus, these properties make the argon gas shielding more preferable.

Besides pure tungsten electrode modified tungsten electrodes exist for GTAW method. Addition of some oxides like thorium oxide, cerium oxide, lanthanum oxide, cesium oxide and zirconium oxide provides more stable arc, better arc starting and increases the electrode life. In welding of aluminum alloys with alternating current pure tungsten electrode is preferred. For high current values zirconium oxide added tungsten electrodes can be used due to extended electrode life and workability at high current values.

CHAPTER 3

EXPERIMENTAL PROCEDURE

3.1. Materials Used

Twin roll cast (TRC) Al-Mg alloys with two different compositions were evaluated for hot cracking susceptibility. The Al-Mg alloys subject to this study were received as sheets with a thickness of 3mm. The alloy compositions are given in Table 3.1. Hot cracking susceptibility of these two twin roll cast (TRC) alloys was evaluated using the Varestraint Test method.

Hot cracking susceptibilities of these two alloys depending on line energy and strain were evaluated by using Varestraint Test method. Also, the effects of different types of fillers on hot cracking susceptibility of the alloys were examined. Two different filler wires were used to obtain weld metals with different compositions. Chemical composition of these filler alloys are given below (Table 3.2).

Table 3.1 Chemical composition of 5049 and 5754 alloys.

Material	Si	Fe	Cu	Mn	Mg	Cr	Zn	Ti
5049	0.092	0.56	0.03	0.858	1.68	0.0075	<0.005	0.314
5754	0.167	0.182	0.0053	<0.001	3.21	0.0016	<0.005	0.0275

Table 3.2 Chemical composition of filler wires.

Filler	Si	Fe	Cu	Mn	Mg	Cr	Zn	Ti
5183	0.0378	0.191	0.0055	0.554	4.30	0.0923	<0.0068	0.101
5356	0.0525	0.178	0.0057	0.0953	4.66	0.1230	<0.0050	0.105

3.2. Specimen Preparation for Hot Cracking Susceptibility Test

Two groups of test specimen were prepared for the evaluation of hot cracking susceptibility of 5049(Al-2wt%Mg) and 5754(Al-3wt%Mg). The first group consisted of 5049(Al-2wt%Mg) and 5754(Al-3wt%Mg) base alloys and the second group consisted of alloys welded with two different filler wires. The test setup and procedures used for the evaluation of hot cracking susceptibility are explained in the following section.

Gas Tungsten Arc Welding (GTAW) method was used for the production of welded specimens. In order to obtain a standard weld seam profile, a semi-automatic welding setup was utilized. This setup consists of a welding power source, a welding torch, a torch carrier (Figure 3.1) and a wire feeder (Figure 3.2). “Rehm Schweißtechnik – Invertig 250 GW” TIG welding machine was used for the production of the welded specimens and hot cracking susceptibility tests. The machine was operated on 3 phases 380 V mains supply. The highest possible welding current at the 100 % duty cycle was 220 A at 19 V. Arc was ignited by a high frequency generator without any contact between the tungsten electrode and the aluminum specimen. The torch and the current conductors were cooled with water circulation. Filler addition was made continuously at a constant feeding rate by a wire feeder which was also equipped with a time adjustable pulse feeding option. Welding speed was kept constant by the torch carrier. The parameters used in the production of the welds are given in Table 3.3.

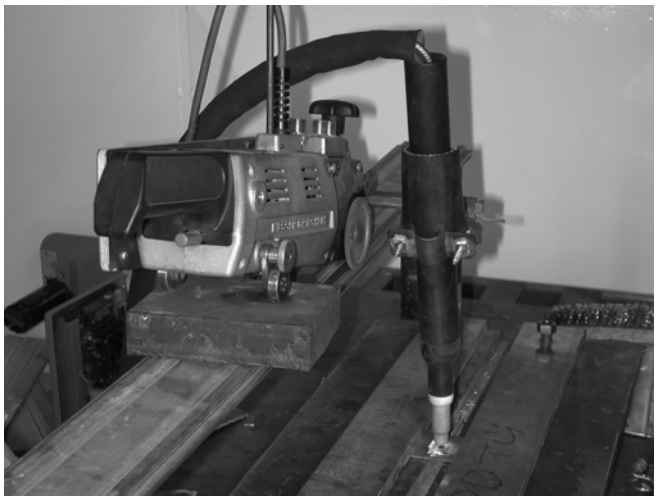

Figure 3.1 Torch carrier used for welding with Gas Tungsten Arc Welding (GTAW) process

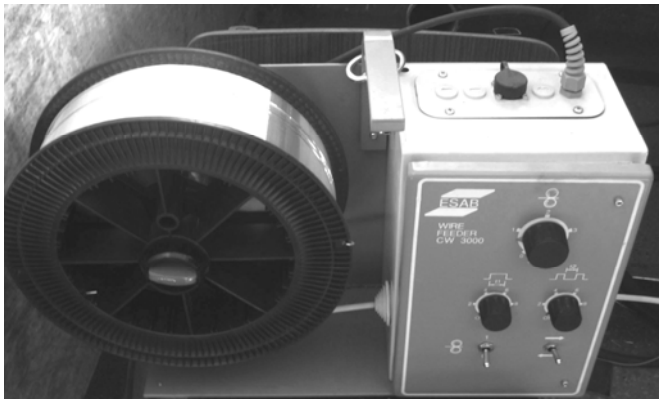

Figure 3.2 Wire feeder used for continuous or pulsed feeding of filler wire during GTAW process

After the completion of the welds, specimens were cut to a size of 40x100x3 mm and weld seams on them were grinded down to the sheet thickness (Figure 3.3). Four weld combinations were used for 5049(Al-2wt%Mg) and 5754(Al-2wt%Mg) alloys with two filler wires 5356 and 5183.

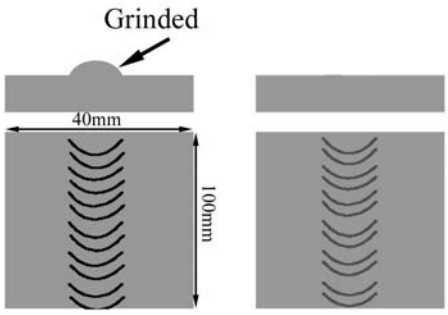

Figure 3.3 Preparation of welded specimens with filler addition for Varestraint Test.

Table 3.3 Welding parameters used for the production of welded specimens

Welding source	**:**	Rehm INVERTIG 250 GV
Current type	**:**	AC (Alternating current)
Electrode type	**:**	Pure tungsten
Electrode diameter	**:**	3.2 mm
Filler wire diameter	**:**	1.6 mm
Filler type	**:**	5754, 5356, 5183
Shielding gas	**:**	Argon
Shielding gas flow rate	**:**	10 lt/min
Welding current	**:**	105 A
Welding speed	**:**	100 mm/min

Specimens were obtained from the 5049(Al-2wt%Mg) and 5754(Al-3wt%Mg) alloy sheets in following dimensions of 100 x 40 x 3 mm (Figure 3.4). To prepare the parts for tests surface oxides and grease were removed from the surface of the specimens using stainless brush and acetone.

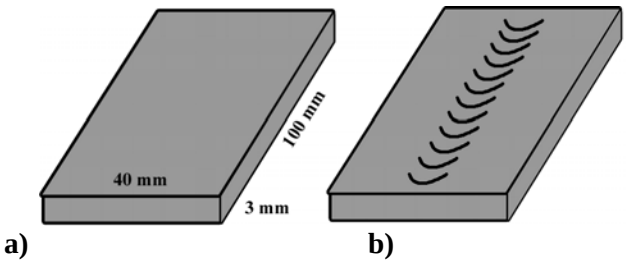

Figure 3.4 Schematic view of the dimensions for a) base alloys and b) welded sheets with filler addition.

3.3. Test Setup and Procedures for Evaluating the Hot Cracking Susceptibility

The hot cracking susceptibility was tested using the Varestraint Test equipment. Varestraint Test is an externally loaded test method. The equipment consists of three main parts (Figure 3.5) which are the electronic control unit, the welding-bending unit and the welding power source connected to the control and bending units.

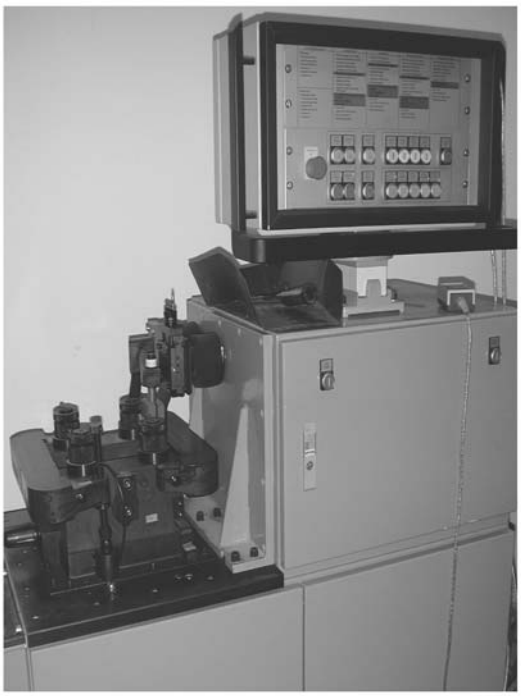

Figure 3.5 Varestraint test equipment

The start and finishing of the welding process, adjustment of welding speed and bending position were controlled on the electronic control unit. All adjustments were made according to the position of the torch. There were three types of tests that could be chosen from the welding-bending unit. These were bending of test specimen without welding, welding of test specimen without bending and bending at the given torch position during welding process.

To start a test, the test piece was placed on the machine and then the equipment was set for the torch positioning. The bending mechanism consisted of two upper and one lower

die. The amount of strain applied on the specimen could be changed through these dies. After placing the specimen between these dies weld seam was formed on the surface of it. At the moment that the welding torch reached the bending position (just at the middle of the specimen), the upper dies were moved towards the lower one simultaneously with the specified bending speed. The welding process during and after bending continued without any interruption. Each of the upper die pressed on the specimen edge.

For welding alternating current was used under technologically pure Argon gas shielding. Bending of the specimens was made during welding operation (Figure 3.6). Also to evaluate the effect of strain level and line energy the die radius and the welding speed were changed. The effective line energy was calculated using the following equation [53]:

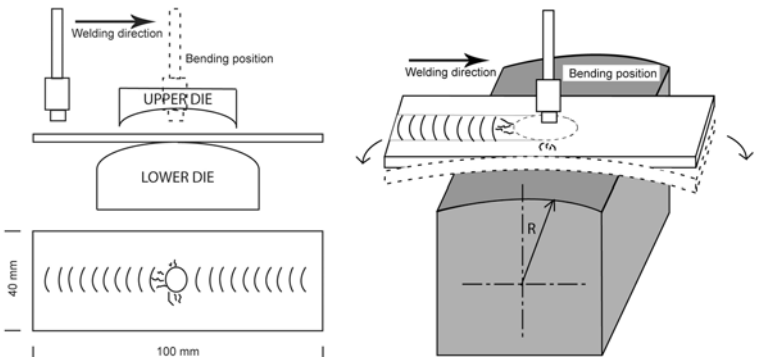

Figure 3.6 Schematic view of the varestraint test method

$$E = \eta \times \frac{U \times I}{v_w} \times 60 \tag{8}$$

E: Line energy; in kJ/cm

η: Efficiency in welding heat input

U: Potential differences across the arc; in V

I: Welding current in the welding circuit; in A

v_w: Relative welding speed; in cm/min

The term "$\eta x\ U\ x\ I$" is called as the effective heat input. The efficiency factor in front of the equation depends on the applied welding process, current type, current level and the shielding gas composition. The main effect of shielding gas composition in heat input efficiency comes from its thermal conductivity. In this investigation TIG-AC welding under argon shielding gas was used and for the applied parameters an efficiency factor of η= 0.84 was taken [54, 55].

Varestraint Test conditions are given in Table 3.4. As can be seen in Table 3.4, the welding current during Varestraint Test was lower than the current used during welding with filler addition (Table 3.3). For tests on base alloys welding speed and strain level were altered as given in Table 3.5. To evaluate of the hot cracking susceptibilities of the weld beads different welding speeds were used on a given die radius as given in Table 3.6.

Table 3.4 Varestraint test conditions and welding parameters used for cracking susceptibility

Test conditions	
Strain	0.5, 1, 2 and 4%
Bending point	Middle of the specimen
Bending speed	200 mm/min
Welding conditions	
Welding process	GTAW (autogenously)
Power source	Rehm INVERTIG 250 GV
Current type	AC (alternating current)
Electrode type	Pure tungsten electrode
Electrode diameter	2.4 mm
Shielding gas type	Argon 99.9%
Shielding gas flow rate	10 lt/min
Welding current	65 A (AC)
Line energy	0.285-0.497 kJ/cm
Weld seam length	80 mm

Table 3.5 Parameters applied during the tests of base alloys with 1.0 Volts and 65 amperes

Welding speed mm/min	Line energy J/cm	Applied strain %
75	436,8	0.5,1.0,2.0,4.0
80	409,5	0.5,1.0,2.0,4.0
85	385,4	0.5,1.0,2.0,4.0
90	364	0.5,1.0,2.0,4.0
95	344,85	0.5,1.0,2.0,4.0
100	327,6	0.5,1.0,2.0,4.0
105	312	0.5,1.0,2.0,4.0
110	297,8	0.5,1.0,2.0,4.0
115	284,85	0.5,1.0,2.0,4.0
120	273	0.5,1.0,2.0,4.0
125	262,1	0.5,1.0,2.0,4.0
130	252	0.5,1.0,2.0,4.0

Table 3.6 Parameters applied during MVT tests of the welded specimens with 1.0 Volts and 65 amperes

Welding speed mm/min	Line energy J/cm	Applied strain %
100	327,6	1
105	312	1
110	297,8	1
115	284,85	1
120	273	1
125	262,1	1
130	252	1

Varestraint Testing of base alloys and welded specimens were done under same welding current. For the welded specimens one strain level was applied to see the hot cracking susceptibilities of the weld beads obtained with different filler additions.

3.4. Crack length measurements

To monitor the cracks formed during strain application specimens were etched to reveal the crack length easily. To remove oxide layer formed during welding Modified Adler

reagent was used and following cleaning was made with 50%HNO_3 – 50% distilled water. Modified Adler reagent is composed of 100 ml Adler base solution and 1 gr potassium metabisulphite [$K_2S_2O_5$] with 70 ml distilled water. Adler base reagent is a solution of 25 ml distilled water, 50ml HCl, 15 gr ferric chloride [$FeCl_3.6H_2O$] and 3gr ammonium chlorocuprate (II) [$(NH_4)2[CuCl_4]$ $.2H_2O$].

Crack length measurement was performed under Nikon SMZ-2T stereomicroscope with 25X magnification. Before starting measurements the scale on the microscope was calibrated with a micrometer. Initially cracks were classified as solidification and liquation cracks and then their lengths were measured. An example for the crack length measurement was given in Figure 3.7. Hot cracking susceptibilities were assessed with respect to total crack length (TCL), total number of cracks (T#C) and maximum crack length (MCL).

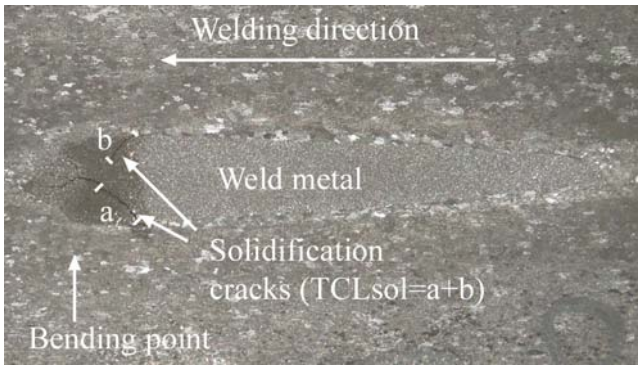

Figure 3.7 An example for the crack length measurement on the specimen. Cracks formed in the weld metal are solidification cracks.

3.5. Quench tests

Quench tests on as received twin roll cast (TRC) Al-Mg alloys were performed. The samples were heated to a temperature range between the solidus and liquidus, and then they were quenched in cold water. Same quenched tests were also repeated in order to find if liquation below the solidus temperature would occur. Thus same specimens were heated up to different temperatures below the solidus temperatures of alloys. Then they

were air cooled. Then quenched specimens were prepared for metallographic examination to find if any second phase liquation has formed.

3.6. Metallographic examination

Specimens were examined both in polished and etched conditions. Chemical and electrolytic etchings were applied. Electrolytic etching with Barker's reagent was used to reveal the grain structure of the base and weld metals. Chemical etching with Weck reagent was applied to reveal any hot cracks and also the weld microstructure. Micrographs were taken by using Nikon "optiphot" and "optiphot 100" metallographic microscopes. Secondary dendrite arm spacing in the weld zones were measured using an image analyzer to correlate the differences in hot cracking susceptibilities of the base alloys.

Solidification and liquation crack surfaces were examined under the scanning electron microscope. Scanning electron microscope examinations were carried out using a Jeol 6400 equipped with "NORAN System 6 X-Ray Microanalysis System". Also phases with low melting point that may increase the solidification range were investigated in the centerline segregation. The types of intermetallic particles in the centerline segregation of both twin roll cast alloys were examined under the optical microscope and microchemical information was obtained using an energy dispersive spectrometer (EDS) attached to the SEM.

3.7. Thermal analysis

It is known that the solidification range of aluminum alloys affects the hot cracking tendency. Therefore, to determine the solidification range of both the alloys differential thermal analysis (DTA) was made using the "Setaram Labsys DTA". Samples were heated above the liquidus temperature up to 750^{o}C at a constant rate of 10^{o}C/min. Endothermic and exothermic peaks were recorded as a function of the temperature.

CHAPTER 4

RESULTS

The aim of this study is to investigate the hot cracking susceptibility of twin roll cast (TRC) aluminum-magnesium alloys with varestraint test method. The scope of this investigation consists of (i) evaluation of hot cracking susceptibility of two twin roll cast aluminum-magnesium alloys with different magnesium contents, (ii) effect of filler alloys on solidification cracking susceptibility of these alloys and (iii) effect of mid-plane segregation on hot cracking susceptibility.

4.1 Hot cracking susceptibility of 5049(Al-2wt%Mg) and 5754(Al-3wt%Mg) alloys

In this section, the Varestraint Test results of hot cracking susceptibility of twin roll cast 5754(Al-3wt%Mg) and 5049(Al-2wt%Mg) alloys are given. Hot cracking behavior of these alloys was investigated by measuring the solidification and liquation cracks as a function of different strain levels and line energies.

4.2 Hot cracking susceptibility with filler added weld beads

As the next step the bead-on-plate welds on the same alloys were produced with different filler wires resulting in different weld metal composition at weld beads. These weld beads were examined after the varestraint test to see the effect of filler additions on the hot cracking susceptibility of the selected alloys.

4.3 Microstructural investigation

Third part contains effects of line energy on weld microstructure with respect to penetration depth and secondary dendrite arm spacing, solidification and liquation cracks and mid-plane segregations.

4.4 Differential thermal analysis

Thermal analysis results of both 5049(Al-2wt%Mg) and 5754(Al-3wt%Mg) alloys were given in this section.

4.5 Scanning electron microscope

Scanning electron microscope study on solidification and liquation crack surfaces were given with EDS results.

4.1. Hot cracking susceptibility of 5049(Al-2wt%Mg) and 5754(Al-3wt%Mg) alloys

Hot cracking susceptibilities of 5049(Al-2wt%Mg) and 5754(Al-3wt%Mg) alloys were examined with Varestraint Test Method. Four different strain levels were applied during the hot cracking test. The effect of heat input on hot cracking susceptibility was investigated by altering the welding speed. To compare the hot cracking susceptibility, alloys were assessed by all cracks formed after Varestraint Test. Cracks were classified as solidification cracks and liquation cracks and measured under x25 magnification. In the following sections crack length measurements are grouped in three sets. The first one gives the total crack length (TCL) consisting sum of the each solidification crack length (TCLsol), and sum of the each liquation crack length (TCLliq). In the second group the total number of cracks for both solidification and liquation cracks (T#Csol and T#Cliq) are given. In the last group the maximum crack length for solidification (MCLsol) are listed.

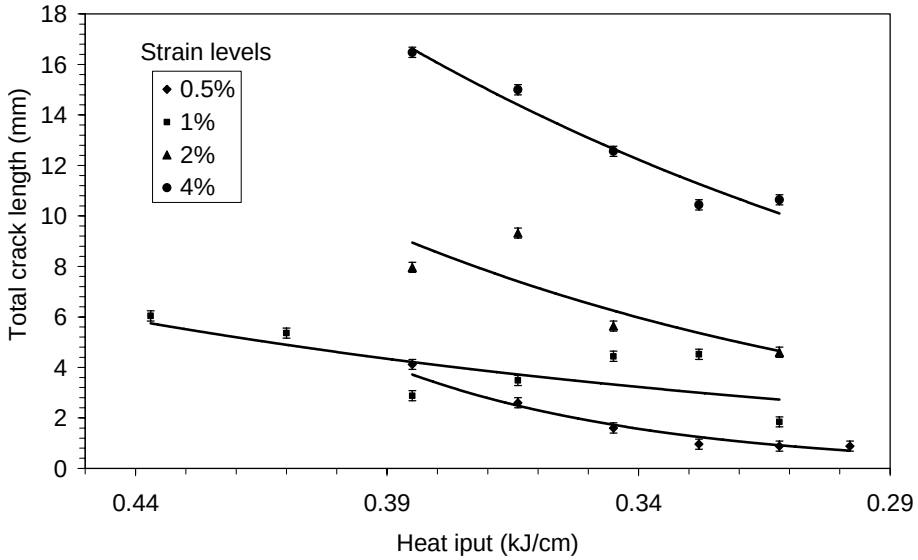

Figure 4.1 Change in total crack length values depending on alternating line energy for different strain levels applied during Varestraint Testing of alloy 5754.

5049(Al-2wt%Mg) alloy has shown almost no liquation cracking. Therefore, total number of cracks and total crack length measurements which are calculated by the addition of solidification and liquation cracks are given only for 5754(Al-3wt%Mg) alloy. Figure 4.1 shows the changes in the *total crack length* values with line energy and strain variations on 5754(Al-3wt%Mg) alloy. As can be seen from the Figure 4.1, increasing strain level resulted in an increase in total crack length. Simultaneously total crack length increased with increasing heat input. At low strain levels of 0.5 to 1%, changes in total crack lengths were minor. Major changes in total crack length occurred in higher strain levels of 2 to 4%. The change in total number of cracks depending on the strain level and heat input is given in Figure 4.2. The total numbers of cracks increased with increasing strain value. With decreasing line energy, i.e. heat input (kJ/cm), total number of cracks decreased for all strain levels.

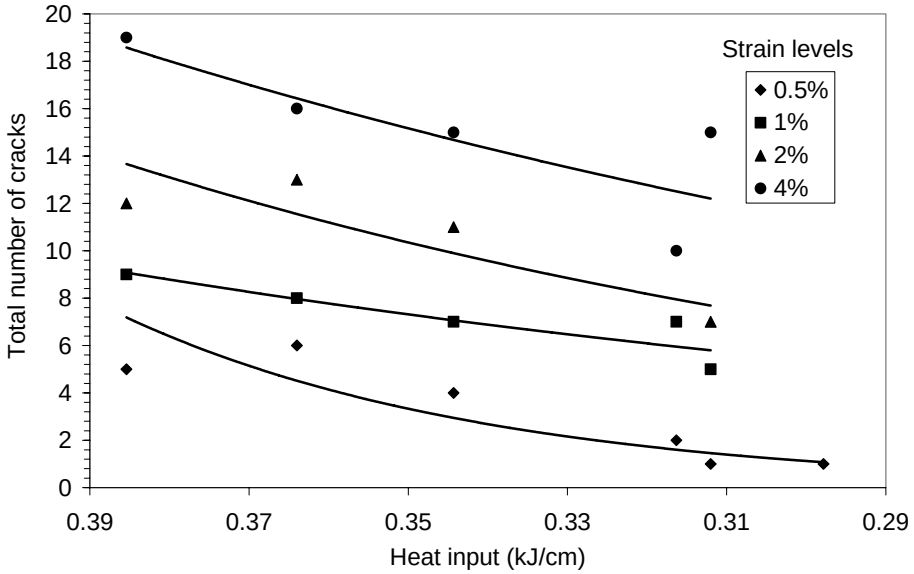

Figure 4.2 Change in total number of cracks depending on alternating line energy for different strain levels applied during Varestraint Testing of 5754(Al-3wt%Mg) alloy.

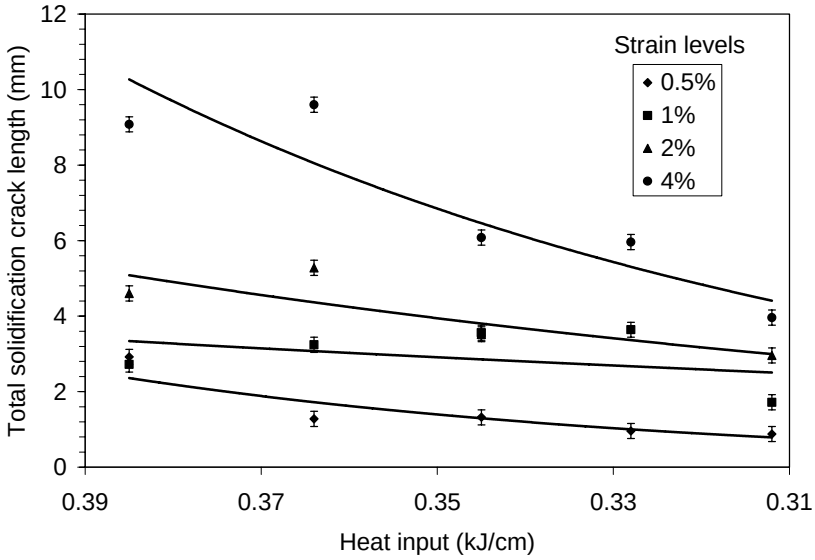

a)

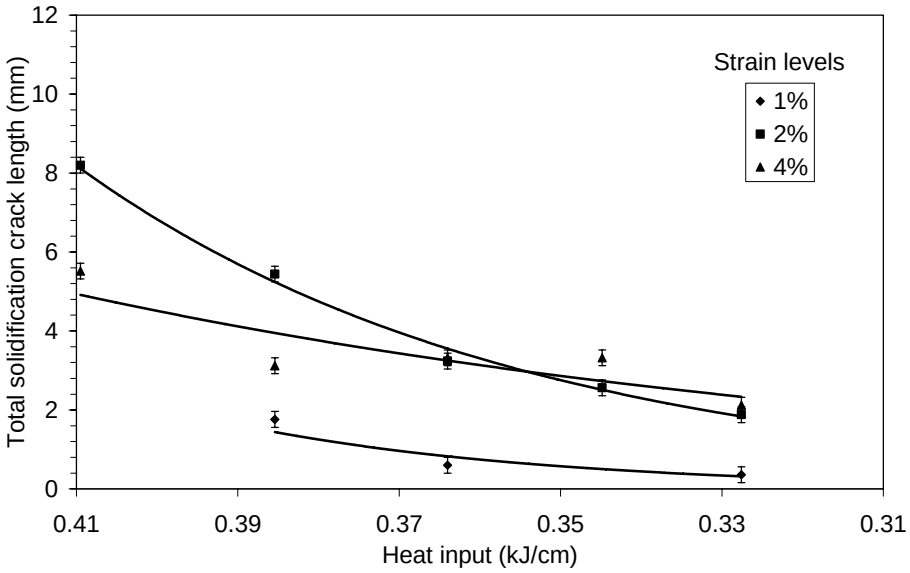

b)

Figure 4.3 Change in total solidification crack length depending on alternating line energy for different strain levels applied during Varestraint Testing of a) 5754(Al-3wt%Mg) alloy and b) 5049(Al-2wt%Mg) alloy.

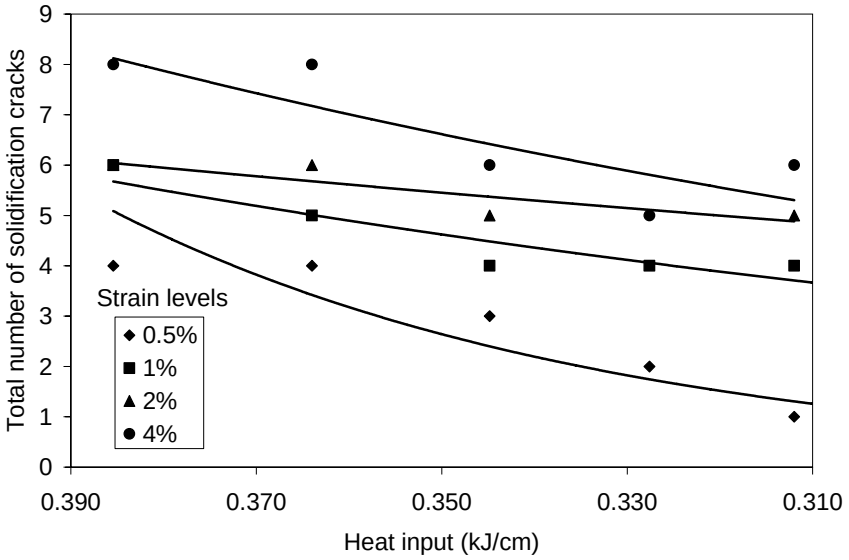

a)

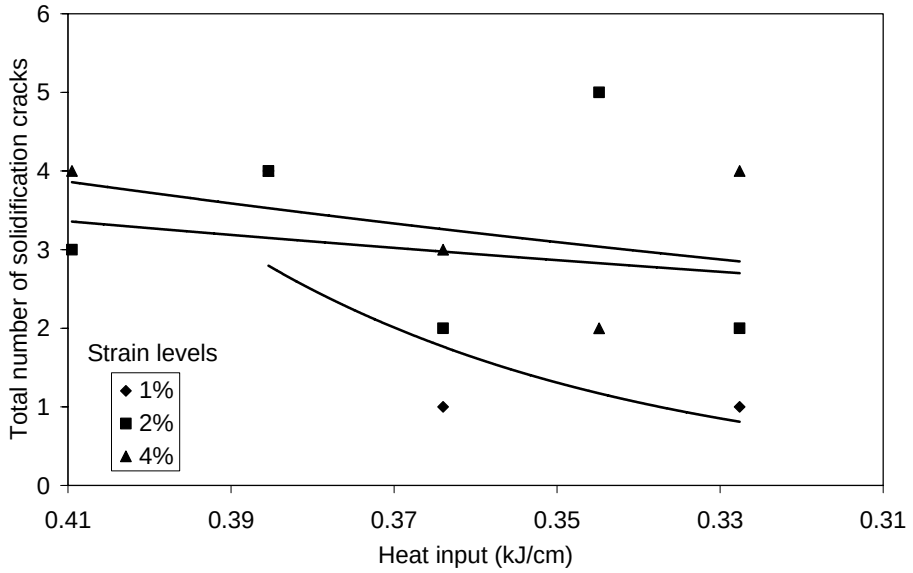

b)

Figure 4.4 Change in total number of solidification cracks depending on alternating line energy for different strain levels applied during Varestraint Testing of a) 5754(Al-3wt%Mg) alloy and b) 5049(Al-2wt%Mg) alloy.

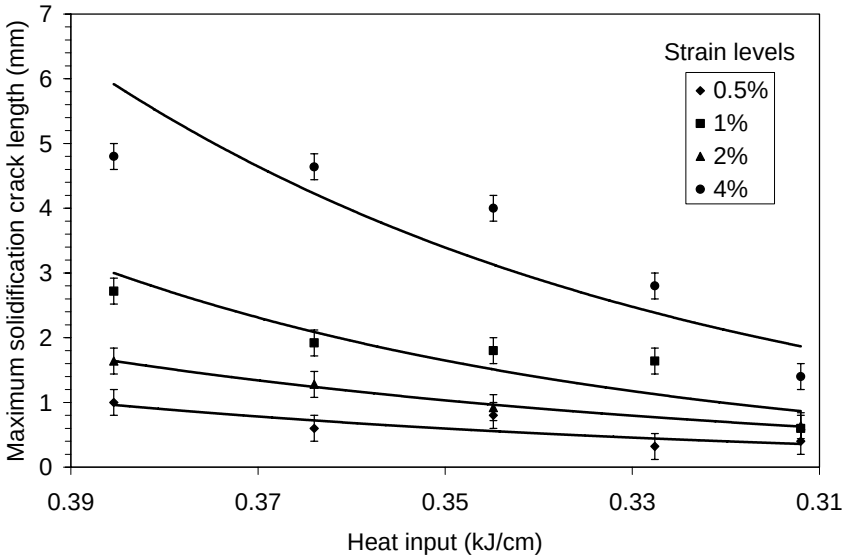

a)

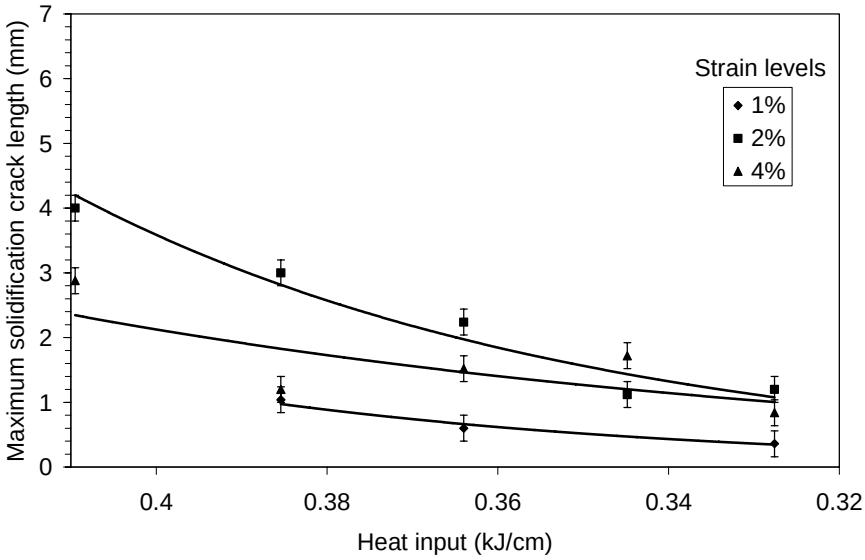

b)

Figure 4.5 Change in maximum solidification crack length (MCLsol) depending on alternating line energy for different strain levels applied during Varestraint Testing of a) 5754(Al-3wt%Mg) alloy and b) 5049(Al-2wt%Mg) alloy.

The change in total solidification crack length of 5049 and 5754 alloys are given in Figure 4.3. Total solidification crack length has increased with increasing line energy for

both alloys. In addition to that, increasing strain level has resulted in higher total solidification crack length. As given in Figure 4.4 number of solidification cracks for both alloys has increased with increasing strain level. Moreover, increasing welding speed (i.e. decreasing line energy) has resulted in a decline in the number of cracks. Maximum solidification crack length of 5754(Al-3wt%Mg) alloy for each strain level and line energy was higher when compared with 5049(Al-2wt%Mg) alloy (Figure 4.5). When the change in maximum solidification crack lengths of 5754(Al-3wt%Mg) and 5049(Al-2wt%Mg) alloys are compared, a similar behavior is observed. Maximum crack length in weld metals has increased with increasing line energy for both alloys.

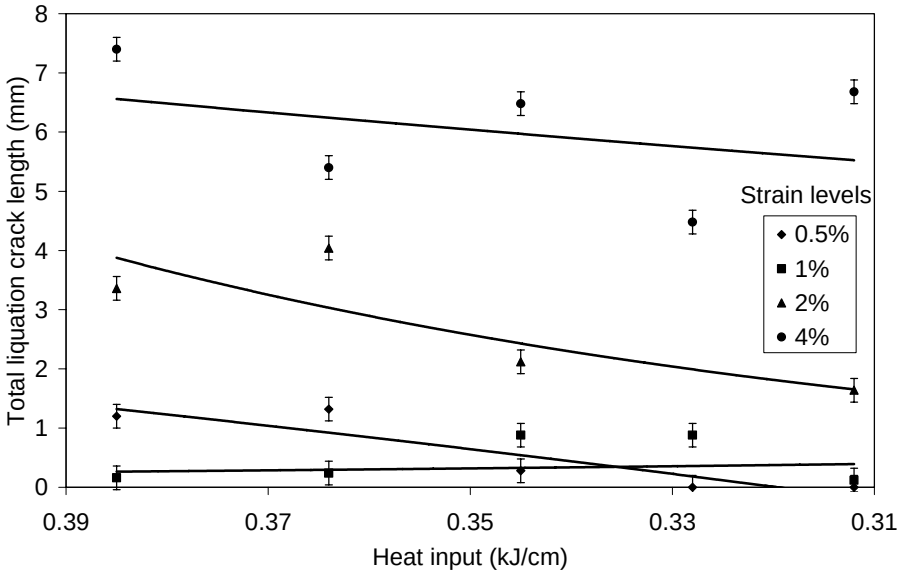

Figure 4.6 Change in total liquation crack length of 5754(Al-3wt%Mg) alloy depending on alternating line energy for strain levels applied during Varestraint Testing.

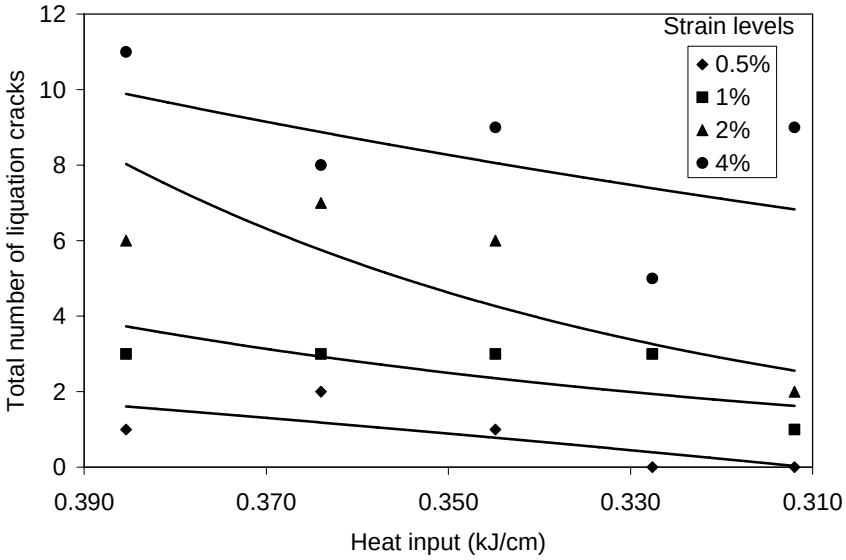

Figure 4.7 Change in total number of liquation cracks of 5754(Al-3wt%Mg) alloy depending on alternating line energy for strain levels applied during Varestraint Testing.

As it was stated above, 5049(Al-2wt%Mg) alloy has shown almost no liquation cracking. Therefore evaluation of liquation cracks was only made for 5754(Al-3wt%Mg) alloy. As it can be seen in Figure 4.6, *total liquation crack length* (TCLliq) reached its maximum value at 4% strain and dropped with the reduction of strain level. Also for all strain levels, reducing line energy has decreased *total liquation crack length. Total number of liquation crack measurements* (T#Cliq) (Figure 4.7) have shown similar results. Total number of liquation cracks has increased with increasing strain level and line energy.

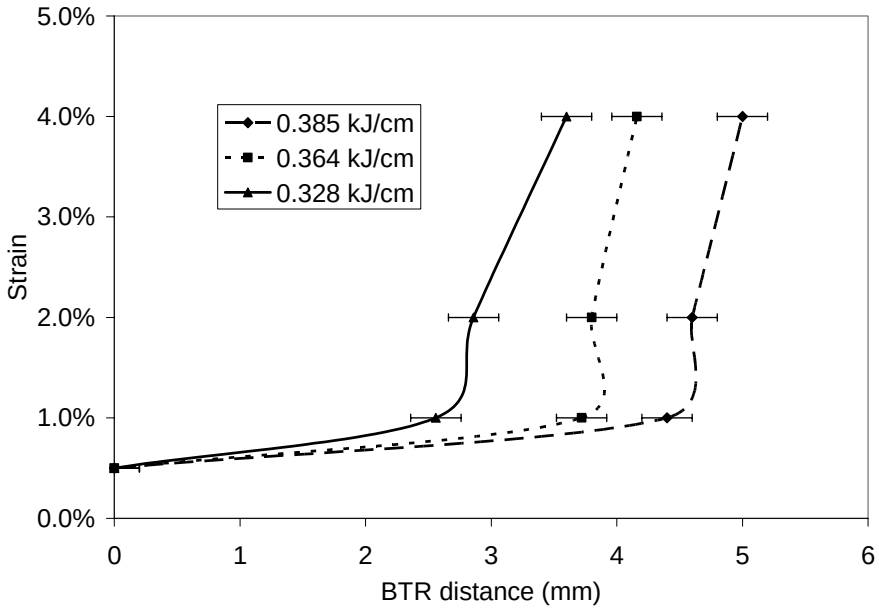

Figure 4.8 Brittle temperature range distance depending on the strain levels applied and line energy of 5049(Al-2wt%Mg) alloy.

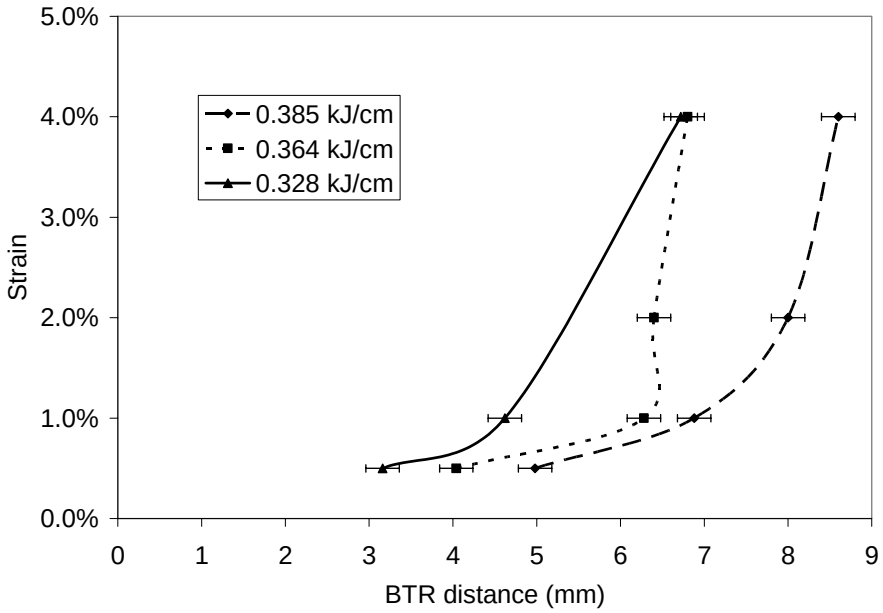

Figure 4.9 Brittle temperature range distance depending on the strain levels applied and line energy of 5754(Al-3wt%Mg) alloy.

As mentioned in section 2.3, hot cracking susceptibility of aluminum alloys can be expressed in turn to its brittle temperature range. Crack tip distance measurements are given in Figure 4.8 and Figure 4.9. Increasing line energy has increased crack tip distance for both 5049(Al-2wt%Mg) and 5754(Al-3wt%Mg) alloys. Moreover, crack tip distance has increased for each strain level. If the two alloys are compared, 5049(Al-2wt%Mg) alloy has narrow range, i.e. its crack tip distances are smaller compared to 5754(Al-3wt%Mg) alloy.

Summary

In this section, the outputs of Varestraint Test outputs were given in terms of total crack length (TCL), total number of crack (T#C), maximum crack length (MCL) and maximum crack tip distance (MCD) were given. In literature, depending on the test methods some of these outputs have been used for defining the hot cracking susceptibility of an alloy. In the present study, each varestraint test output used for the evaluation of hot cracking susceptibility of two twin roll cast (TRC) Al-Mg alloys gave similar results. It was found that hot cracking tendency could be determined with each TCL, T#C, MCL and MCD outputs. Varestraint Test method has provided valuable data for assessing the hot cracking susceptibility of alloys as a function of different strain levels applied and welding parameters.

4.2. Hot cracking susceptibility with filler added weld beads

Weld beads were obtained with different filler additions (5183 and 5356) by Gas Tungsten Arc Welding (GTAW) process. Filler addition has resulted in a change in the weld bead composition of 5049(Al-2wt%Mg) and 5754(Al-3wt%Mg) alloys. Varestraint test was used to find the effect of filler addition on hot cracking susceptibility. The changes in the crack lengths are determined for different *base alloy/filler alloy* combinations. Crack length measurement results for different *base alloy/filler alloy* combinations are given in Figure 4.10 and Figure 4.11.

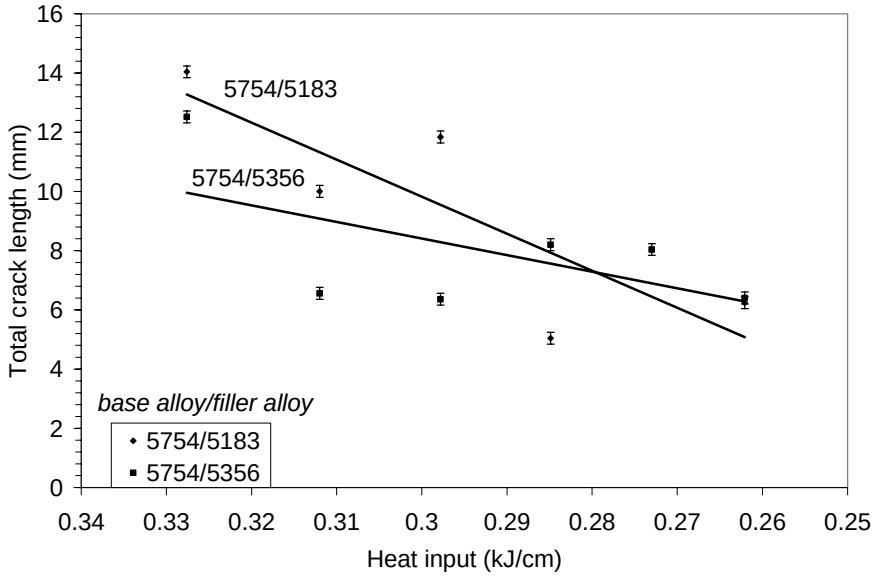

a)

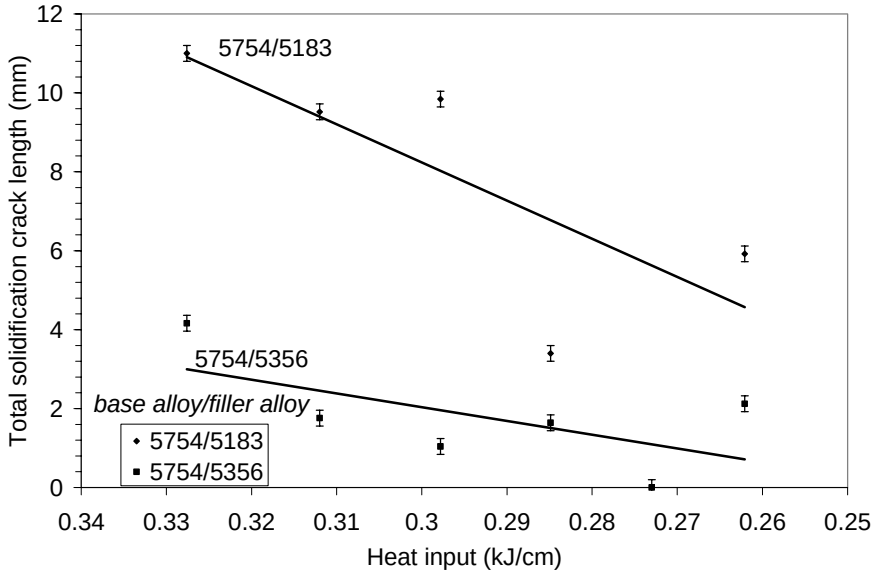

b)

Figure 4.10 Hot cracking susceptibilities of the weld metals obtained with different filler additions to the 5754(Al-3wt%Mg) alloy. a) Total crack length, b) Total solidification crack length and c) Total liquation crack length. Fillers: 5183 and 5356.

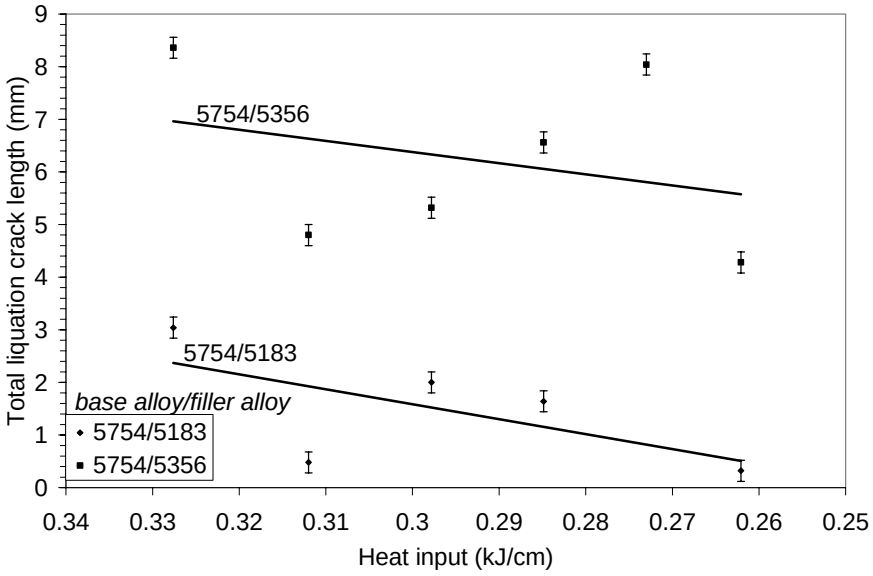

c)

Figure 4.10 Hot cracking susceptibilities of the weld metals obtained with different filler additions to the 5754(Al-3wt%Mg) alloy. a) Total crack length, b) Total solidification crack length and c) Total liquation crack length. Fillers: 5183 and 5356 *(continued)*.

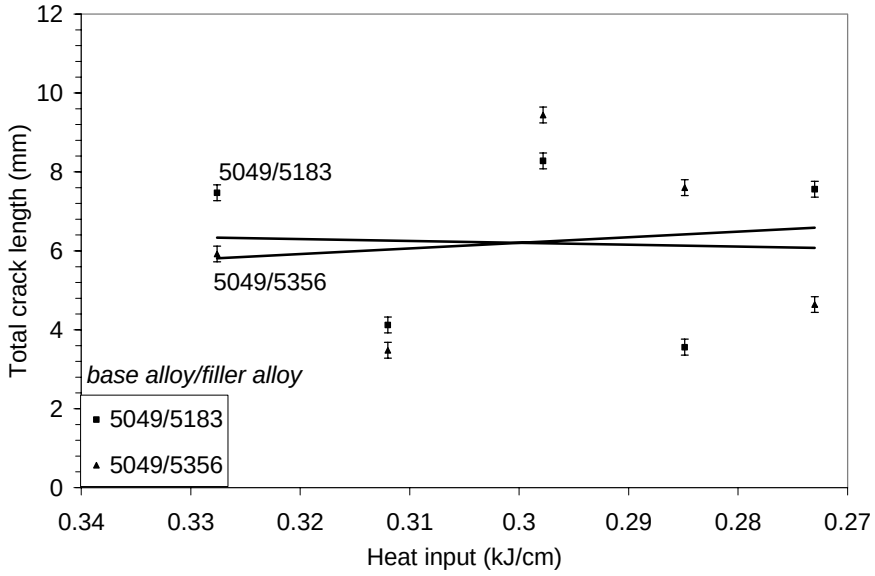

a)

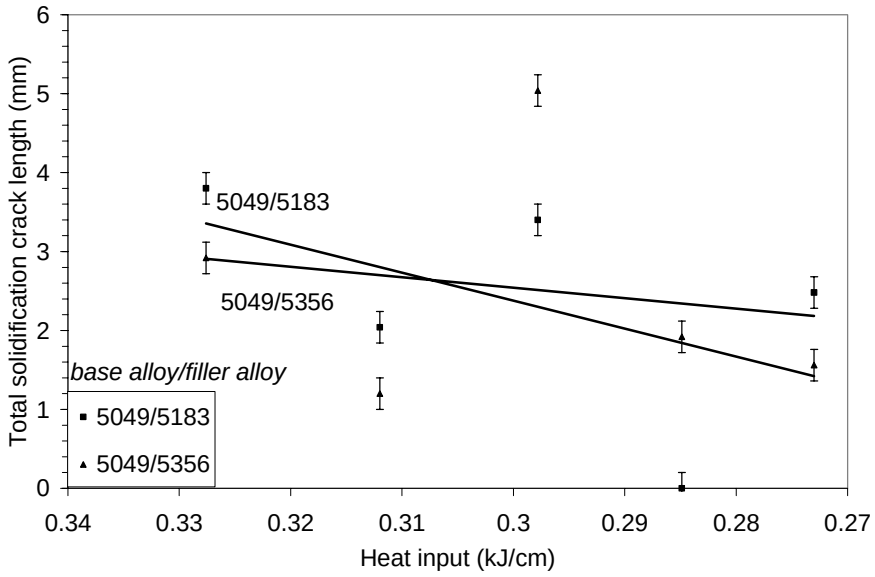

b)

Figure 4.11 Hot cracking susceptibilities of the weld metals obtained with different filler additions to the 5049(Al-2wt%Mg) alloy. a) Total crack length, b) Total solidification crack length and c) Total liquation crack length. Fillers: 5183 and 5356.

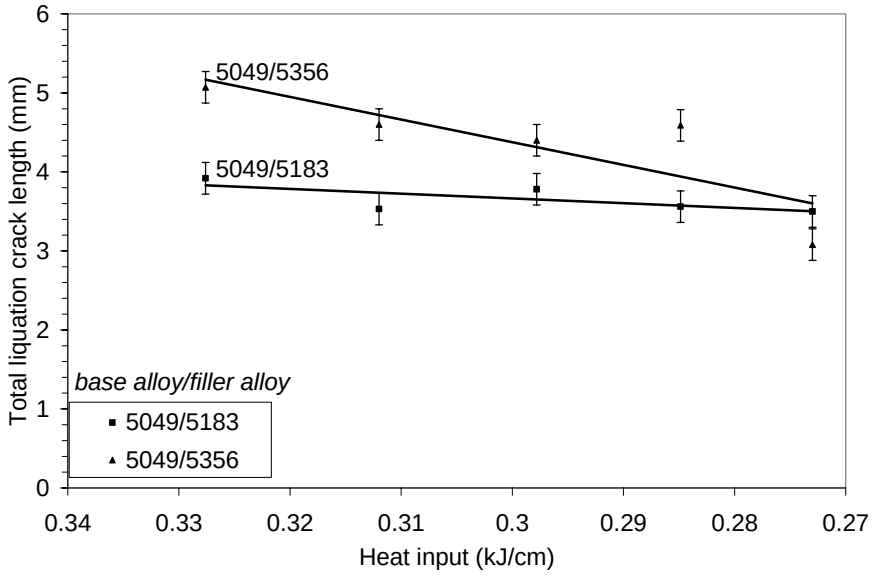

c)

Figure 4.11 Hot cracking susceptibilities of the weld metals obtained with different filler additions to the 5049(Al-2wt%Mg) alloy. a) Total crack length, b) Total solidification crack length and c) Total liquation crack length. Fillers: 5183 and 5356 *(continued)*.

The weld seam on 5754(Al-3wt%Mg) alloy produced with the addition of 5183 filler alloy has shown higher solidification cracking susceptibility compared to the weld seam produced with 5356 filler alloy (Figure 4.10b). For both of the filler wires, a decrease in the heat input also decreased the total lengths of solidification cracks. When the liquation cracks are compared, it was seen that the cracking susceptibility of the weld seam produced with 5356 filler alloy is higher with respect to the ones produced with 5183 filler alloy. The liquation crack lengths have decreased with decreasing heat input just like the solidification cracks for both 5183 and 5356 filler alloys.

No significant difference could be observed in the total solidification crack lengths on bead-on-plate welds of 5049(Al-2wt%Mg) alloy when produced with 5183 and 5356 filler alloys. Further, the total solidification crack lengths decreased with with decreasing line energy for both 5183 and 5356 filler alloys. When the liquation crack

length data are compared, maximum total crack length was measured for the weld metal of 5356 filler alloy compared to 5183 filler alloy.

It has been stated in section 3.2 and 3.3 that the bead-on-plate welds produced by addition of filler alloys are wider than the width of the melted zone during the Varestraint test. Therefore, liquation cracks formed at the filler added weld metal not on the base alloy sheet. The evaluation of the liquation cracks here should be considered as different from the ones formed in the base metals.

Summary

Total solidification crack length results for 5049(Al-2wt%Mg) and 5754(Al-3wt%Mg) alloys have been given in section 4.1. Total solidification crack length results for *base alloy/filler alloy* combinations were given in this section. Magnesium content is important for hot cracking susceptibility since it determines the solidification range of aluminum-magnesium alloy. Therefore, these results can be combined to compare the effect of magnesium content on solidification cracking of aluminum-magnesium alloy.

4.3. Microstructural investigation

Metallographic studies were given as follows:

1. Effect of line energy on weld profile (weld width and penetration)
2. Effect of line energy on solidification microstructure (secondary dendrite arm spacing measurements
3. Solidification and liquation cracks on Varestraint test specimens
4. Microstructure of mid-plane segregation

4.3.1. Microstructure of the base alloys and of welds

In the previous section Varestraint Test was used for the determination of hot cracking susceptibility of 5049(Al-2wt%Mg) and 5754(Al-3wt%Mg) at different strain and line energy levels. The variation of hot cracking susceptibility of weld metals obtained using

different filler alloys was also evaluated. The effect of heat input on weld width, penetration and microstructure are examined in this section.

To evaluate the effect of heat on the weld zone, welding was made at different welding speeds in order to vary the heat input, i.e. line energy, during welding. Tests were made at heat inputs between 0.413 and 0.273kJ/cm during welding. Weld width and penetration measurements for different line energies were given below for both 5049 and 5754 alloys.

Both alloys have shown that increasing line energy resulted in wider weld seams (Figure 4.12). When the two alloys are compared, it was found that the 5049(Al-2wt%Mg) alloy has narrower weld widths than 5754 alloy for all heat input values applied. As can be seen in Figure 4.13, penetrations decreased with decreasing heat input. Full penetration depth was reached at line energy of 0.36kJ/cm for 5754(Al-3wt%Mg) alloy but even at line energy of 0.41kJ/cm maximum penetration reached for 5049(Al-2wt%Mg) alloy was only about 1.5mm even.

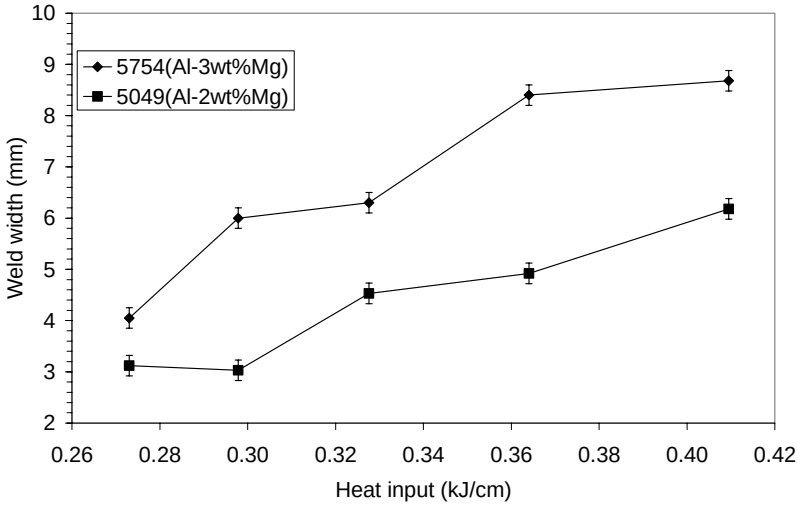

Figure 4.12 Change in the width of weld seam for different heat inputs.

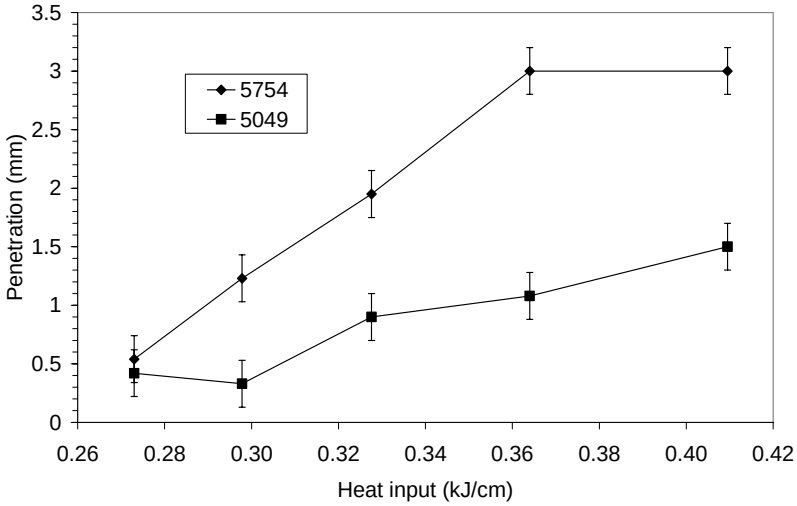

Figure 4.13 Change in penetration depth measurements of the weld seam for different heat inputs.

Microstructures of the base alloys and fusion line between the weld metal and heat affected zone (HAZ) are given in Figure 4.14 and Figure 4.15 respectively. When the microstructures of two base alloys are compared it can be stated that 5049(Al-2wt%Mg) alloy has smaller grain size than the 5754(Al-3wt%Mg) alloy (Figure 4.14).

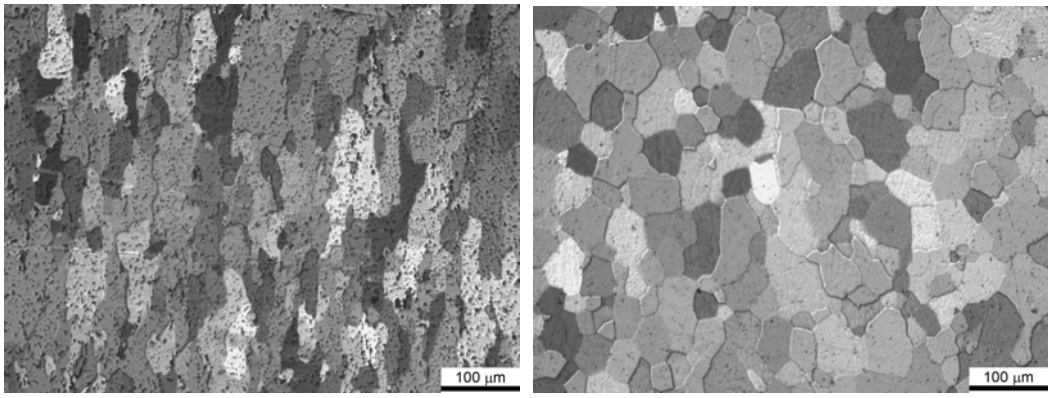

a) b)

Figure 4.14 Optical microstructures taken from the base metals a) 5049(Al-2wt%Mg) alloy and b) 5754(Al-3wt%Mg) alloy. Electrolytic etching with Barker's reagent was applied

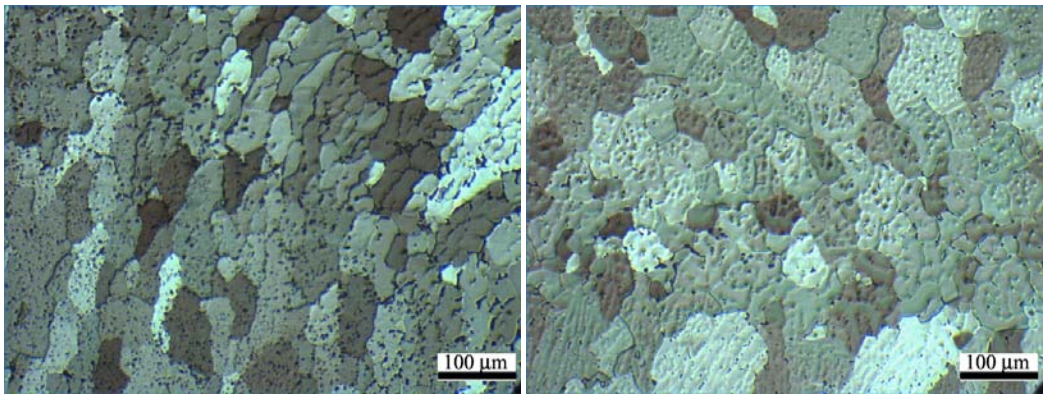

a) b)

Figure 4.15 Optical microstructures taken from the fusion line a) 5049(Al-2wt%Mg) alloy and b) 5754(Al-3wt%Mg) alloy. Electrolytic etching with Barker's reagent was applied.

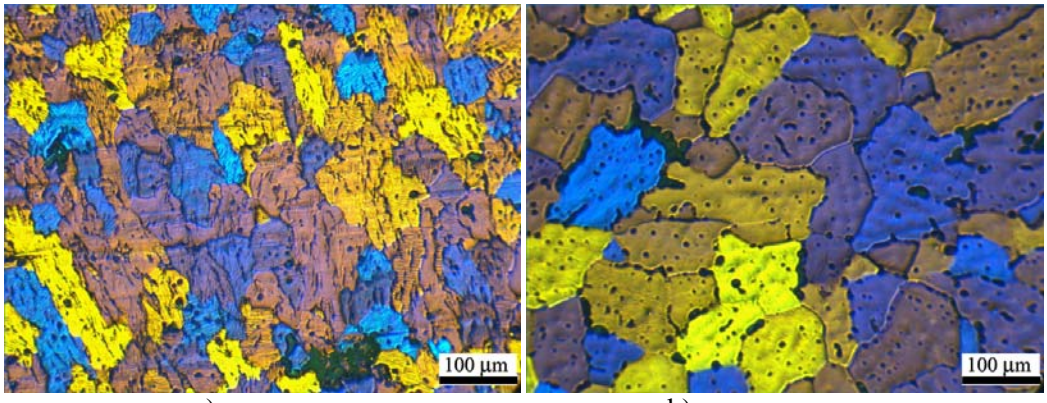

a) b)

Figure 4.16 Optical microstructures taken from the weld zone a) 5049(Al-2wt%Mg) alloy and b) 5754(Al-3wt%Mg) alloy obtained with 0.41kJ/cm heat input. Welding speed: 80mm/min

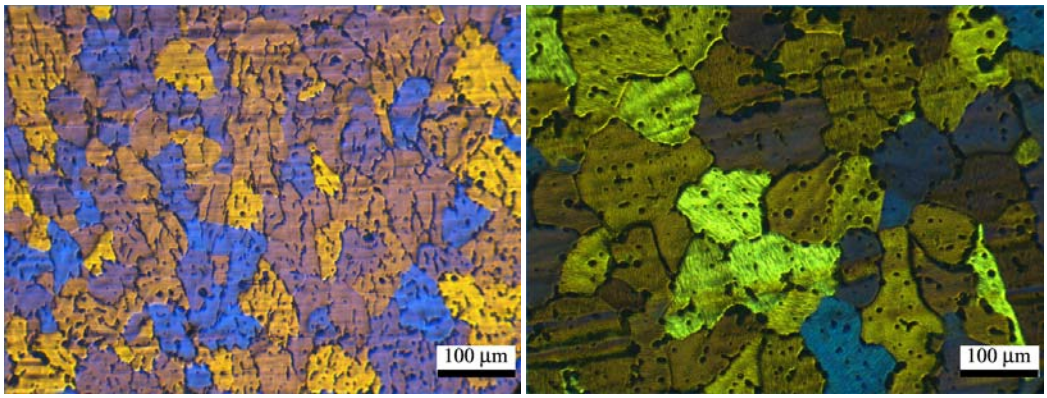

a) b)

Figure 4.17 Optical microstructures taken from the weld zone a) 5049(Al-2wt%Mg) alloy and b) 5754(Al-3wt%Mg) alloy obtained with 0.36kJ/cm heat input. Welding speed: 90mm/min

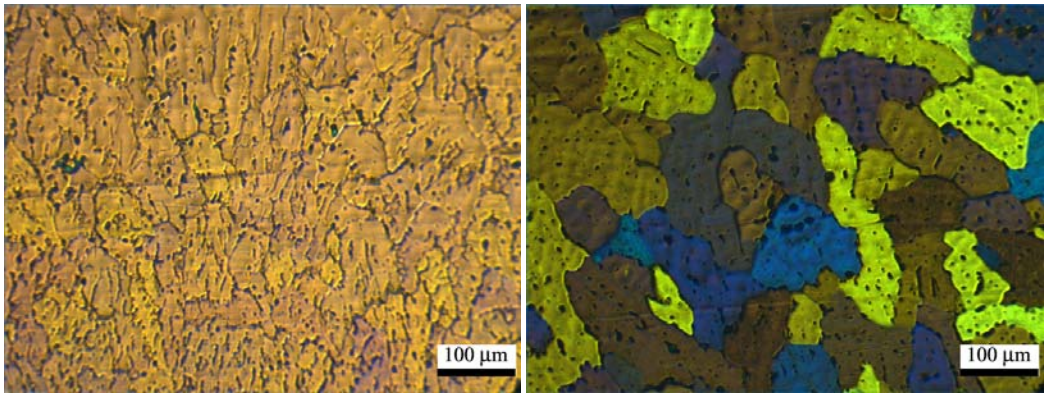

a) b)

Figure 4.18 Optical microstructures taken from the weld zone a) 5049(Al-2wt%Mg) alloy and b) 5754(Al-3wt%Mg) alloy obtained with 0.33kJ/cm heat input. Welding speed: 100mm/min

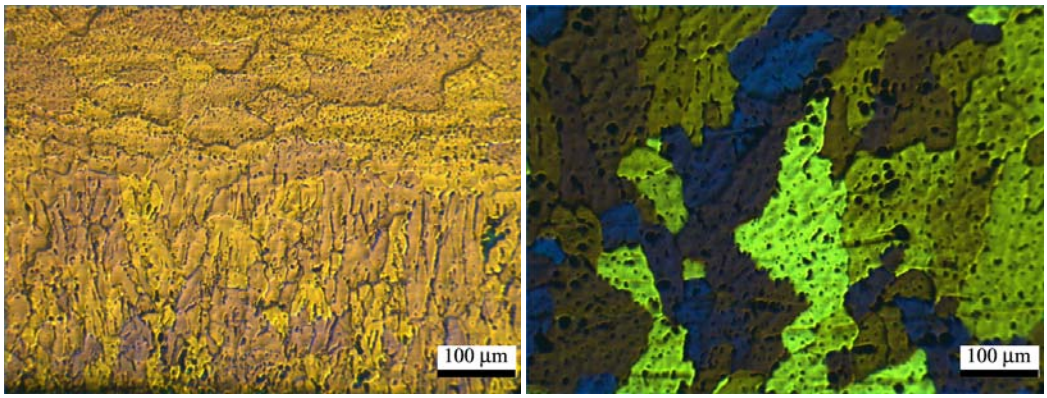

a) b)

Figure 4.19 Optical microstructures taken from the weld zone a) 5049(Al-2wt%Mg) alloy and b) 5754(Al-3wt%Mg) alloy obtained with 0.29kJ/cm heat input. Welding speed: 110mm/min

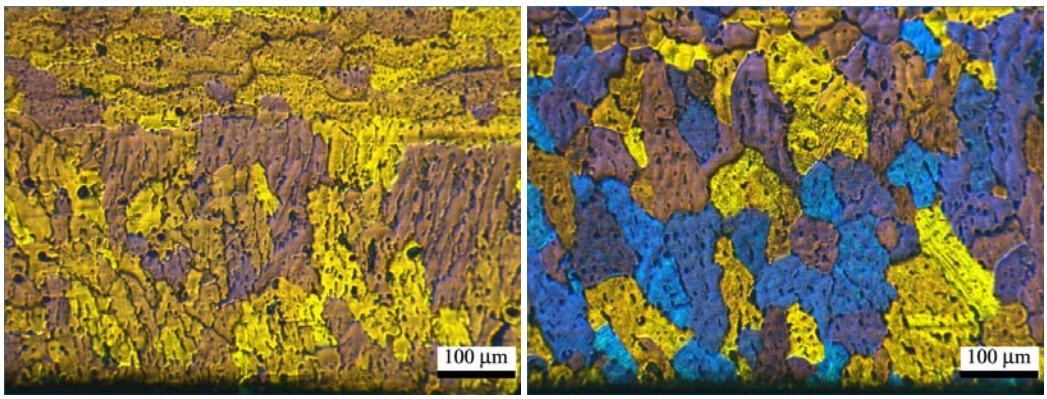

a) b)

Figure 4.20 Optical microstructures taken from the weld zone a) 5049(Al-2wt%Mg) alloy and b) 5754(Al-3wt%Mg) alloy obtained with 0.27kJ/cm heat input. Welding speed: 120mm/min

The microstructure images of the weld seams obtained by changing welding speed are given in Figure 4.16, Figure 4.17, Figure 4.18, Figure 4.19 and Figure 4.20. Secondary dendrite arm spacing (SDAS) has been measured on these microstructures as shown in

Figure 4.21. Effect of line energy on secondary dendrite arm spacing can be seen in Figure 4.22.

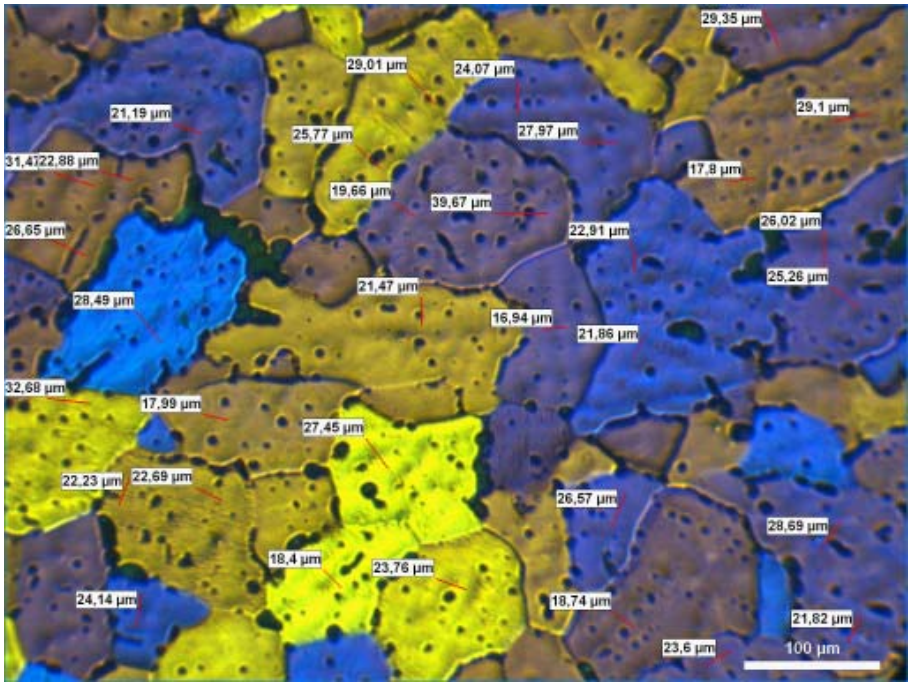

Figure 4.21 An example of secondary dendrite arm spacing measurement in the weld microstructure.

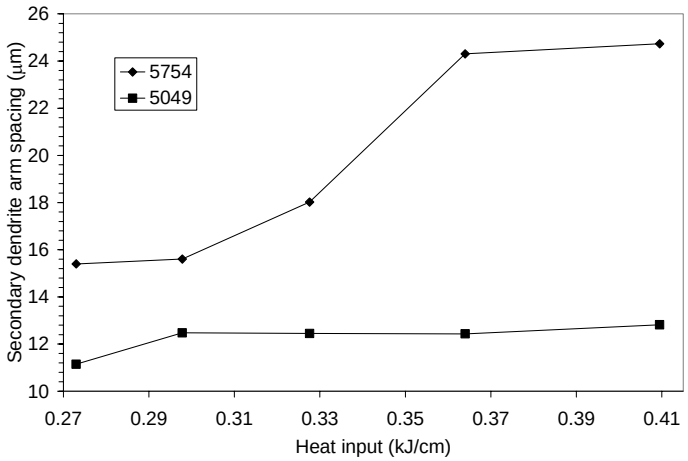

Figure 4.22 Change in secondary dendrite arm spacing in the weld zone of 5049 and 5754 alloys for different heat inputs.

Secondary dendrite arm spacing (SDAS) measurements have shown that the solidification microstructure of 5049(Al-2wt%Mg) alloy revealed finer microstructure when compared to 5754(Al-3wt%Mg) alloy. Solidification microstructure of 5754(Al-3wt%Mg) alloy showed coarsening with increasing line energy. Although the same behavior was observed for the 5049(Al-2wt%Mg) alloy, the change in secondary dendrite arm spacing (SDAS) values was not as significant as in 5754(Al-3wt%Mg) alloy.

Weld microstructures of the specimen produced with filler additions are given in Figure 4.23. Since very high heat input was used for the production of the weld seam (Figure 4.23a) it revealed a coarse structure. This weld zone was remelted during the Varestraint Testing at low line energies resulting in finer microstructure (Figure 4.23b).

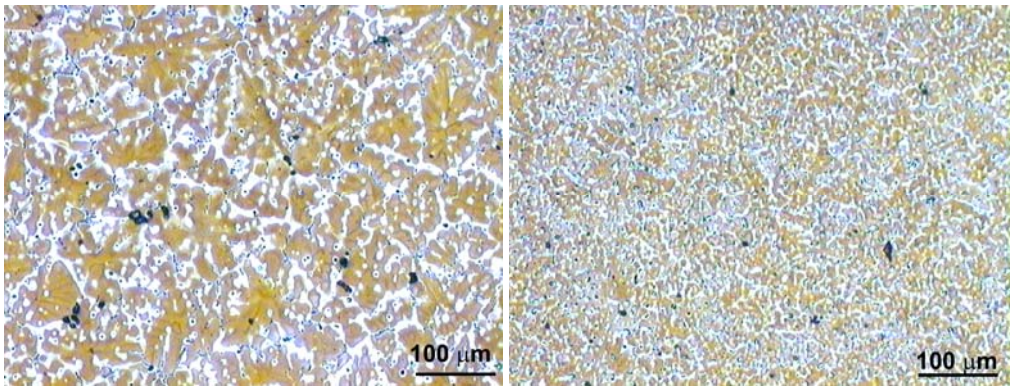

a) b)

Figure 4.23 a) Weld metal microstructure of 5049 alloy obtained with 5356 filler alloy. b) Remelted weld zone with lower heat input during varestraint testing.

4.3.2. Microstructure of the MVT specimens

In this section, the liquation and solidification cracks formed by the Varestraint Test Method have been examined under the optical microscope. Cracks on the weld metal are called *solidification cracks*. Figure 4.24 is an example of solidification cracks. Strain has been applied externally to form cracks during varestraint test. As the strain level is increased the length and number of cracks have also increased. This situation has been shown in section 4.1 with various graphic representations.

The cracks formed in the heat affected zone (HAZ) closer to the fusion line are called *liquation cracks*. It is known that these cracks are formed between grains in the partially melted zone. Liquation cracks formed by the varestraint test are given in Figure 4.25. In 5049(Al-2wt%Mg) alloy liquation cracks are negligible. On the other hand, just like the solidification cracks, increasing strain level and line energy has resulted in higher TCLliq and T#Cliq for 5754(Al-3wt%Mg) alloy.

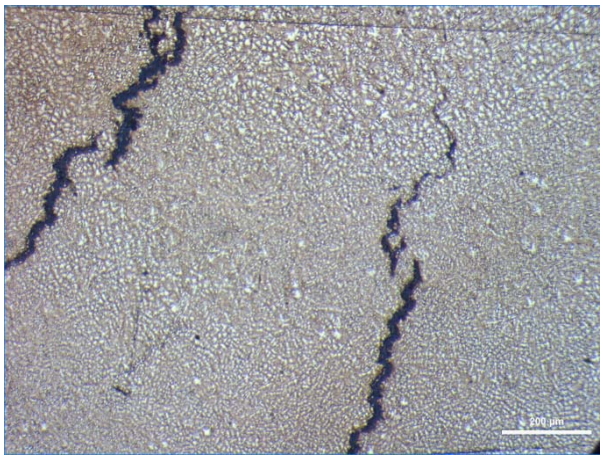

Figure 4.24 Solidification cracks formed in the weld metal of the alloy 5754

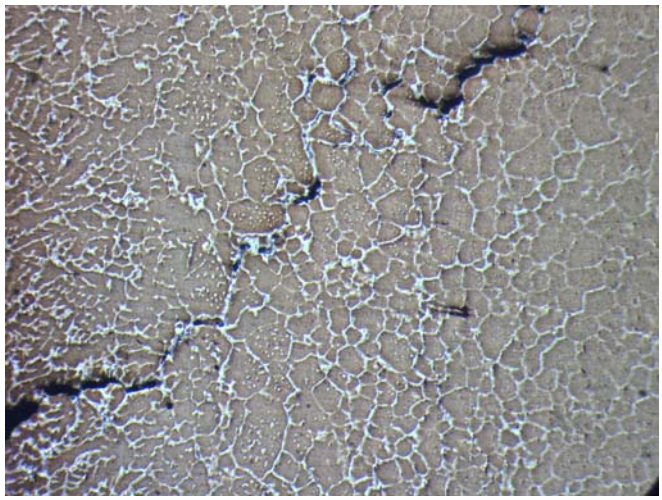

Figure 4.25 Liquation crack formed in the partially melted zone (PMZ) of the alloy 5754(Al-3wt%Mg)

When the grain boundaries in the heat affected zone (HAZ) are observed, it can be seen that the second phase particles precipitated (Figure 4.26). This is interpreted as to facilitate the formation of liquation cracking.

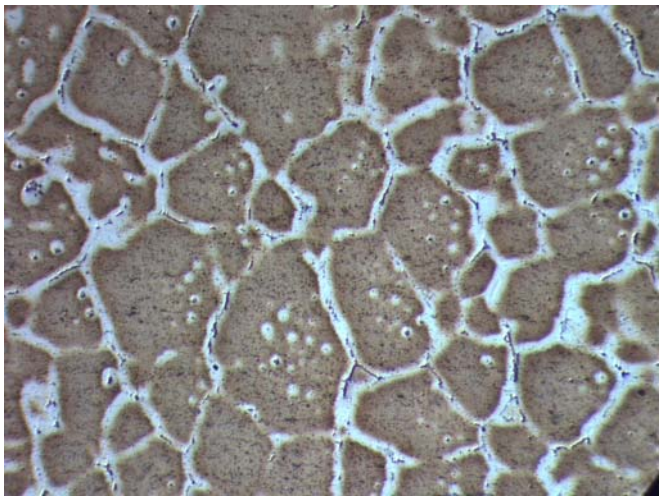

Figure 4.26 Micrograph of heat effected zone (HAZ) of the alloy 5754(Al-3wt%Mg).

4.3.3. Microstructure of mid-plane segregation

It is known that in the aluminum alloys produced by Twin Roll Casting centerline segregation forms [37]. Between the two alloys 5754(Al-3wt%Mg) alloy has higher amount of segregation in the mid-thickness. Optical micrograph of the centerline segregations is given in Figure 4.27. As seen in Figure 4.27 there are two types of second phase particles in the segregation zones. EDS analysis taken from the intermetallics are given in Table 4.1. EDS analysis shows that *large* light gray particles (I) and *fine* light gray particles (II) are the same type of intermetallics containing Mg and Fe. Type III particles are black and contain high amount of Mg, Si and Fe.

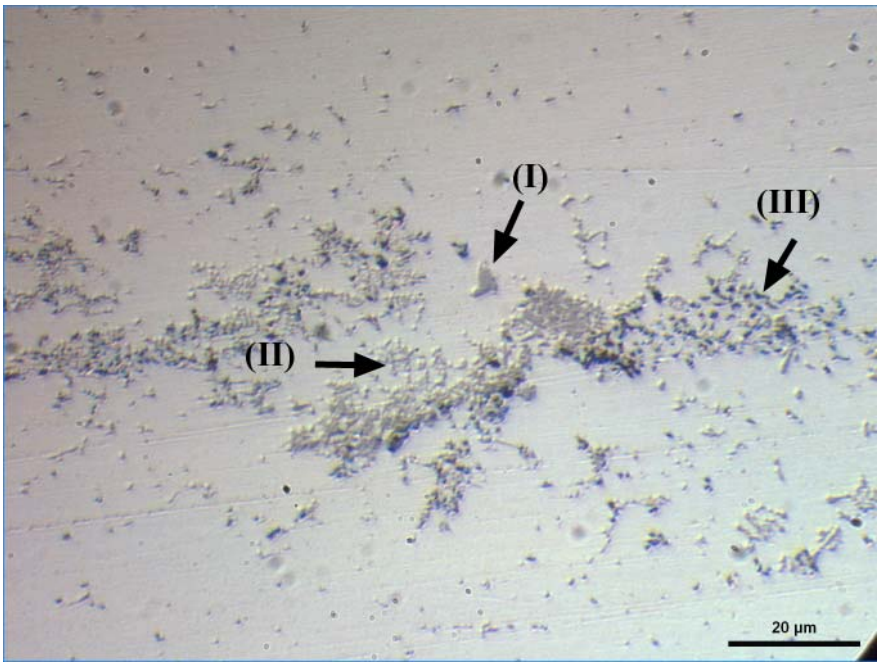

Figure 4.27 Optical micrograph of centerline segregation zone of alloy 5754(Al-3wt%Mg)

Table 4.1 Compositions (at%) of particles in 5049 and 5754 alloy

Second phase particles	**Mg**	**Fe**	**Si**	**Al**
I	5.07	7.02	0.79	Bal.
III	29.13	3.86	19.82	Bal.

In the present study the effect of heat input on mid-plane segregation was also investigated. The image obtained from the segregation zone under the optical microscope is given in Figure 4.28. When the cross section of the fusion zone was examined under optical microscope, it was seen that there were some variations in the mid-plane segregation of 5754(Al-3wt%Mg) alloy. There are three regions (pointed out with arrows) affected from the heat input during welding. Two of them are in heat affected zone (HAZ) and third one is at the base metal side.

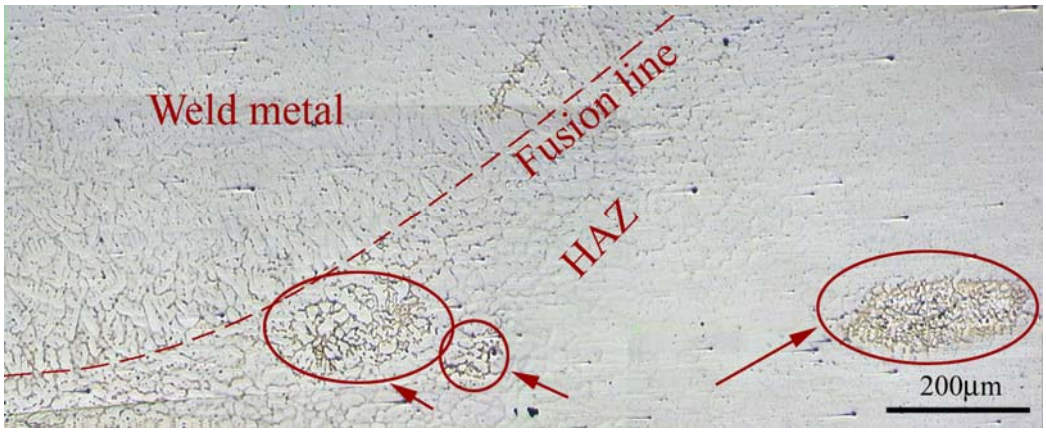

Figure 4.28 Microstructure of the mid-plane segregation near the weld zone. Etched with Weck

Microstructure images of the segregation zones are given in Figure 4.28. Changes in the second phase particles in the heat affected segregation zones after welding have been investigated. As can be seen in the microstructure images (Figure 4.29c), the second phase particles in "Chinese script" form are observed. Also it can be seen that these second phase particles are formed along the grain boundaries (Figure 4.29c).

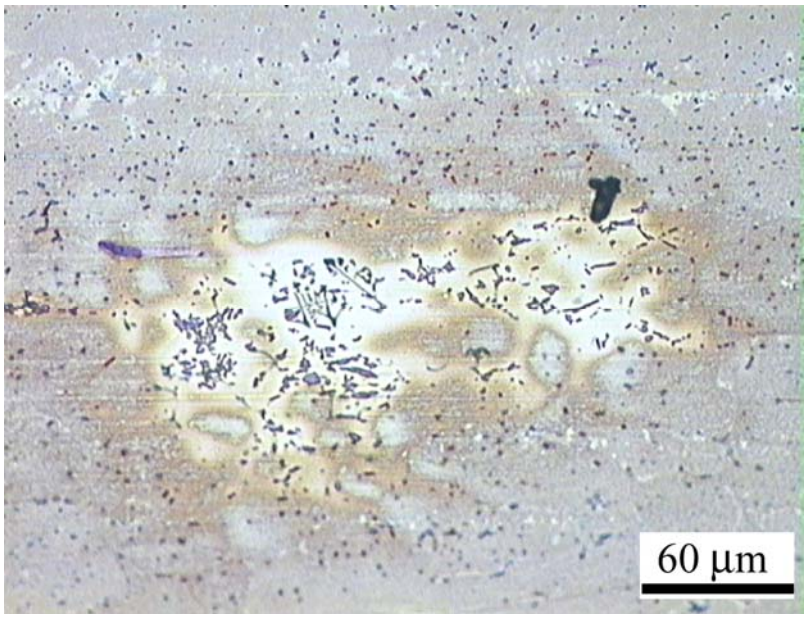

a)

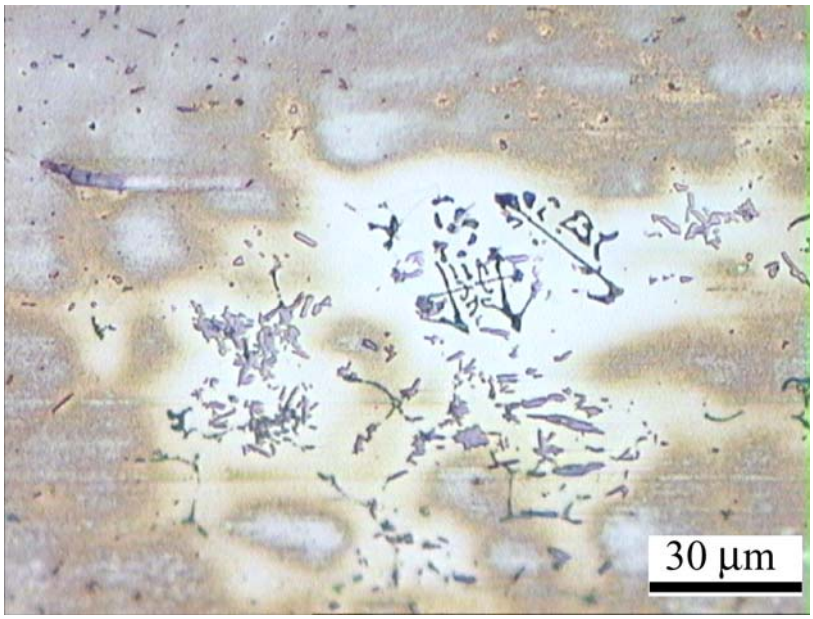

b)

Figure 4.29 Second phase particles formed near the weld zone due to heat effect. a) Lower magnification of segregation zone. b) Higher magnification of (a). c) Another example of second phase particles formed at the grain boundaries in the heat affected segregation zone.

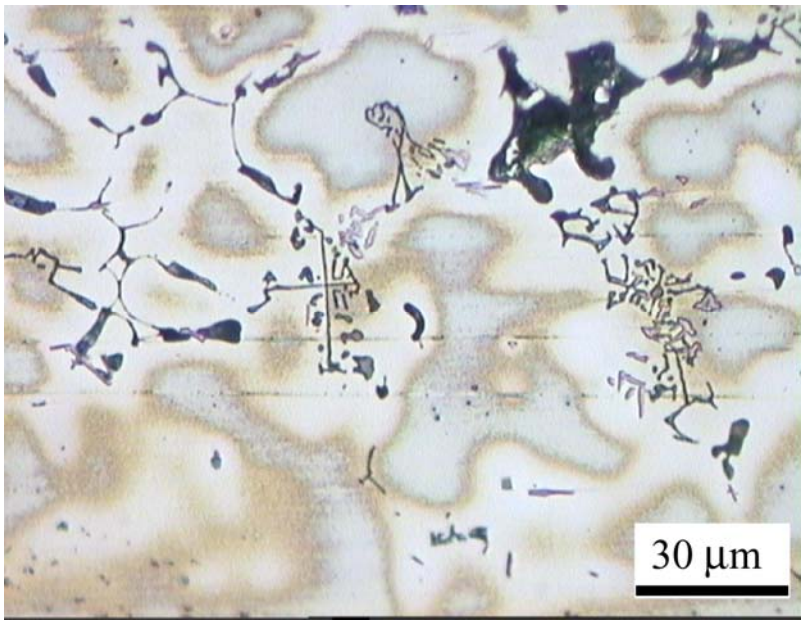

c)

Figure 4.29 Second phase particles formed near the weld zone due to heat effect. a) Lower magnification of segregation zone. b) Higher magnification of (a). c) Another example of second phase particles formed at the grain boundaries in the heat affected segregation zone *(continued)*.

These changes taking place close to the heat affected zones were investigated using the quench test method. In this method samples were heated up to temperatures below the solidus temperature and they were quenched in water. Liquation in the grain boundaries within the segregation zones has been observed in these samples (Figure 4.30). This situation proposes that second phase particles may be formed by a eutectic reaction in mid-plane segregation region.

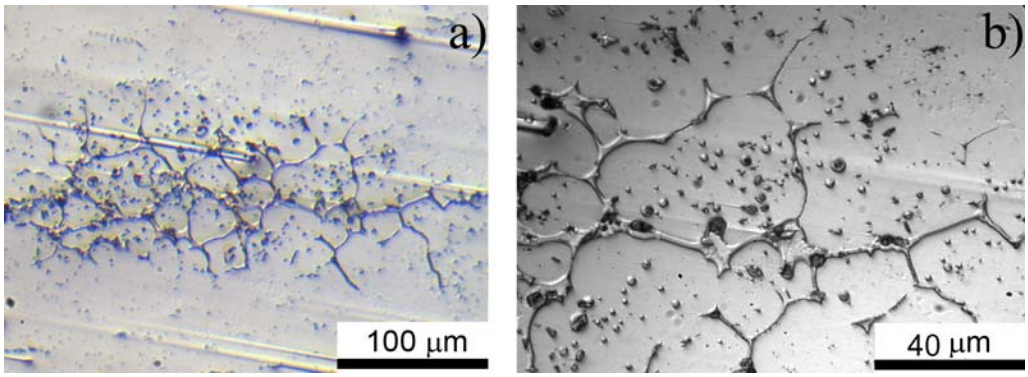

a) b)

Figure 4.30 Micrographs of centerline segregation region after quench test

To determine the liquation temperature of mid-plane segregation zone additional tests were applied at various temperatures below the solidus of 5754 alloy. Samples were heated up to temperatures below solidus and then air cooled and examined under the optical microscope. As can be seen in Figure 4.31 samples heated up to 575^{o}C and air cooled, contain second phase particles in "Chinese script" form in 5754 alloy. EDS analysis were taken from point A and B from second phase particles (Figure 4.32) and results are given in Figure 4.33 and Figure 4.34.

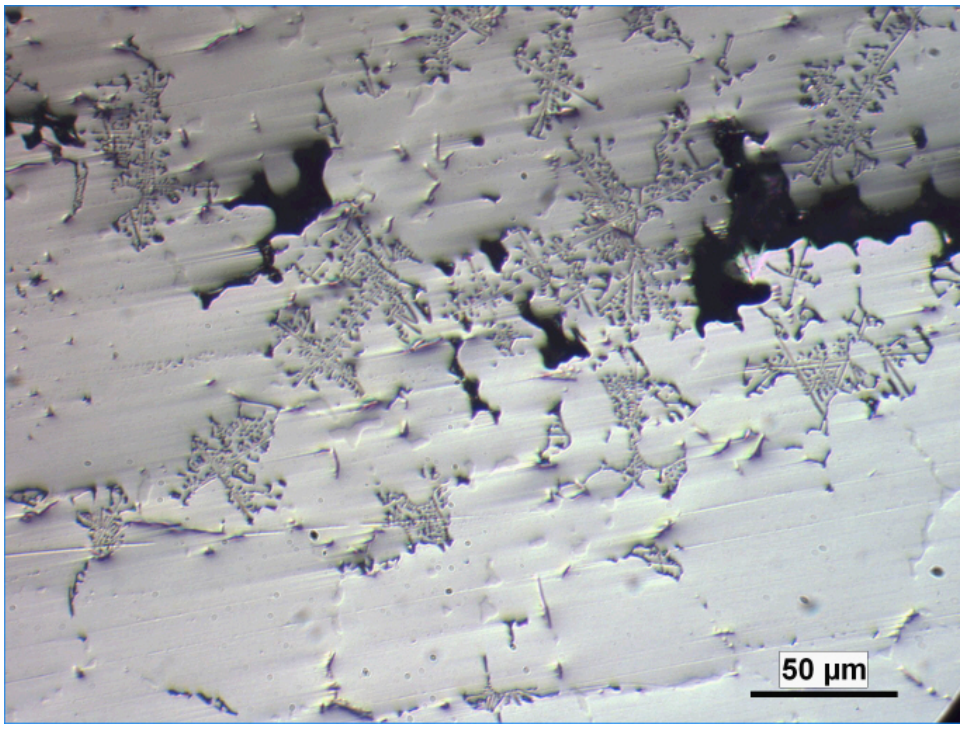

Figure 4.31 Mid-plane segregation on 5754(Al-3wt%Mg) alloy. Heated up to 575^{o}C and air cooled. Second phase particles in "Chinese script" form observed with cavities left from eutectic melting

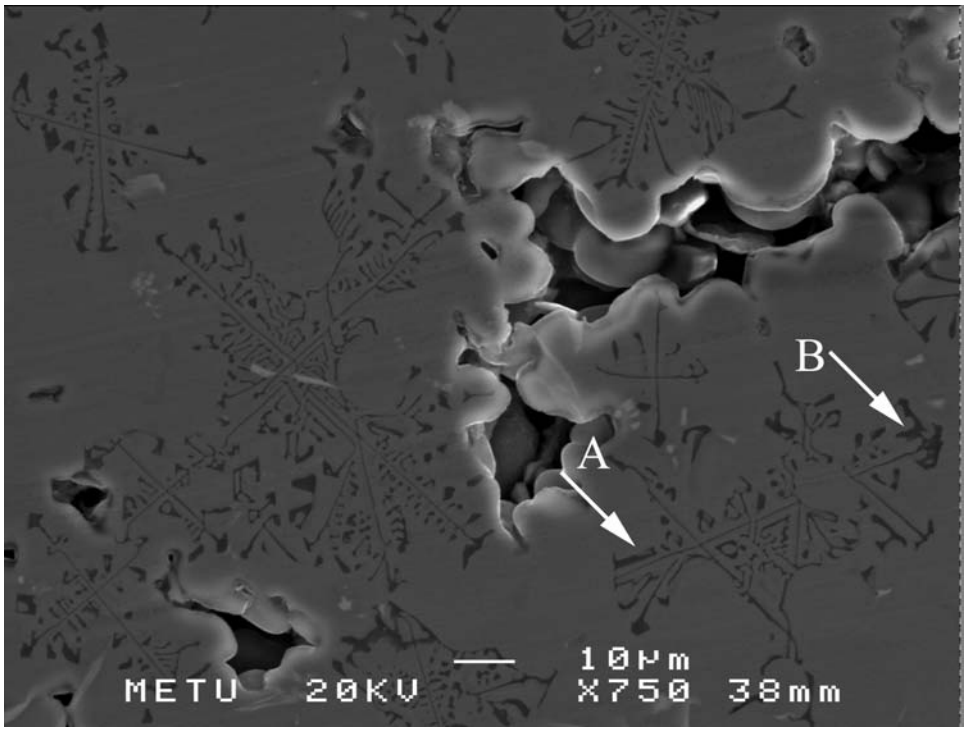

Figure 4.32 Scanning electrom microscope (SEM) image of mid-plane segregation on 5754(Al-3wt%Mg) alloy. EDS analysis was taken from points labeled as A and B.

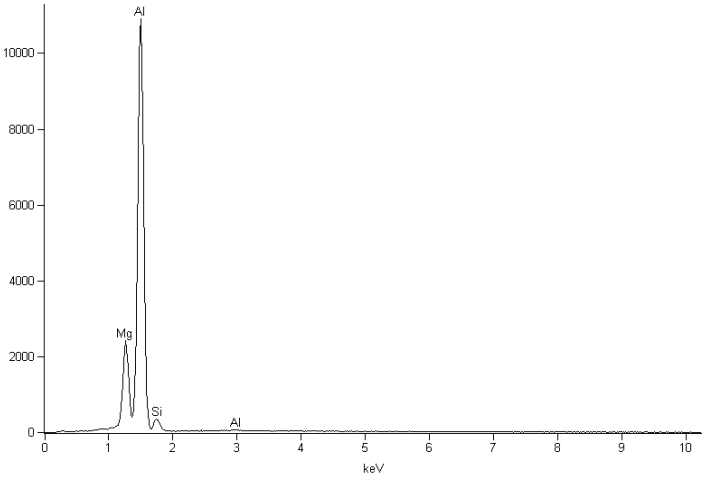

Element	*Weight Conc %*
Mg	12.32
Al	82.20
Si	5.47

Figure 4.33 EDS analysis taken from point A.

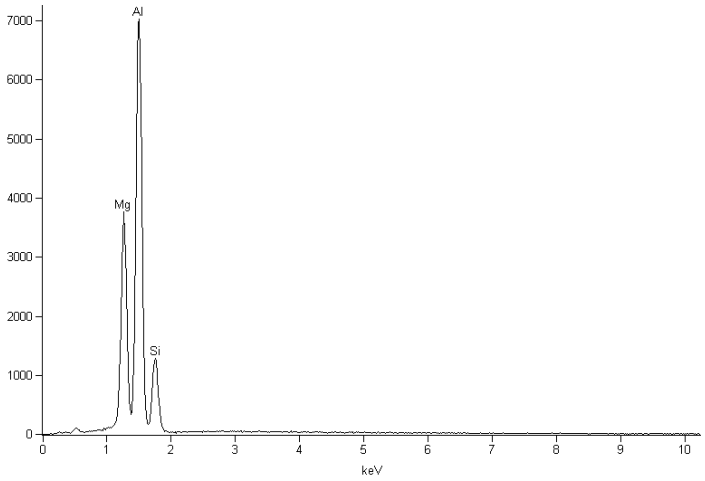

Element	*Weight Conc %*
Mg	20.73
Al	61.09
Si	18.18

Figure 4.34 EDS analysis taken from point B

These results show that there is a reaction in mid-plane segregation zone. Also, the temperature at which this reaction occurs is below the solidus temperature of 5754(Al-3wt%Mg) alloy. As previously mentioned, partially melted zone is limited between the liquids and solidus temperature of the alloy. High amount of solute segregation and eutectic reactions below solidus expands partially melted zone. Thus, wider partially melted zone (PMZ) causes a wider region susceptible to liquation cracking. In other words, presence of mid-plane segregation can increase the hot cracking susceptibility since it broadens the partially meted zone.

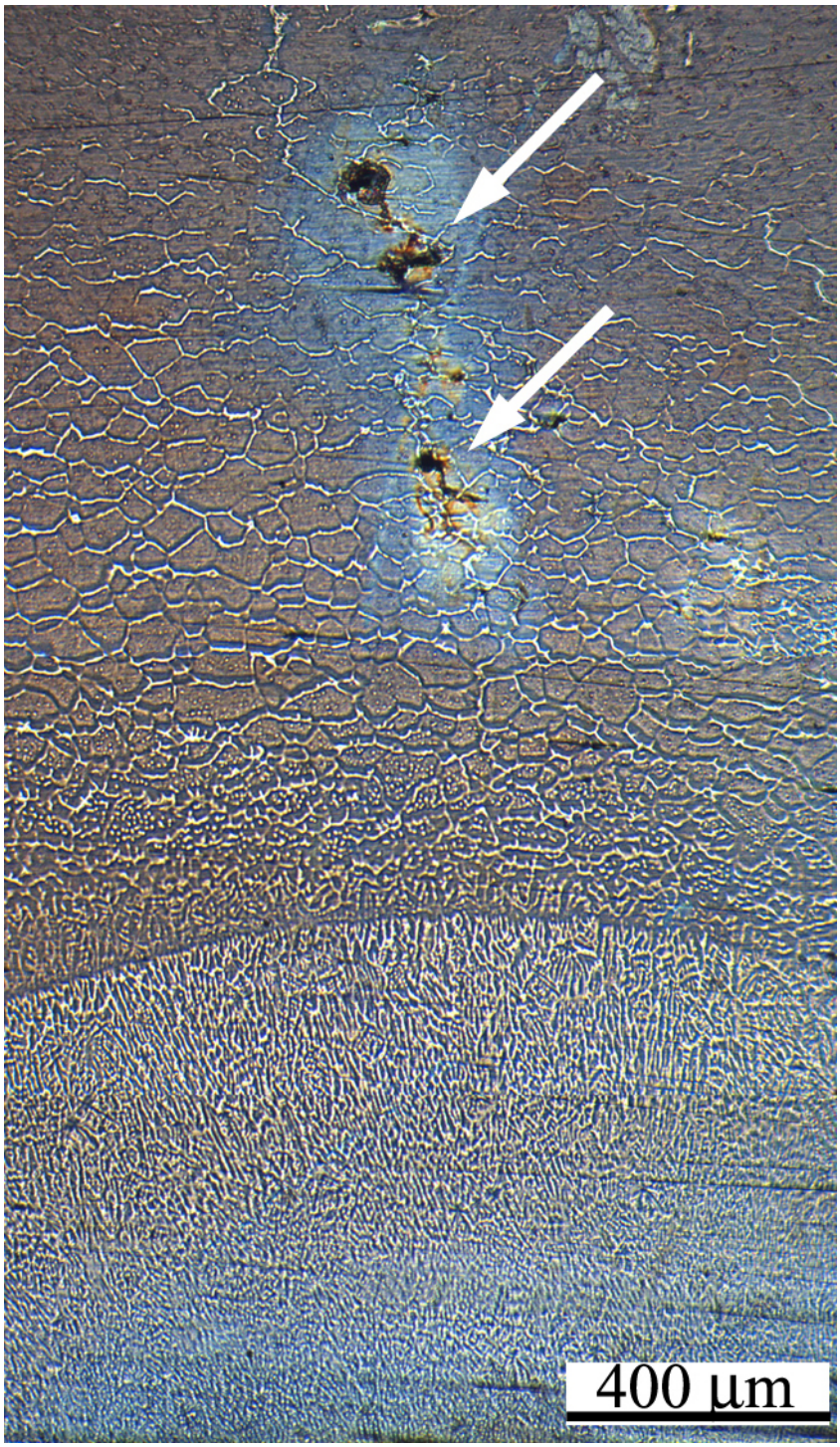

Figure 4.35 Microstructure of weld zone and partially melted zone with internal cracks formed in mid-plane segregation. Varestraint test specimen: strain level: 2%. Etchant: Weck

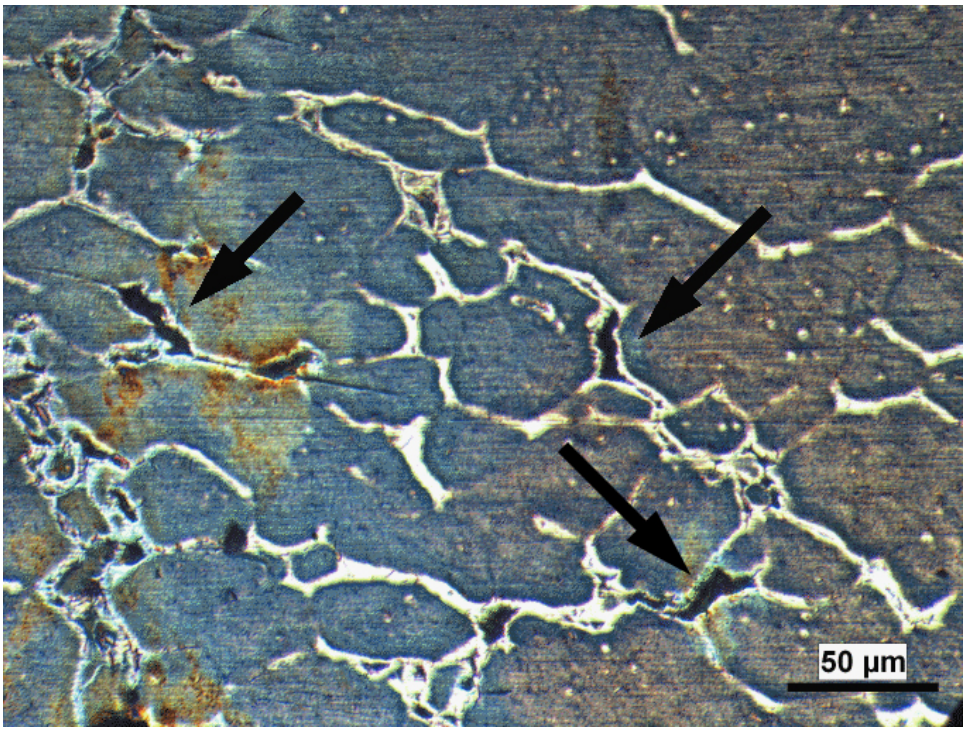

Figure 4.36 Internal liquation cracks formed at the mid-plane segregation zone. Higher magnification of Figure 4.35.

Longitudinal cross section of Varestraint Test specimens were examined to investigate any liquation cracking at the mid-plane segregation zones. In Figure 4.35 and Figure 4.36 internal cracks can be observed out side of the fusion zone after Varestraint Test. As mentioned above, in addition to high solute segregation, presence of low temperature eutectics increases the zone vulnerable zone to any liquation cracking.

Summary

The effect of welding parameters used at Varestraint Test method on the microstructures was studied. Line energy was changed with welding speed and its effects were studied with the optical microscope. Penetration depth, weld width and secondary dendrite arm spacing (SDAS) measurements were made by the Clemex vision image analyzer. It was observed that decreasing line energy resulted in finer microstructure. Moreover, 5049(Al-2wt%Mg) alloy has finer microstructure obtained for each line energy level during welding. In addition to that, it was seen that, 5049(Al-2wt%Mg) alloy has narrow

weld width and shallow penetration depth compared to 5754(Al-3wt%Mg) alloy. Also, images of solidification cracks in weld metal and liquation cracks in partially melted zone (PMZ) were displayed.

Optical micrograph of autogeneous bead-on-plate welding of twin roll cast 5754(Al-3wt%Mg) alloy has shown that, mid-plane segregation zone was affected from weld heat input. Then, quench test was applied and liquation was observed at the mid-plane segregation below the solidus temperature of the 5754 alloy. Further furnace experiments have shown that there was a liquation due to eutectic reaction at around 575^{o}C. Second phase particles in "Chinese script" form and voids were observed verifying this liquation due to eutectic reaction. To investigate the effect of liquation at the mid-plane segregation, varestraint test specimens were examined. And it was seen that, there were internal liquation cracks formed after the Varestraint Test. Presence of high segregation at the mid-thickness has resulted in formation of eutectic reaction and wider partially melted zone.

4.4. Thermal analysis of 5049 and 5754

It is known that the susceptibility of forming solidification and liquation cracks is related to the solidification range. For this reason the difference of solidus and liquidus temperatures of 5049(Al-2wt%Mg) and 5754(Al-3wt%Mg) alloys has been determined with thermal analysis. It should be noted at this point that the major difference in the compositions of the two base alloys is the amount of Mg which is affecting the solidus and liquidus temperatures. Heating and cooling stage of the 5049(Al-2wt%Mg) alloy is given in Figure 4.37. The temperature where liquation starts was determined as 623^{O}C. And the complete melting was reached at 661^{O}C for 5049(Al-2wt%Mg) alloy.

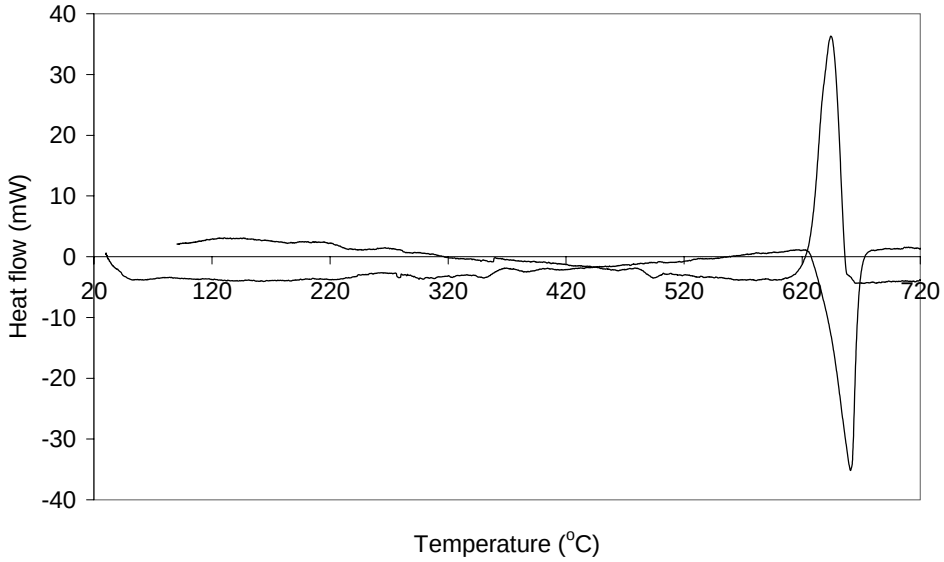

Figure 4.37 Heat flow with temperature measurements of the 5049 alloy during heating and cooling in thermal analysis

Figure 4.38 shows the thermal analysis results of the 5754(Al-3wt%Mg) alloy. Melting range was determined from heating stage. First liquid formation started at 605^{O}C and melting completed at 653^{O}C. Solidification ranges determined from differential thermal analysis are given in Table 4.2.

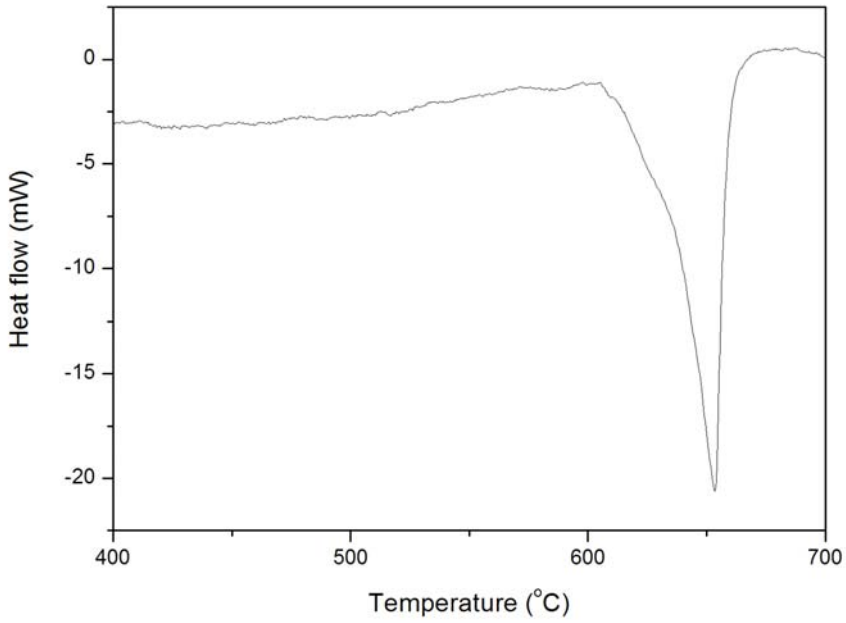

a)

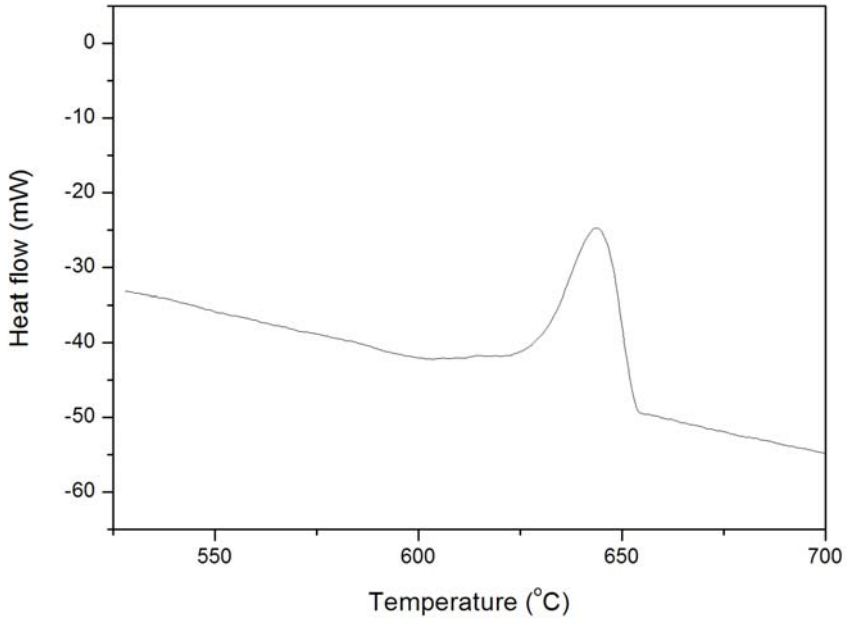

b)

Figure 4.38 Heat flow with temperature measurements of the 5754(Al-3wt%Mg) alloy during heating (a) and cooling (b) in thermal analysis.

Table 4.2 Solidus and liquidus temperatures of 5049(Al-2wt%Mg) and 5754(Al-3wt%Mg) alloys obtained from DTA.

Alloy	Temperature		ΔT
5754	T_s	605	48
	T_l	653	
5049	T_s	623	38
	T_l	661	

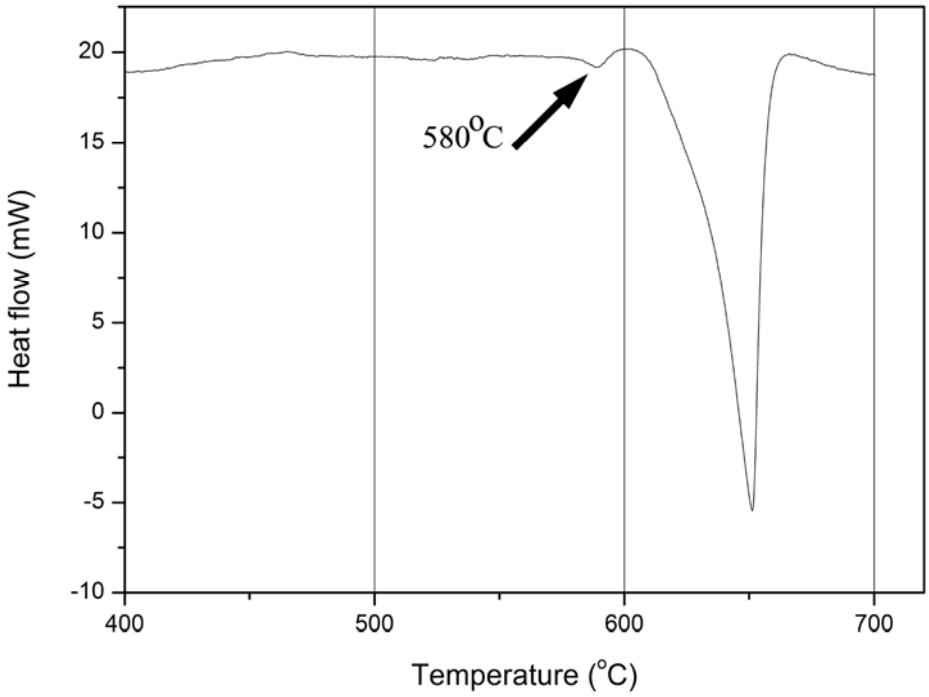

Figure 4.39 Heat flow with temperature measurements of the 5754(Al-3wt%Mg) alloy during heating in thermal analysis. Specimen was taken from mid-section of 5754(Al-3wt%Mg) alloy.

As mentioned above, there is a mid-plane segregation in the 5754(Al-3wt%Mg) alloy and quench tests have shown that liquation occurs below the solidus temperature in mid-plane segregation. Therefore, thermal analysis was applied to a sample from mid-section of 5754(Al-3wt%Mg) alloy. As seen in Figure 4.39 there is an exothermic reaction before solidus temperature is reached at around 580°C and this temperature is close to results of quench experiments.

Summary

Thermal analysis of 5049(Al-2wt%Mg) and 5754(Al-3wt%Mg) alloys have shown that 5754(Al-3wt%Mg) alloy has wider solidification range than 5049(Al-2wt%Mg) alloy. And it is consistent with magnesium contents of both alloys. In addition to that, thermal analysis was applied to a sample taken from the mid-section of 5754(Al-3wt%Mg) alloy to investigate if there are any eutectic reactions below the solidus of 5754(Al-3wt%Mg) alloy. DTA curve has pointed out an exothermic peak around 580^{o}C which is below the solidus temperature of 5754(Al-3wt%Mg) alloy. This temperature is almost the same with the temperature obtained during the quench tests.

4.5. Scanning electron microscope analysis

As it was mentioned in section 4.1, solidification and liquation cracks have formed in 5754(Al-3wt%Mg) alloy after the application of the Varestraint Test. However, for 5049(Al-2wt%Mg) alloy since the liquation cracks were negligible only the solidification cracks were evaluated. In this section the fracture surfaces of the solidification cracks for both alloys and fracture surface of liquation crack of 5754(Al-3wt%Mg) alloy were examined.

The solidification crack fracture surfaces are given in three parts. Fracture surface given in Figure 4.40 was taken from a point close to the weld pool, i.e. low solid fraction when fracture occurred. In Figure 4.41, fracture surface of semi-solid structure with higher solid fraction is given. And the final micrograph was taken from the tip of solidification fracture surface where solidification is almost complete with interdendritic liquid. Solidification fracture surfaces of crack tips from 5754(Al-3wt%Mg) and 5049(Al-2wt%Mg) alloys are given in Figure 4.42 and Figure 4.43 respectively.

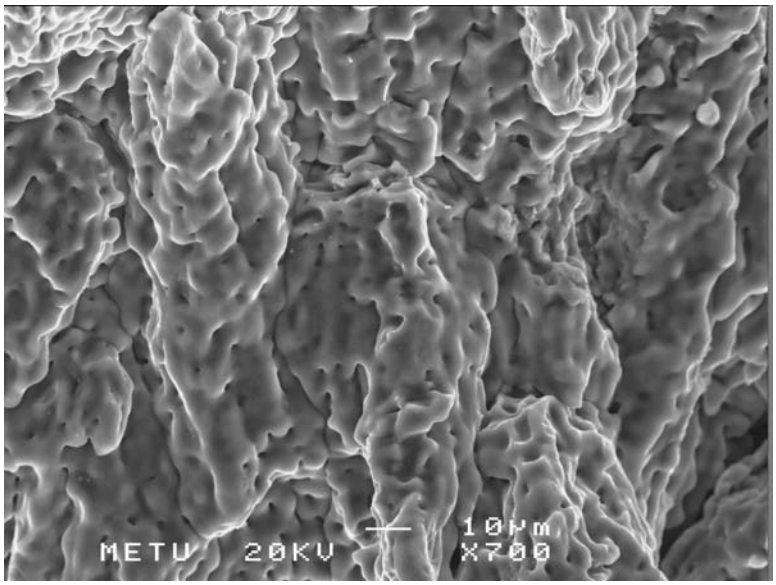

Figure 4.40 Fracture surface of solidification crack close to weld pool of 5754(Al-3wt%Mg) alloy. Crack formed near the weld pool where solid fraction was low.

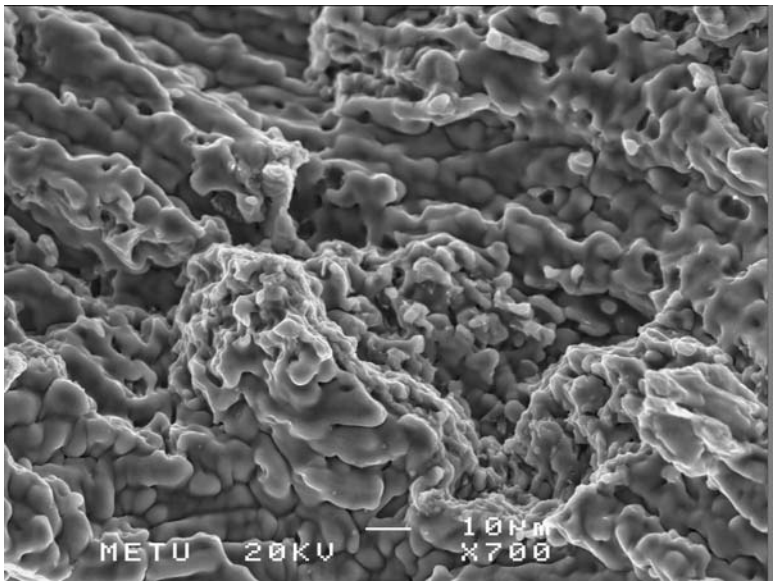

Figure 4.41 Fracture surface of solidification crack of 5754(Al-3wt%Mg) alloy. Crack formed at the point where solid fraction was higher than the crack Figure 4.40.

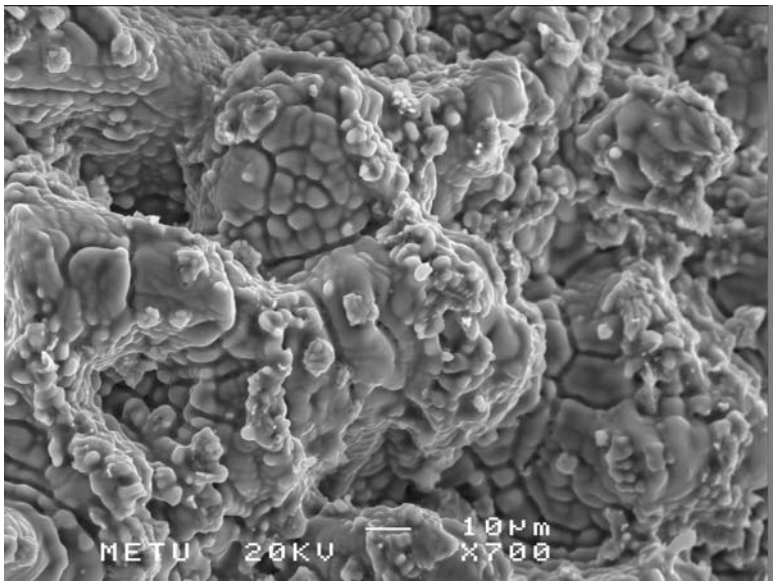

Figure 4.42 Fracture surface of the solidification crack of 5754(Al-3wt%Mg) alloy taken from solidification crack tip.

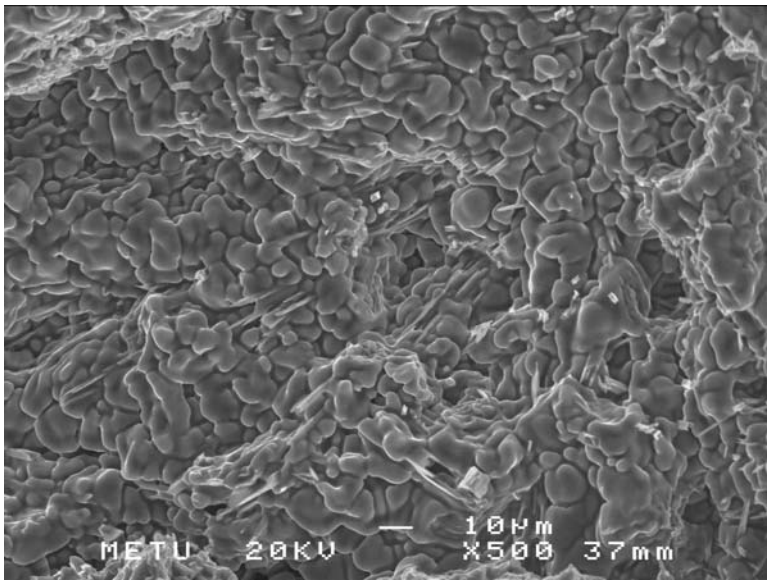

Figure 4.43 Fracture surface of the solidification crack of 5049(Al-2wt%Mg) alloy taken from solidification crack tip.

Intermetallic constituents have formed at the grain boundaries during the solidification of fusion zone in 5754 alloy (Figure 4.44). The EDS analysis has revealed that the

intermetallics contain 6.09at%Mg, 27.77at%Fe 0.36at%Si 65.78at%Al (Figure 4.45). It is known that, in Al-Mg alloys, in the absence of Mn and Cr, iron may form $FeAl_3$ [47]. For this reason, it is assumed that the iron rich intermetallics observed on the solidification cracks of 5754 alloy are $FeAl_3$ (Figure 4.44).

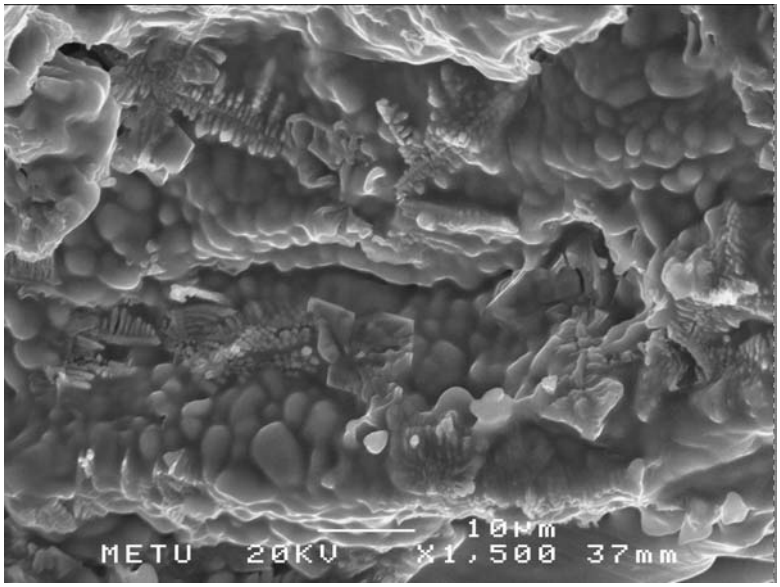

Figure 4.44 Iron rich intermetallics formed in the interdendritic region during solidification of 5754 alloy.

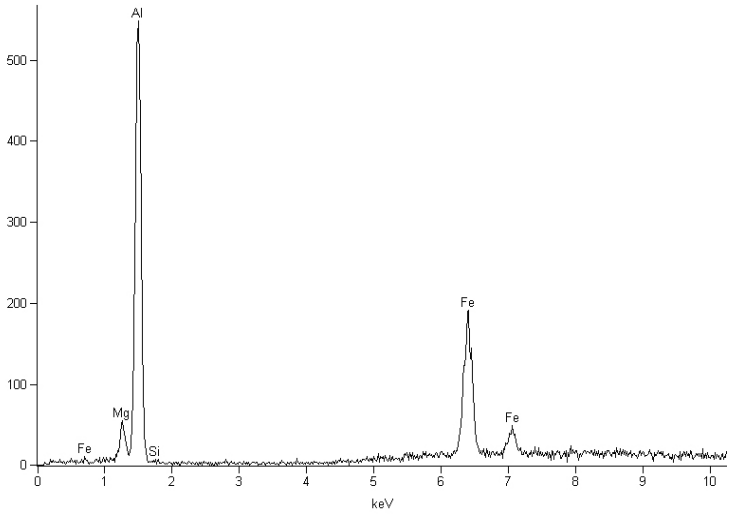

Figure 4.45 EDS analysis taken from the solidification fracture surface.

The reason for the formation of liquation cracks has been searched for on liquation cracks and fracture surfaces. Optical micrograph of liquation crack on 5754(Al-3wt%Mg) alloy is given in Figure 4.46. Liquation fracture surface of 5754 alloy is given in Figure 4.47. High amount of magnesium and silicon segregation was observed on the liquation cracks. EDS analysis taken from liquation crack surface (Figure 4.47) has shown that Mg is 7.89wt% and Si is 8.24wt%. Increasing solute content at the grain boundaries decreases melting temperature of the intergranular liquid below the solidus temperature of the alloy.

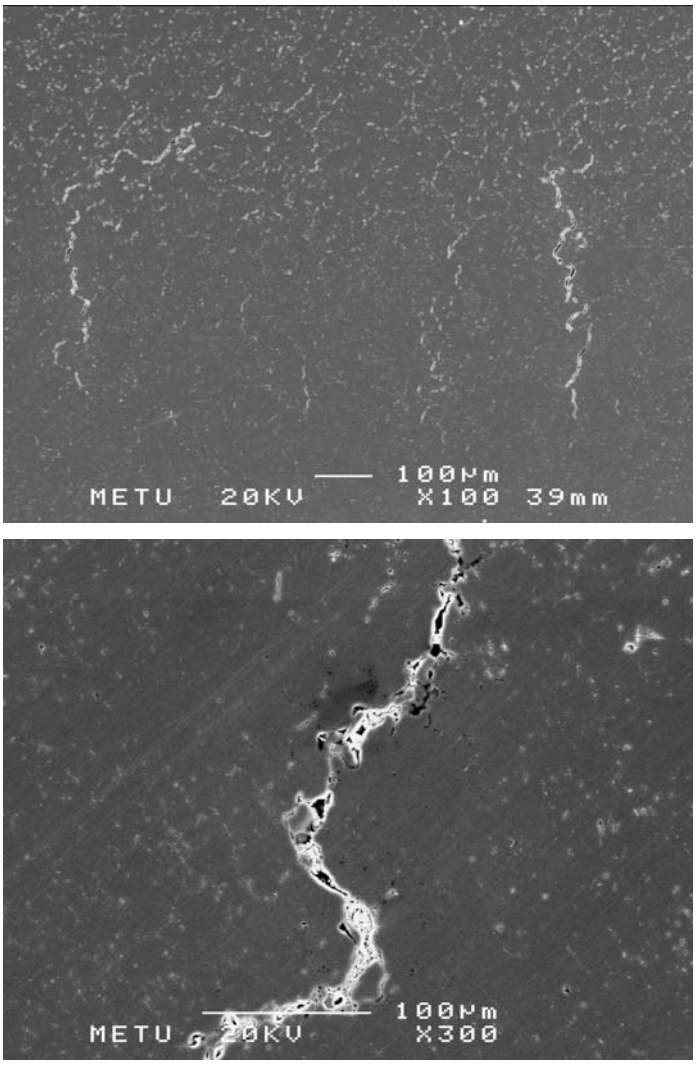

Figure 4.46 Liquation cracks near the fusion line of 5754 alloy.

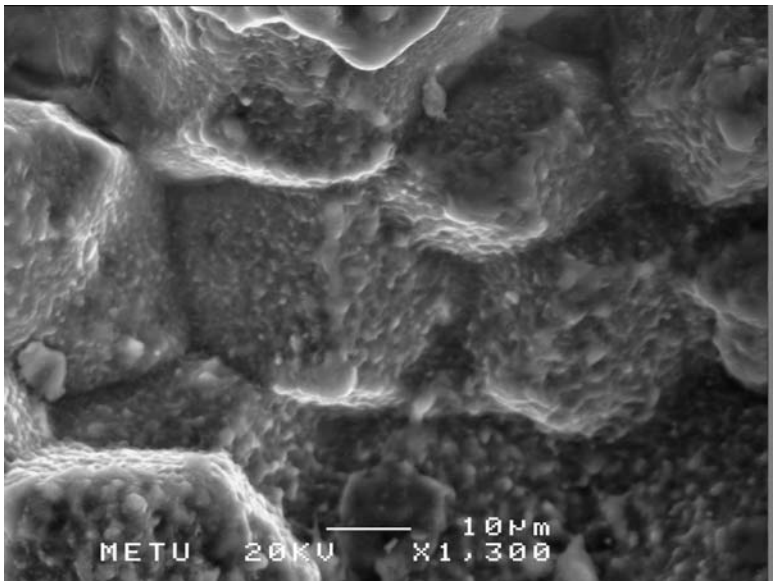

Figure 4.47 Liquation fracture surface of 5754 alloy

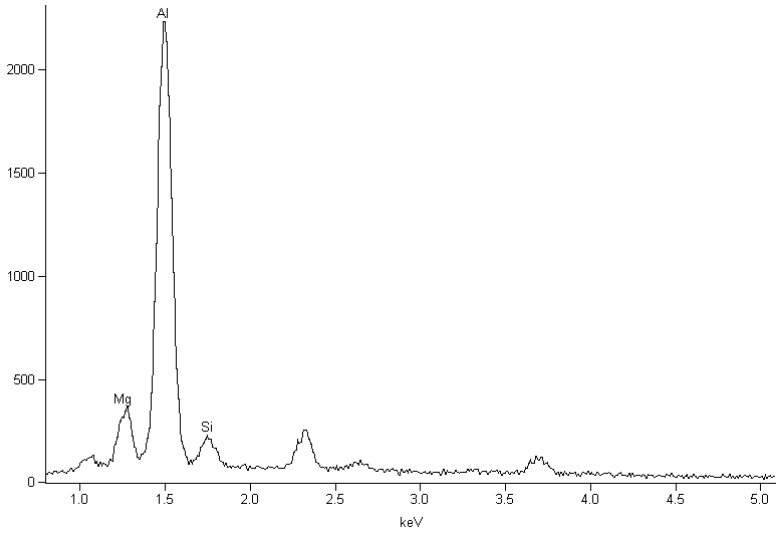

Element	Weight Conc %	AtomConc %
Mg	7.89	8.71
Al	83.88	83.42
Si	8.24	7.87

Figure 4.48 EDS analysis taken from liquation fracture surface shown in Figure 4.47

Two types of intermetallics one mainly composed of Fe, the other composed of Si have been observed on the fracture surfaces. The intermetallic particles composed of mainly

iron is similar to the one seen on the surface of the solidification crack surface shown above. The images of these intermetallic particles (Figure 4.49) and the EDS analysis obtained from both are given below (Table 4.3).

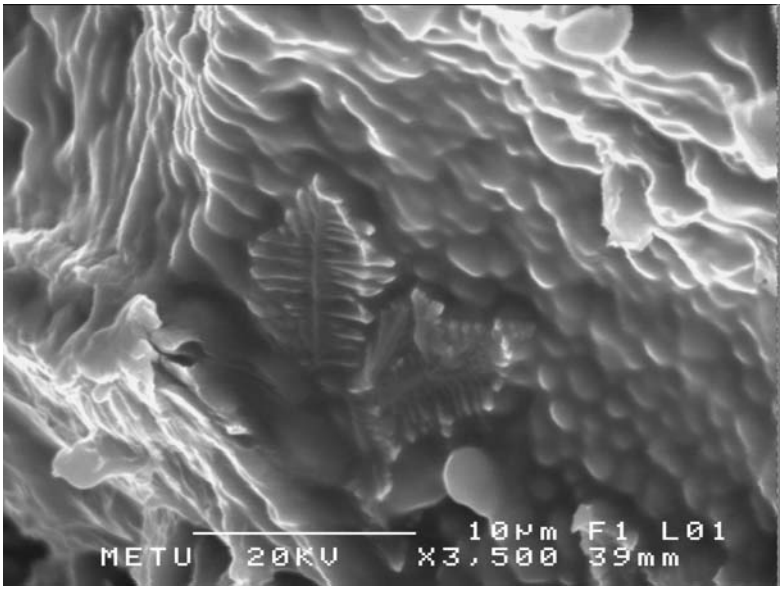

a)

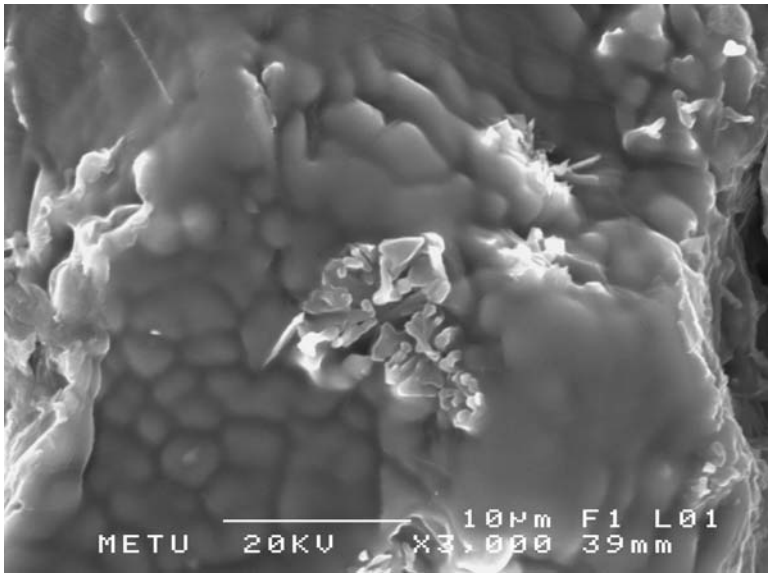

b)

Figure 4.49 a) Fe rich and b) Si rich intermetallics on the liquation crack surface

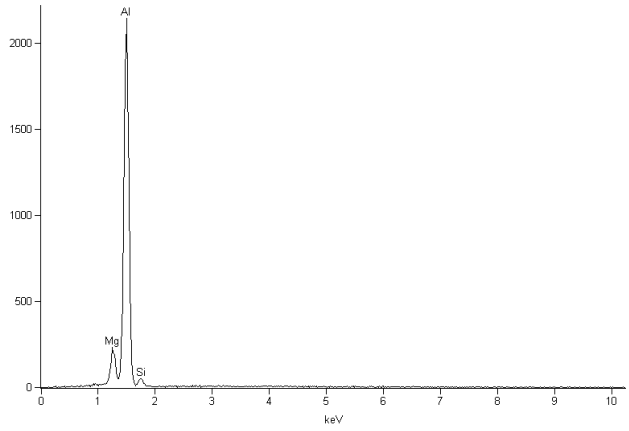

a)

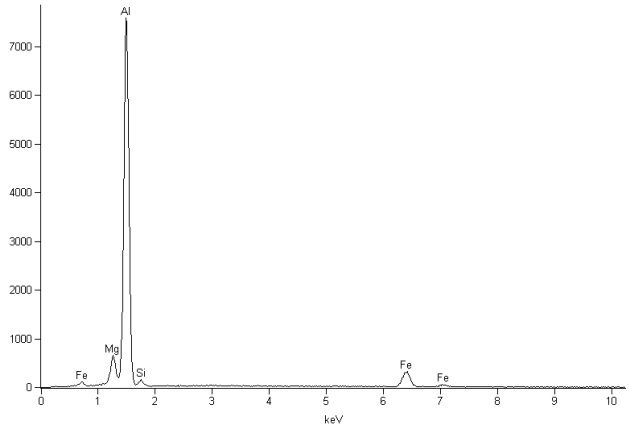

b)

Figure 4.50 EDS analysis taken from two types of intermetallics given in Figure 4.49

Table 4.3 EDS analysis of the two types of intermetallics.

Element	Fe rich intermetallic (wt%)	Si rich intermetallic (wt%)
Al	78.99	89.07
Mg	4.63	5.92
Si	2.54	5.01
Fe	13.83	-

It is thought that the intermetallic particles observed on the fracture surfaces that belong to the liquation cracks examined with the electron microscope are formed during the solidification of partially melted zone (PMZ). The microstructure images given in section 4.3.3 show these intermetallics. It can be assumed that these intermetallics that cannot be observed in the microstructure images that belong to the base alloys have been formed after the liquation and solidification in the high segregation zones.

CHAPTER 5

DISCUSSION

The discussion aims to establish a relation between the hot cracking susceptibility differences of 5049(Al-2%Mg) and 5754(Al-3%Mg) alloys as a function of welding and straining parameters. In addition to that, effect of filler alloys and mid-plane segregation zone are evaluated. In this frame, the discussion will be given under the following headings:

5.1 The effect of weld heat input on 5049(Al-2%Mg) and 5754(AlMg3) alloys
5.2 General behavior of hot cracking susceptibility of the 5049(Al-2%Mg) and 5754(Al-3%Mg) alloys
5.3 Hot cracking susceptibility of the alloys with filler additions
5.4 Mid-plane segregation zone in 5754(Al-3%Mg) alloy

5.1. Effect of weld heat input on 5049(Al-2%Mg) and 5754(Al-3%Mg) alloys

In the welding process, line energy, i.e. heat input per unit length, can be changed by altering the welding parameters. These parameters differ depending on the welding process used. In Gas Tungsten Arc Welding process (GTAW) which was used in this study, welding current and welding speed are the parameters that establish line energy. Effect of line energy on weld metal was studied for both 5049(Al-2%Mg) and 5754(Al-3%Mg) alloys. Welding current was kept constant and welding speed was changed in order to alter line energy. It was seen that weld metal width and penetration depth changed on both alloys depending on the line energy. The changes in weld width and

penetration depending on line energy were given in Figure 4.12 and Figure 4.13 respectively. As seen in these figures weld width and penetration increased with increasing line energy for both alloys. Moreover, both weld width and penetration depth of 5754(Al-3%Mg) alloy was found higher than 5049(Al-2%Mg) alloy. Therefore, increasing weld width with increasing line energy in 5754(Al-3%Mg) alloy results in a more susceptible region for solidification cracking since the mushy zone expands.

5.2. Hot cracking susceptibility of 5049(Al-2%Mg) and 5754(Al-3%Mg) alloys

Hot cracking appears as solidification cracking in the weld metal and liquation cracking in the heat affected zone. In Varestraint Test, the results are classified as total crack length, total number of crack and maximum crack length and they are given in Figure 4.3, Figure 4.4 and Figure 4.5 for solidification cracks, and liquation crack measurements are given in Figure 4.6 and Figure 4.7.

Solidification cracking susceptibility

Solidification cracking behavior of both alloys has been assessed according to the number of cracks and crack length measurements. Both alloys have shown that increasing line energy resulted in increasing cracking susceptibility of the weld metal. As mentioned in the previous section, the width of the weld metal increases with increasing line energy. Therefore, a wider mushy zone (the region susceptible to cracking) is formed by increasing the weld width. Moreover, increasing line energy causes decreasing cooling rate due to higher heat input. Thus, the amount of local interdendritic liquid which is not yet solidified increases. With increasing heat input since the amount of local interdendritic liquid increased with increasing line energy, the susceptibility to solidification cracking as expected has increased.

Weld microstructure of both alloys was evaluated according to secondary dendrite arm spacing (SDAS). As mentioned in section 2.2.1, the cooling rate depends on line energy and the growth rate depends on welding speed. Line energy was decreased by increasing welding speed and in return it increased the cooling rate. Therefore, decreasing line energy with increasing welding speed causes an increase in the cooling rate to growth rate ratio and formation of a finer microstructure [10]. As seen in Figure 4.22 secondary

dendrite arm spacing (SDAS) measurement has shown that finer solidification structure was obtained by increasing the welding speed, i.e. decreasing line energy.

Solidification temperature range is an important factor affecting hot cracking susceptibility of an alloy [35]. As the solidification temperature range increases, strain accumulation due to solidification shrinkage and thermal gradients increases on the mushy zone. Thus, solidification cracking susceptibility increases with solidification range. Differential thermal analysis (DTA) have shown that solidification range of 5754 alloy is higher than 5049 alloy as seen in Table 4.2, Figure 4.37 and Figure 4.38. During the varestraint test at the time when the strain is applied the amount of liquid is higher in the 5754(Al-3%Mg) alloy due to its wider solidification range. This makes 5754(Al-3%Mg) alloy more susceptible to cracking. As seen in Figure 4.3 and Figure 4.5, total number of solidification crack and total crack length measurements support these results.

In addition to total crack length (TCL), total number of crack (T#C) values and maximum crack length (MCL), *maximum crack tip distances* were evaluated. Maximum crack tip distance provides information about the ductility of the solidifying weld metal. As it was mentioned before, upper boundary of brittle temperature range is liquidus temperature and lower boundary is crack tip temperature. Nakata et. al. [39] have studied various aluminum alloys and stated that brittle temperature range is related to the solidification range of the alloy. In other words, increasing solidification range increases the brittle temperature range of the alloy. In the present study, it was seen that 5049(Al-2%Mg) alloy has no cracks at 0.5% strain level. Moreover, crack tip distance of 5049(Al-2%Mg) alloy at each strain level and line energy is shorter. It can be stated that crack stops at higher temperatures compared to 5754(Al-3%Mg) alloy (Figure 4.8 and Figure 4.9.). As a result, 5049(Al-2%Mg) alloy with a smaller solidification range has a narrower brittle temperature range.

In the solidifying weld metal interdendritic liquid with a low melting point, as well as its distribution along the grain boundaries affect the brittle temperature range. Nakata et al. [39] has shown that decreasing wetting angle results in higher cracking susceptibility. If the total number of solidification crack and maximum crack length results are

considered, higher resistance to solidification cracking of 5049 alloy can be related with less amount of low melting point liquid and/or its wetting angle.

When the *chemical compositions* of the two alloys are compared, first of all the difference of magnesium contents is significant. 5754(Al-3%Mg) alloy has higher amount of magnesium compared to 5049 alloy. And differential thermal analysis (DTA) results have revealed that the solidification range is wider for 5754(Al-3%Mg) alloy as expected. Second difference is manganese contents between two alloys. 5049 alloy contains about 0.86wt% Mn while 5754(Al-3%Mg) alloy contains below 0.001wt%Mn. Matsuda et.al [41] have studied the effect of some alloying elements on the solidification cracking susceptibility. It has been stated that although it was not as effective as Ti+B on grain refining, Mn addition has resulted in a finer microstructure.

Liquation cracking susceptibility

Partially melted zone (PMZ) is the region vulnerable to liquation cracking during welding due to the wide solidification range of aluminum alloys. Partially melted zone (PMZ) starts from fusion line where temperature is the liquidus temperature and expands to the point where it reaches the solidus temperature. As mentioned above, thermal analyses have shown that solidification range of 5754(Al-3%Mg) alloy is wider compared to 5049(Al-2%Mg) alloy. Thus, the partially melted zone (PMZ) of 5754(Al-3%Mg) alloy is expected to be wider than 5049(Al-2%Mg) alloy. Results have shown that there was almost no liquation cracking on 5049(Al-2%Mg) alloy. On the other hand, liquation cracking occurred for each strain level and line energy on 5754(Al-3%Mg) alloy. In addition to that, liquation cracking increased with increasing strain level and line energy n the partially melted zone (PMZ) of 5754(Al-3%Mg) alloy.

High segregation on grain boundary area increases partially melted zone (PMZ). Increasing solute content decreases the melting temperature of the interdendritic region resulting in higher amount of liquation and wider region vulnerable to liquation cracking. Strain accumulated during welding causes intergranular cracking due to liquation at the grain boundaries. EDS analyses (Figure 4.48) taken from the liquation fracture surface (Figure 4.47) have shown that 5754(Al-3%Mg) alloy has high magnesium and silicon content at the grain boundaries where liquation has occurred.

Due to high solute content melting temperature of the intergranular region may decrease resulting in higher liquation [14, 51]. Moreover, SEM images of liquation crack surfaces of 5754(Al-3%Mg) alloy have shown that there are two types of intermetallics that form at the grain boundaries. And these intermetallic particles may act as crack nuclei [52]

5.3. Hot cracking susceptibility of the weld metals with filler additions

The effects of filler additions on the hot cracking susceptibility of 5049(Al-2%Mg) and 5754(Al-3%Mg) alloys were evaluated. Hot cracking susceptibilities of different weld metals were studied for different line energies at a constant strain level. Crack length measurements were given in Figure 4.10 and Figure 4.11 for base alloy/filler alloy combinations.

Crack length measurements have shown that welds obtained with 5183 and 5356 filler additions to 5754(Al-3%Mg) alloy gave almost similar total crack length values. However, total solidification and total liquation crack length results are different for both 5754/5183 and 5754/5356 weld combinations. Solidification cracking susceptibility of the weld metal obtained with 5183 filler alloy is higher. If the chemical compositions of weld metals are compared 5754/5183 and 5754/5356 combinations has 3.5wt%Mg and 4.3wt%Mg respectively. As mentioned in the previous section, solidification range increases with increasing amount of magnesium. It is expected that as the solidification range increases solidification cracking susceptibility increases. However, in the 5754/5183 and 5754/5356 welds this was not the case. Thus, it can be assumed that cracks can be healed by solute-rich liquid with low melting point during solidification of 5754/5356 weld metal having 4.3wt%Mg resulting in lower cracking. Crack length measurements of 5049/5183 and 5049/5356 *base alloy/filler alloy* combinations have shown that solidification cracking susceptibilities of both weld metals were almost similar. When magnesium contents are considered, 5049/5183 and 5049/5356 welds have 2.6wt% and 2.85wt% magnesium respectively. Thus, it can be assumed that solidification ranges of both weld metals are approximately equal and it is consistent with the results.

Solidification cracking susceptibility of four weld metals has decreased with decreasing line energy. As it was mentioned before, decreasing line energy results in smaller weld

zone and finer microstructure. Therefore, weld metal has higher resistance to cracking with decreasing line energy.

When evaluating liquation cracking susceptibility, weld metal microstructure should be considered. As mentioned in section 4.2, re-melted region during varestraint testing of weld metals is narrower than width of weld metal. Therefore, while cracks formed in the re-melted zone are named as *solidification cracks*, cracks formed at the weld metal region which has not been re-melted during testing are named as *liquation cracks*. As a result, liquation cracking susceptibility mentioned in this part is the resistance of welds with filler additions to liquation cracking.

Liquation crack length measurements of weld metals which are 5754/5183 and 5754/5356 were given in Figure 4.10c. The combination of 5754/5356 has higher susceptibility to liquation cracking compared to alloy 5754/5183. The weld metal obtained with 5356 filler alloy contains higher amount of magnesium resulting in a wider solidification range. In addition to that, high solute content causes more segregation on grain boundaries and it decreases solidus temperature of the intergranular liquid below the weld metal. Thus, weld metal obtained with 5356 filler alloy is more susceptible to liquation cracking.

Liquation cracking of bead-on-plate welds obtained with 5183 and 5356 filler alloys on 5049(Al-2%Mg) alloy was also evaluated. Weld metal of 5049/5356 which has higher amount of Mg content showed higher liquation cracking compared to 5049/5183 having lower magnesium content. As mentioned above increasing magnesium content resulted in wider solidification range. Increasing solidification range resulted in wider partially melted zone (PMZ) which is vulnerable for liquation cracking.

5.4. Mid-plane segregation zone in 5754(Al-3%Mg) alloy

Both 5754(Al-3%Mg) and 5049(Al-2%Mg) alloys have centerline segregation at the mid-thickness of the sheets. And it was seen that 5754(Al-3%Mg) alloy has higher amount of segregation compared to 5049(Al-2%Mg) alloy. Two types of second phase particles were found in both alloys (Figure 4.27). First type of second phase particle

which is grey mainly includes iron and second type is black and rounded shape and contains silicon, magnesium and iron.

As given in Figure 4.26 cross section of bead-on-plate welds of 5754(Al-3%Mg) alloy has shown that centerline segregation zones close to the fusion zone were affected from the weld heat input. Second phase particles with different shapes were seen in these segregation zones under the optical microscope (Figure 4.28). It was concluded that these second phase particles were formed below the solidus temperature since they were seen outside the partially melted zone.

Heat treatment experiments were applied for segregation zone to see any changes that would take placejust below the solidus temperature. As given in Figure 4.28, intergranular liquation were observed at the mid-thickness of the 5754 alloy. Additional experiments were conducted to determine the lowest temperature at which these second phase particles were formed. It was seen that second phase particles in black color and "Chinese script" shape (Figure 4.29 and Figure 4.30) were formed at a temperature around 575^{o}C. These second phase particles contained mainly magnesium, silicon and iron as given in EDS analysis (Figure 4.32). It can be stated that, there is as a eutectic reaction below the solidus of the 5754(Al-3%Mg) alloy.

Differential thermal analysis (DTA) was applied to the mid-section of 5754(Al-3%Mg) alloy sheet to observe the effects of this mid-plane segregation zone. As given in Figure 4.37 there is an endothermic peak at around 580^{o}C during heating stage. Moreover, this curve has not been observed in the differential thermal analysis (DTA) curve of the 5754(Al-3%Mg) alloy sample as a whole. When these results are compared with heat treatment experiments mentioned above, it can be stated that there could be a eutectic reaction at around 580^{o}C at mid-plane segregation. Mg_2Si, Si and aluminum are possible phases forming eutectic reaction [47].

Partially melted zone is limited between liquidus and solidus temperature of the base alloy during welding. However, in twin roll cast (TRC) alloys the size of PMZ can increase due to high solute content in the mid-plane segregation zone. Moreover, presence of eutectic reaction below the solidus temperature also increases the width of partially melted zone (PMZ). Therefore, liquation cracking susceptibility of an alloy

increases due to mid-plane segregation. At the beginning, varestraint test specimens were investigated only for surface cracks. Due to the presence of liquation at mid-thickness of the sheet internal cracks were investigated. Micrographs were taken from longitudinal cross section varestraint test specimen with partial penetration. As given in Figure 4.35 and Figure 4.36, internal cracks at the grain boundaries due to liquation below the fusion zone were determined. Transverse cross sections were also examined to see if there are any internal cracks near the fusion zone but there were none. Results revealed that, mid-plane segregation also increases the liquation cracking susceptibility in the heat affected zone during welding.

CHAPTER 6

CONCLUSION

The present study contains results of hot cracking susceptibility of two twin roll cast (TRC) Al-Mg alloys. The quantitative comparison was made using the varestraint test outputs and reasons for the hot cracking susceptibility difference of two Al-Mg alloys were discussed. The conclusions obtained based on the results are given as follows:

1. The hot cracking susceptibility of 5049(Al-2%Mg) and 5754(Al-3%Mg) alloys increased with increasing strain level and line energy.

2. Differential thermal analysis results showed that solidification range of 5754 alloy is wider than 5049 alloy and hot cracking susceptibility depends on Mg content. Further 5049 has shown no solidification cracking at 0.5% strain level and liquation cracking was not observed at each line energy.

3. Varestraint test for hot cracking susceptibility determination can be used either by total crack length (TCL), or by total number of crack (T#C) or by maximum crack length (MCL) mesurements.

4. Addition of filler alloys (5183 and 5356) changed the magnesium content and solidification cracking tendency of the weld zone.

5. Decreasing line energy resulted in finer microstructure and decreased solidification cracking tendency. Thus, solidification cracking susceptibility can be decreased by obtaining finer microstructure in the weld zone.

6. In 5754 alloy welding heat input changed the type of segregation and since the segregation decreases the melting point of the intergranular region partially melted zone expands.

7. Eutectic reaction at mid-plane segregation solidifies below the solidus of 5754 alloy. Liquation due to eutectic reaction can cause higher liquation cracking tendency during welding.

REFERENCES

1. R. Cook, P. G. Grocock, P. M. Thomas, D. V. Edmonds and J. D. Hunt, "Development of the twin-roll casting process" Journal of Materials Processing Technology 55 (1995) 76-84.

2. T. Haga "Semisolid strip casting using a twin roll caster equipped with a cooling slope" Journal of Materials Processing Technology 130–131 (2002) pp558–561.

3. T. Haga, S. Suzuki "Study on high-speed twin-roll caster for aluminum alloys" Journal of Materials Processing Technology 143–144 (2003) pp895–900

4. S. A. Lockyer, Ming Yun, J. D. Hunt, and D. V. Edmonds, "Micro- and macro defects in thin sheet twin-roll cast aluminum alloys" Materials Characterization 37 (1996) pp301-310

5. T. Haga, K. Takahashi, M. Ikawa and H. Watari, "A vertical type twin roll caster for aluminum alloy strips" Journal of Materials Processing Technology 140 (2003) pp610–615

6. D. J. Monaghan, M. B. Henderson, J. D. Hunt and D. V. Edmonds, "Microstructural defects in high productivity twin-roll casting aluminum" Materials Science and Engineering, A173 (1993) pp251-254

7. M. Yun, S. Lokyer, J.D. Hunt "Twin roll casting of aluminium alloys" Materials Science and Engineering A280 (2000) pp116-123

8. B Cantor, K O'Reilly, "Solidification and casting" IOP publishing, 2003

9. G. E. Totten and D. S. MacKenzie “Handbook of Aluminum”. Vol. 1 2003 CRC Press Taylor&Francis Group

10. S. Kou “Welding Metallurgy” 2nd edition (2002) pp285-296 John Wiley & Sons

11. S. Kou, “Solidification and liquation cracking issues in welding” JOM vol. 55, No. 6 (2003) pp37-42

12. A. Chojecki, I. Telejko and P. Kozelsky, “Influence of calcium on cracking of steel during the welding or casting process” Theoretical and Applied Fracture Mechanics 31 (1999) pp41-46

13. E. Cicala, G. Duffet, H. Andrzejewski, D. Grevey and S. Ignat, “ Hot cracking in Al-MgiSi alloy laser welding –operating parameters and their effects” Materials Science and Engineering A 395 (2005) pp1–9,

14. C. M. Cheng, C. P. Chou, I. K. Lee and H. Y. Lin, “Hot cracking of welds on heat treatable aluminium alloysScience and Technology of Welding and Joining” 2005 Vol 10 No 3 pp344-352

15. O.A. Ojo, Y.L. Wang and M.C. Chaturvedi “Heat affected zone liquation cracking in electron bean welded third generation nickel base superalloys” Materials Science and Engineering A 476 (2008) pp217–223

16. R. Hermann, S.S. Birley and P. Holdway, “Liquation cracking in aluminum alloy welds” Materials Science and Engineering A212 (1996) pp247-255

17. G. Cao and S. Kou, “Liquation cracking in full-penetration Al-Si” Welding Journal 84(4) (2005) pp63-71

18. C. Huang and S. Kou, “Liquation cracking in full-penetration Al-Cu welds” Welding Journal 83(2) (2004) pp50-58

19. C. Huang and S. Kou, “Liquation cracking in full-penetration Al-Mg-Si” Welding Journal 83(4) (2004) pp111-122

20. C. Huang, G. Cao and S. Kou, “Liquation cracking in partial penetration aluminum welds: assessing tendencies to liquate, crack and backfill” Science and Technology of Welding and Joining Vol. 9 No. 2 2004 pp149–157

21. C. Huang and S. Kou, “ Liquation mechanisms in multicomponent aluminum alloys during welding” Welding Journal 81(10) (2002) pp211-222

22. G.D. Janaki Ram, T.K. Mitra, V. Shankar and S. Sundaresan, “Microstructral refinement through inoculation of type 7020 Al-Zn-Mg alloy welds and its effect on hot cracking and tensile properties” Journal of Materials Processing Technology 142 (2003) pp174–181

23. H. T. Kim, S. W. Nam and S. H. Hwang, Journal of Materials Science 31 (1996) pp2859-2864

24. G. M. Reddy, A. K. Mukhopadhyay and A. S. Rao, “Influence of scandium on weldability of 7010 aluminum alloy” Science and Technology of Welding and Joining Vol 10 No 4 (2005) pp432-441.

25. S. Lathabai and P.G. Lloyd, “The effect of scandium on the microstructure, mechanical properties and weldability of a cast Al-Mg alloy” Acta Materialia 50 (2002) pp4275–4292

26. A.F. Norman,, K. Hyde, F. Costello, S. Thompson, S. Birley and P.B. Prangnell, “Examination of the effect of Sc on 2000 and 7000 series aluminum alloy castings: for improvements in fusion welding” Materials Science and Engineering A354 (2003) pp188-198

27. Y. P. Yang, P. Dong, J. Zhang and X. Tian, “ A hot-cracking migitation technique for welding high-strength aluminum alloy” Welding Journal 79(1) (2000) pp9-17

28. T. W. Nelson, J. C. Lippold, W. Lin and W. A. Baeslack, Welding Journal 76(3) (1997) pp110-119

29. F. Matsuda, K. Nakata, K. Arai and K. Tsukamoto, "Assessment of solidification cracking test for aluminum alloy welds" Trans. of JWRI Vol11 No1(1982) pp67-77

30. W. F. Savage and C.D Lundin, Welding Journal 44 (1965) pp433-442

31. M. M. Mossman and J. C. Lippold, "Weldability testing of dissimilar combinations of 5000- and 6000-series aluminum alloys" Welding Journal 81(9) (2002) pp188-194

32. D.G. Eskin, Suyitno, L. Katgerman "Mechanical properties in the semi-solid state and hot tearing of aluminium alloys" Progress in Materials Science 49 (2004) pp629–711

33. Novikov II, Novik FS. Doklady Akad Nauk SSSR, Ser Fiz 1963 vol.7 pp1153.

34. Prokhorov NN. Russian Castings Production 1962 vol.2 pp172.

35. H. T. Kim, S.W. Nam "Solidification cracking susceptibility of high strength aluminum alloy weldment" Scripta Materialia 1996 Vol.34 No.7 pp1139-1145

36. F. Matsuda, K. Nakata, K. Tsukamoto, T. Uchiyama "Effect of additional element on weld solidification crack susceptibility of Al-Zn-Mg alloy (Report III)" Transactions of JWRI, vol. 13 No. 1 1984 pp57-66

37. M. Slamova, M. Karlık, F. Robaut, P. Slama, M. Veron "Differences in microstructure and texture of Al–Mg sheets produced by twin-roll continuous casting and by direct-chill casting" Materials Characterization 49 (2003) pp231– 240

38. V Shankar, T P S Gill, S L Mannan and S Sundaresan "Solidification cracking in austenitic stainless steel welds" Sadhana Vol. 28, Parts 3 & 4, June/August 2003, pp359–382

39. K. Nakata, and F. Matsuda, “Ductility characteristics of commercial aluminum alloys between liquids and solidus temperatures during welding and evaluation of weld solidification cracking susceptibility” Welding Journal 9 (1995) pp706-716.

40. F. Matsuda, K. Nakata, Y. Shimokusu, K. Tsukamoto, K. Arai “Effect of additional element on weld solidification crack susceptibility of Al-Zn-Mg alloy (Report I)” Transactions of JWRI, vol.12 No.1 1983 pp81-87

41. F. Matsuda, K. Nakata, K. Tsukamoto, T. Uchiyama “Effect of additional element on weld solidification crack susceptibility of Al-Zn-Mg alloy (Report III)” Transactions of JWRI, vol. 13 No. 1 1984 pp57-66.

42. C Huang, and S. Kou, “Partially melted zone in aluminum welds — liquation mechanism and directional solidification” Welding Journal 79(5) 2000 pp113-120.

43. C Huang, and S. Kou, “Partially melted zone in aluminum welds — planar and celluar solidification” Welding Journal 80(2) 2001 pp 46-53.

44. C Huang, and S. Kou, “Partially melted zone in aluminum welds — solute segregation and mechanical behavior” Welding Journal 80(1) 2001 pp9-17.

45. F. Matsuda, K. Nakata, K. Arai, K. Tsukamoto “Assesssment of solidification cracking test for aluminum alloy welds” Transactions of JWRI vol.11No.1 (1982)pp67-77.

46. M. Karlík, M. Slámová, M. Janeèek and P. Homola “Microstructure Evolution of Twin-Roll Cast Al-Mg Alloys During Downstream Processing” Kovové Materiály, 40, 2002, pp330-340.

47. L.F. Mondolfo, “Aluminum Alloys: Properties And. Structure” Butterworth & Co (Publisher) Ltd, (1976).

48. G.D.J. Ram, T.K. Mitra, M.K. Raju, S. Sundaresan “Use of inoculants to refine weld solidification structure and improve weldability in type 2090 Al-Li alloy” Materials Science and Engineering A276 (2000) pp48–57.

49. G.D.J. Ram, T.K. Mitra, V. Shankar, S. Sundaresan “Microstructural refinement through inoculation of type 7020 Al-Zn-Mg alloy welds and its effect on hot cracking and tensile properties” Journal of Materials Processing Technology 142 (2003) pp174–181.

50. N. Ramanaiah, K.S. Rao, B. Guha and K.P. Rao “Effect of modified AA4043 filler on partially melted zone cracking of Al-alloy gas tungsten arc welds” Science and Technology of Welding and Joining 2005 Vol 10 No 5 pp591-596.

51. R.K. Gupta and S.V.S.N. Murty, “Analysis of crack in aluminium alloy AA2219 weldment” Engineering Failure Analysis 13 (2006) pp1370–1375.

52. L. Katgerman, D.G. Eskin, “In Search of the Prediction of Hot Cracking in Aluminium Alloys” In Hot Cracking Phenomena in Welds II pp3-18.

53. M. Schellhase, “Der Schweißlichtbogen; ein technologisches Werkzeug” Fachbuchreihe Schweißtechnik, Band 84 Deutscher Verlag für Schweißtechnik (DVS), (1985) Düsseldorf.

54. J. Cornu, “Advanced welding systems” Vol. 3: TIG and related processes. Springer Verlag, (1988). Berlin.

55. Ø. Grong, “Metallurgical Modelling of Welding” The Institute of Materials. (1994) London.

56. J.J Pepe and W.F Savage, “Effect of constitutional liquation in 18-Ni maraging steel weldments” Welding Journal, vol.46: (1967) pp411-422.

57. J.J Pepe and W.F Savage, Welding Journal, vol.49 (1970) pp545.

58. W.S Pellini,. “Strain theory of hot tearing”. The Foundry vol. 80(11) (1952) pp. 125-199.

59. W.I. Pumphrey and P.H. Jennings “A consideration of the nature of brittleness and temperature above the solidus in castings and welds in aluminum alloys” J. Inst. Metals 75 (1948) 235-256.

60. N. Coniglio, “Aluminum Alloy Weldability: Identification of Weld Solidification Cracking Mechanisms through Novel Experimental Technique and Model Development” PhD Thesis Berlin, BAM (2008).

61. N. N Prokhorov “The problem of the strength of metals while solidifying during welding” Svar Proiz (1956) vol. 6 pp5–11.

62. T Senda, F Matsuda and G. Takano “Studies on solidification crack susceptibility for weld metals with trans-varestraint test” J Japan Weld Soc Vol.42 (1973) pp48–56.

63. I.I. Novikov. “Hot Shortness of Non-Ferrous Metals and Alloys” Nauka, Moscow, (1966) pp209.

64. J.C Borland “Generalized theory of super-solidus cracking in welds (and castings)” Br. Weld. J. Vol.7 (1960) pp508–512.

65. D.G. Eskin L. Katgerman “A Quest for a New Hot Tearing Criterion” Metallurgical and Materials Transactions Volume 38A, July 2007 pp1511-1519.

66. T.W Clyne, G.J Davies, “Solidification and casting of metals” London Metals Society (1979) pp275.

67. U Feurer. In: Nieswaag H, Schut JW, editors. “Quality control of engineering alloys and the role of metals science” Delft, Delft University of Technology (1977) pp131.

68. M. Wolf, H. Schobbert, T. Böllinghaus “Influence of the Weld Pool Geometry on Solidification Crack Formation” In: Hot Cracking Phenomena in Welds, Springer Pub.,pp245-268.

69. L Katgerman. “A mathematical model for hot cracking of aluminum alloys during DC casting” JOM 1982 vol.34 (20) pp46.

70. J.N DuPont, C.V Robino and A.R Marder “Modelling solute redistribution and Microstructural development in fusion welds of Nb-bearing superalloys” Acta Materialia, vol.46 (1998) pp4781-4790.

71. R.A Chihoski, “The character of stress fields around a weld arc moving on aluminium sheet” Welding Journal, vol. 51(1) (1972) pp9-18.

72. R.A. Chihoski, “Understanding weld cracking in aluminum sheet” Welding Journal. Vol.51 (1972) pp24-30.

73. C. Batıgün, Ph.D thesis “Determination of welding parameter dependent hot cracking susceptibility of 5086-H32 aluminium alloy with the use of MVT method” METU, Ankara (2005).

APPENDIX A

PHASE DIAGRAM OF Al-Mg and Al-Mg-Si

Aluminum–magnesium phase diagram is given to evaluate the hot cracking susceptiblity differences between two different Al-Mg alloys with respect to solidification range. Also liquidus projection of Al-Mg-Si phase diagram is given to evaluate the eutectic reactions at the mid-plane segregation.

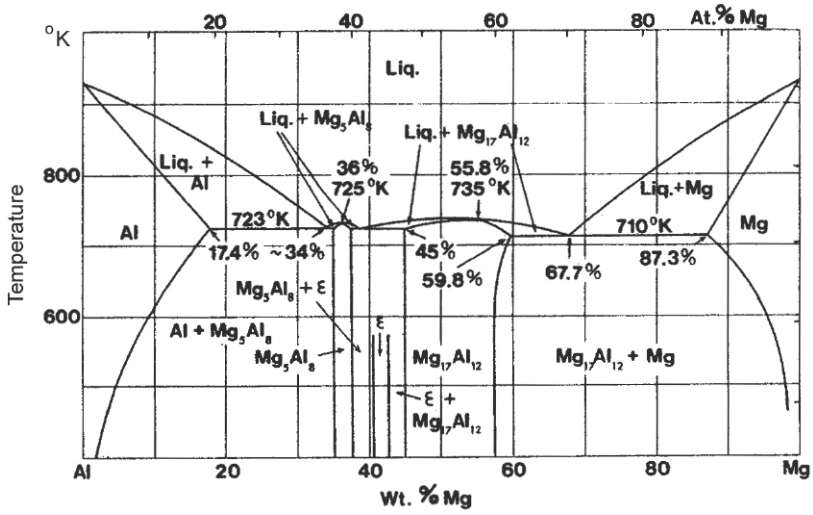

Figure A1 Al-Mg phase diagram[47].

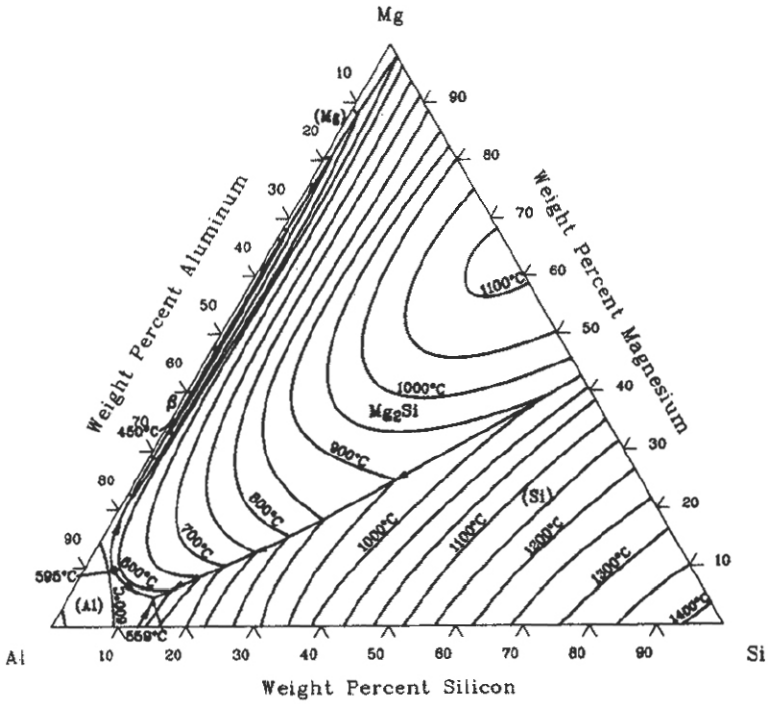

Figure A2 Liquidus projection of Al-Mg-Si ternary phase diagram[47].

VITA

PERSONAL INORMATION

Last Name, Name	: Tirkeş, Süha
Nationality	: Turkish (TC)
Date and Place of Birth	: June 26, 1977, Ankara
Marital Status	: Married
Voice	: +90-506-474-1993
E-mail	: stirkes@metu.edu.tr

EDUCATION

Degree	**Institution**	**Year of Graduation**
MS METU,	Metallurgical and Materials Eng.	2002
BS METU,	Metallurgical and Materials Eng.	1999
High School	Antalya High School	1994

WORK EXPERIENCE

Year	**Place**	**Enrollment**
2000-present	METU, Welding Tech. & NDT Center	Research Assistant
1998 August	Cer Döküm	Intern Engineering Student
1997 June	Toprak Seramik	Intern Engineering Student

PUBLICATIONS

1. M. Akkuş, S. Tirkeş, C. Batıgün, Effects of welding on the mechanical properties of Al-Zn-Mg alloys, Proceedings of The 14th International Metallurgy and Materials Congress and Fair, Istanbul, 16-18 October 2008

2. M.T. Ertürk, S. Tirkeş, C. Batıgün, Determintion of the hot crcking tendency of 7075 aluminum alloy during welding using the circular patch test, Proceedings of The 14th International Metallurgy and Materials Congress and Fair, Istanbul, 16-18 October 2008

3. C. Batıgün, S. Tirkeş, Al-Mg alaşımlarının MIG kaynağında hat enerjisinin kaynak dikişi geometrisine ve kaynak metalindeki magnezyum oranına etkisi, Proceedings of The 6th National Welding Technology Congress, Ankara, 9-11 November 2007

4. S. Tirkeş, C. Batıgün, Al-Mg alaşmlarının kaynak esnasındaki sıcak çatlama eğiliminin TIG nokta kaynağı metodu ile belirlenmesi, Proceedings of The 6th National Welding Technology Congress, Ankara, 9-11 November 2007